THE STRUCTURE AND CIRCULATION OF DEEP AND BOTTOM WATERS IN THE ANTARCTIC OCEAN

Jeffrey Edwin Callahan

THE STRUCTURE AND CIRCULATION OF DEEP AND BOTTOM WATERS IN THE ANTARCTIC OCEAN

by

Jeffrey Edwin Callahan

A dissertation submitted to The Johns Hopkins University in conformity with the requirements for the degree of Doctor of Philosophy.

Baltimore, Maryland

1971

ABSTRACT

The circulation of deep and bottom waters in the Antarctic Ocean is studied by analyzing the distributions of heat, salt, and dissolved oxygen in the ocean south of 40°S. The discussion of the deep-water flow is based on maps showing the depth, salinity, and dissolved-oxygen content of the surfaces where potential steric anomaly equals 50 and 30 centiliters per ton (potential density equals 27.60 and 27.81 grams per liter). The 50-cl/t surface is close to the vertical minimum of dissolved oxygen in the antarctic. This feature is shown to originate in the eastern South Pacific Ocean. The 30-cl/t surface nearly coincides with the deep salinity maximum, which originates in the North Atlantic Ocean.

Maps showing the potential temperature, salinity, and dissolved oxygen in the bottom layer (depth > 3500 m) of the Antarctic Ocean are also included in the report. Bottom water is shown to be produced in both the Ross and Weddell seas. Ross Bottom Water is characterized by high salinities relative to Weddell Bottom Water. The distributions in the bottom layer indicate that the Weddell Sea is a much stronger source of bottom water than is the Ross Sea.

The velocity field south of Australia is examined through geostrophic computations and direct current measurements. The eastward Antarctic Circumpolar Current is shown to be divided into two distinct zones separated by weak westward flow. The narrow

westward countercurrent is found near the crest of the Indian-Antarctic Ridge. The net eastward flux between Australia and Antarctica is 233×10^6 m^3/s, which is nearly equal to the flux through Drake Passage.

ACKNOWLEDGEMENTS

In preparing this dissertation, I have been assisted by many people. Foremost among them are Professor Raymond Montgomery of The Johns Hopkins University and Mr. Joseph Reid, Jr. of the Scripps Institution of Oceanography. Professor Montgomery, in his capacity as dissertation advisor, has paid careful attention to this project and has made numerous suggestions for improving the final product. The method of analysis upon which much of the dissertation rests is itself based primarily on the research of Professor Montgomery.

Mr. Joseph Reid has, over the past few years, frequently encouraged and assisted me in my study of oceanography. The opportunities which he provided to participate in oceanographic cruises in the antarctic have had an obvious impact on my choice of research topics. I have greatly enjoyed my associations with both of these gentlemen.

I have benefited from discussions with members of The Johns Hopkins University Department of Earth and Planetary Sciences. The advice of Professors Owen Phillips and Francis Bretherton and of Associate Professors James Carpenter and Blair Kinsman (now at the University of Delaware) has been particularly helpful.

I have received expert technical assistance from the staff of the Chesapeake Bay Institute. Mr. Michael Karweit and Mrs. Carol Feister helped write the computer programs required for data processing. Mr. William Wilson and Mrs. Dean Pendleton pre-

pared the many figures included in the dissertation. Mrs. Arlene Sullivan has done all the typing.

I am grateful to the United States Navy for financial support provided under the Burke Scholar Program. The National Science Foundation supported my work on *Eltanin* Cruise 41.

Finally, I wish to record my gratitude to my wife for the steady support she has given me during my studies.

TABLE OF CONTENTS

TABLE OF FIGURES

TABLE OF FIGURES (continued)

I. INTRODUCTION

I.A. Purpose and Significance

The Antarctic or Southern Ocean, which I will take to be the region between 40°S and the Antarctic continent, plays a central role in the deep and bottom circulation of the world ocean. There are two fundamental reasons for its importance in these phenomena: (1) The Antarctic Ocean is by far the largest connection among the Atlantic, Indian, and Pacific oceans. Enormous amounts of water, heat, salt, and nutrients are exchanged among the oceans. The exchange helps maintain the observed temperature, salinity, and dissolved-oxygen fields in the world ocean, thereby affecting the earth's heat budget and the distributions of marine organisms. (2) The extreme southern reaches of the Antarctic Ocean are among the few regions of the world where climatic conditions may lead to navifacial[1] water becoming sufficiently dense to overturn and replenish the deep and bottom water. These sources of bottom water are critical elements in the thermohaline circulation of the ocean.

Insight into the various dynamic and thermodynamic processes which determine the antarctic circulation may be gained from taking several points of view. Theoretical attacks on the problem

---

[1] The term "naviface" (Montgomery, 1969) will be used to distinguish the air-sea interface from the several other surfaces discussed in this paper.

have so far centered on modeling the quasi-zonal Antarctic Circumpolar Current, which is the dominant flow in the region. These studies have been reviewed in the author's masters essay (1968, unpublished).

The present paper takes a different approach, an essentially empirical one. The horizontal and vertical distributions of temperature, salinity, and dissolved oxygen in the abyssal layers are examined in detail. Within the limitations of certain simplifying assumptions, to be discussed later, conclusions are then reached concerning the large-scale structure of the circulation.

Similar studies have been undertaken previously. Most of them were based on data gathered prior to World War II. Within the last decade a large amount of hydrographic work has been carried out in the antarctic. Much of this work has been done in areas that were previously very poorly sampled (*e.g.*, the Weddell Sea) or in areas where old measuring techniques were not sufficiently sensitive to detect differences in water characteristics (*e.g.*, the Pacific Ocean). Further, the recent stations include samples taken closer to the sea floor than on the early stations. Although the new data have been discussed in relation to specific sections of antarctic waters, notably by A. L. Gordon, the present paper represents the first attempt to incorporate these data into a general analysis of the circumpolar region.

In part, this study was prompted by the availability of a large body of new data and a desire to find out what new features

might be revealed in the deep and bottom waters of the antarctic. The investigation was also motivated by an interest in some specific aspects of the antarctic circulation which are not yet well understood. These include the structure of the velocity field and the transport of the Antarctic Circumpolar Current, the meridional exchange of deep water between the antarctic and the oceans to the north, and the importance of the Ross Sea as a source of bottom water.

I.B. Previous Work

Our present understanding of the large-scale structure and circulation of antarctic waters has been pieced together from the efforts of many individuals. Most of this work has been carried out within the last forty years, and my review will therefore focus on this period. However, it is interesting to note that at least a partial appreciation of the role of the antarctic in the deep oceanic circulation was evident somewhat earlier. Buchan (1895, p. 8) concluded from the deep-sea temperature measurements made by the *Challenger* (1872-76) that, "There can be no doubt that these very low deep-sea temperatures have their origin in the Southern or Antarctic Ocean, the icy-cold waters of which are propagated northwards... ." Buchan (p. 27) also deduced the existence of a warm deep current flowing from the North Atlantic to the South Atlantic. This water mass, now known as North Atlantic Deep Water, is another major component of the abyssal circulation in the antarctic.

During the 1920's, substantial improvements were made in the hydrographic coverage of the South Atlantic, Indian, and Pacific oceans. For the first time, oceanographers could begin to understand the character of the general circulation. On the basis of *Carnegie* (1928-29) stations taken in the Pacific Ocean, Sverdrup (1931) was able to show that the deep circulation of the Pacific must be qualitatively different from that of the Atlantic and Indian oceans. He concluded that the Pacific deep water is a mixture of deep water from the Atlantic and Indian oceans with bottom water from the antarctic. Owing to a scarcity of data, Sverdrup was unable to venture beyond these general conclusions, and some of the details of the flow he deduced were later proved incorrect. Nonetheless, the concept of inter-ocean exchange which he formulated is basic to our present understanding of the abyssal circulation.

In 1933, three papers dealing with the characteristics and circulation of Atlantic-Antarctic waters were published. Wüst (1933) discussed at length the distributions of potential temperature and salinity near the sea floor in water deeper than 4000 m. His maps, which were based on all data available at that time, showed in a very striking fashion the propagation of cold bottom water out of the Weddell Sea, northward along the western trough of the Atlantic and eastward into the Indian Ocean. Wüst's maps have become the classic piece of evidence for the importance of the Weddell Sea as a source of bottom water, although there is some ambiguity in Wüst's salinity map.

A more general description of the hydrography of the western Atlantic-Antarctic was written by Deacon (1933). His study was based on the early cruises of the *Discovery* and *Discovery II*. In a brief section on the bottom water, Deacon reviewed several proposed mechanisms for bottom-water formation. He concluded that the bottom water is probably formed over the continental shelf of the Weddell Sea, as Brennecke (1921, referenced by Deacon, 1933) had proposed somewhat earlier.

The question of exchange between the Atlantic and Pacific oceans via Drake Passage was examined by Clowes (1933) in his study of the deep water of the Scotia Sea. Noting that the deep water of the Scotia Sea is somewhat less saline than that farther to the east, he concluded that most of this water must come from the Pacific. Clowes computed the geostrophic transport relative to 3500 db through Drake Passage and arrived at a net eastward flux of 110×10^6 m^3/s. This was the first quantitative estimate of the exchange of water through Drake Passage.

A broad account of the hydrography of the Atlantic-Antarctic sector south of 55°S, between 40°W and 40°E, was given by Mosby (1934). A large part of his data were from the *Norvegia* Expeditions of 1927-28, 1929-30, and 1930-31, but *Deutschland* (1911-12), *Meteor* (1925-26), and *William Scoresby* (1931) stations were also included. In addition to describing and classifying the water masses of the region, much as Deacon (1933) had done, Mosby discussed two dynamical features of interest:

(1) His maps of dynamic topography (*e.g.*, his Figure 28) show clearly a weak, elongated cyclonic gyre centered in the northeastern Weddell Sea and extending as far as 15°E. Mosby pointed out that this flow pattern is consistent with the drift of the *Deutschland*, which was icebound in the Weddell Sea during the winter of 1912. Noting that the winds in this region also have a roughly cyclonic pattern, shifting from westerlies north of 60°S to easterlies along the antarctic coast, he concluded that the Weddell gyre is driven by the wind.

The existence of a cyclonic gyre in the Weddell Sea is also suggested by Mosby's map of maximum sub-surface temperatures, on which a westward intrusion of relatively warm water along the antarctic coast can be seen. According to Mosby, this feature had been observed in the *Deutschland* data by Brennecke (1921), who theorized that the warm water comes directly from the Indian Ocean. Mosby, however, recognized the warm water as the uniform deep water found elsewhere around Antarctica, and ruled out a direct Indian Ocean influence.

(2) Mosby devoted considerable space to the question of bottom-water formation. After reviewing the theories of bottom-water formation, he, like Deacon, concluded that Brennecke's (1921) explanation is correct. Brennecke had proposed that bottom water is formed in the Weddell Sea from navifacial water which is overturned during winter. The postulated vertical convection, which takes place in shallow water, is driven by cooling and the

addition of salt at the naviface during the formation of sea ice. Dense, uniform shelf water then flows down the slope, mixes with warmer, saltier deep water, and forms a dense mixture which sinks to the bottom. In accepting this mechanism for bottom-water formation, Mosby pointed out that to produce bottom water with the observed characteristics, the shelf water (assumed to be at the freezing point) must have a salinity of at least 34.62‰.

Mosby rejected Wüst's (1933) suggestion that the mechanism proposed by Brennecke is supplemented by deep vertical convection occurring "at the edge of the convergence area created by pack ice..." (Wüst, 1933, p. 47). Wüst's theory seemed highly unlikely because (1) no such convergence has been detected (in fact, the prevailing wind field would suggest the existence of a region of divergence), and (2) the observed vertical temperature and salinity distributions are inconsistent with deep overturning.

The first study of the circumpolar characteristics of the Antarctic Ocean was by Deacon (1937). The principal source of data for Deacon's work was the circumpolar cruise of the *Discovery II* in 1932-33, during which nineteen sections were made in the antarctic zone.

Several highly significant features of the deep and bottom flow around Antarctica were revealed in Deacon's paper. It became clear for the first time that bottom water is not formed all around the antarctic coast, as proposed by Sverdrup (1931), but is instead formed primarily in the Weddell Sea. Deacon also showed that the bottom water formed in the Weddell Sea flows

around Antarctica towards the east, not, as Sverdrup had deduced, towards the west. (These conclusions were later confirmed by Sverdrup (1940) on the basis of data taken in the Indian-Antarctic Ocean during the BANZAR Expedition[2](1929-31).) Another valuable result of the *Discovery* data was to confirm the extreme uniformity of the deep water around Antarctica, which Sverdrup (1931) had predicted from the limited data available to him.

In his BANZARE Report Sverdrup acknowledged the defects in his earlier theory of the deep circulation, and he proposed a revised version. He again emphasized the importance of the Atlantic Ocean as the primary source of deep water in the world ocean and the role of the Antarctic Circumpolar Current as the agent by which Atlantic deep water is transported to the Indian and Pacific oceans. Sverdrup computed the eastward water transport relative to 3000 db across a section from Tasmania to Antarctica (145°E). His result, 144×10^6 m^3/s, was the first estimate of the flux of water from the Indian to the Pacific ocean.

Another significant aspect of the circumpolar circulation was pointed out by Sverdrup in his discussion of the general circulation in *The Oceans* (Sverdrup *et al.*, 1942). Sverdrup noted a systematic deflection of the predominantly zonal transport lines by major topographic features (see his Figure 163). The direction

---

[2] British, Australian & New Zealand Antarctic Research Expedition

of the deflection (equatorward on approaching a ridge; poleward after crossing over the ridge) is in agreement with qualitative predictions made by assuming conservation of potential vorticity. One implication of these deflections is that the Circumpolar Current must extend to great depths.

During the period from World War II through the mid-1950's little oceanographic research was carried out in the antarctic, and few papers were published on the subject. One paper from this period which is notable in the present context is Fofonoff's (1956) study of bottom-water formation. Using temperature and salinity data collected in the northern Weddell Sea, Fofonoff gave quantitative support to Brennecke's model of bottom-water formation.

The International Geophysical Year (1957-58) brought about a resurgence in all phases of antarctic research including oceanography. Over the past decade, research ships from the United States and the Soviet Union have been very active in the antarctic, and many hydrographic stations have been occupied. The substantial increase in field activity has resulted in numerous published reports on antarctic oceanography.

Ishino (1963) presented circumpolar plots of temperature, salinity, and density at several depths from 50 m to 3000 m, using mainly *Discovery* (1925-37) and *Ob'* (1956-58) stations. He attempted to discuss seasonal variations in characteristics down to 2000 m, but this effort was severely limited by the lack of winter data. Perhaps the strongest conclusion that may be drawn

from Ishino's maps is that no systematic seasonal variations in temperature and salinity are evident below 200 m, at least in those areas where sufficient data are available for comparison. Ishino (p. 166) apparently believed that large amounts of bottom water are produced in shallow regions along the Indian Ocean sector of the antarctic coast. This conclusion conflicts with the evidence presented by Sverdrup (1940), Deacon (1937), and the present work.

The most recent descriptive studies of the Antarctic Ocean are those by Gordon (1966, 1967b, 1970) and Reid and Nowlin (1971). The first two papers by Gordon are analyses of the sector from 20°W to 170°W, utilizing the early *Eltanin* data. Gordon (1970) has extended his study of bottom water into the eastern Indian Ocean. Gordon and Goldberg (1970) have prepared a folio containing maps of temperature, salinity, and dissolved oxygen at constant depths and sections showing the general structure of antarctic waters. Pertinent aspects of these studies will be discussed in later sections.

Reid and Nowlin (1971) discuss the deep circulation in the Drake Passage region. By using deep current measurements made in the Passage as reference values for geostrophic computations, they have determined that the net eastward mass flux through Drake Passage is well over 200×10^6 m^3/s (their value is 237×10^6 m^3/s). Most previous estimates were on the order of 100×10^6 m^3/s.

The results of the above studies may be summarized in the following brief description of deep and bottom waters in the

antarctic: Circumpolar Deep Water (Sverdrup, 1940) is a thick, uniform layer of relatively warm and salty water found in all longitudes around Antarctica. It has the following characteristics: θ = 1.0 - 2.0°C, S = 34.70 - 34.76 ‰, O_2 = 4.0 - 4.6 ml/l. Circumpolar Deep Water flows in a broad, quasi-zonal current eastward around the continent at speeds of roughly 5 cm/s, and participates in a much slower meridional exchange with the oceans to the north. The mean zonal transport of the Antarctic Circumpolar Current is probably in excess of 200 × 10^6 m^3/s. Permanent large-scale meanders in the zonal flow are found over major topographic features.

A major constituent of Circumpolar Deep Water is North Atlantic Deep Water, which moves south and mixes into the circumpolar flow in the Atlantic and Indian ocean. The magnitude of the southward flux of North Atlantic Deep Water is difficult to determine, but calculations by Wright (1969) and Sverdrup *et al.* (1942) indicate that it is on the order of 20 × 10^6 m^3/s at 30°S. As the Circumpolar Deep Water flows around Antarctica, its properties are further modified by lateral and vertical mixing, ultimately producing the extremely uniform deep water (Common Water, Montgomery, 1958) of the Pacific Ocean.

The second major water mass found in the abyssal depths of the antarctic zone is Antarctic Bottom Water. (For the present, Antarctic Bottom Water will be referred to as a single water mass. Later I will show that two distinctive water types can be recognized within this mass.) Antarctic Bottom Water has the char-

acteristics: $\theta = -0.8 - 0°C$, $S = 34.65 - 34.71$ ‰, $O_2 = 5.4 - 7.0$ ml/l.

The primary source of bottom water is the Weddell Sea, although the Ross Sea probably does produce limited quantities (Gordon, 1966, 1970). The bottom water formed in the Weddell Sea is a mixture of very cold, moderately salty shelf water and warmer, more saline deep water. The dense shelf water is supposed to be produced during winter when sea ice forms. This mechanism is only inferred from summer observations, since no observations of shelf water have ever been made in winter.

I.C. Method of Analysis

In this paper the circulation is studied by means of maps and sections showing the distributions of salt and dissolved oxygen in the deep and bottom waters. These substances act as tracers with which the mean flow field can be deduced using a model based on the diffusion equation.

Several assumptions and approximations have been made in order to simplify the interpretation of the maps. The first of these is that the large-scale ($> 10^2$km) distributions of heat, salt, and dissolved oxygen are in a steady state below the shallow navifacial layer. In view of the demonstrated reproducibility of temperature and salinity measurements below the naviface (compare Wüst, 1936, Teil A and Fuglister, 1960) this appears to be a reasonable approximation, although the period over which such measurements have been

made is admittedly short in comparison with the residence time of water in the deep ocean.

Both salt and dissolved oxygen are treated as conservative properties, meaning that there are no sources or sinks below the naviface. In the case of dissolved oxygen this is obviously not strictly true. Phytoplankton concentrated in the upper 100-200 m provide a source of oxygen, and decaying organic matter throughout the water column acts as a distributed sink. Below the euphotic zone the net effect is equivalent to a weak sink, the strength of which is not well known. Wright (1969) quoted deep O_2-depletion rates of $4.3 - 53.0 \times 10^{-4}$ ml/l per year; data collected on the 1969 GEOSECS test station suggest an average rate of 25×10^{-4} ml/l per year (Craig and Weiss, 1970). The time scale of the deep circumpolar flow is roughly 20 years. At an average depletion rate of 25×10^{-4} ml/l per year, changes in oxygen-concentration due to the sink term would amount to 0.05 ml/l over 20 years. This change is small compared with the probable error of the oxygen data.

The third fundamental assumption behind the analysis is that large-scale flow in the ocean tends to take place along surfaces of uniform potential density or potential steric anomaly. Because of geostrophy, such surfaces often have a small ($< 1:10^3$) slope relative to level (*i.e.*, uniform-depth) surfaces. Over oceanic scales, these small slopes may be significant, and it is therefore important to distinguish between surfaces of uniform depth and surfaces of uniform potential steric anomaly. Processes oc-

curring along the latter surfaces will be designated as "lateral" processes (*e.g.*, lateral mixing) as opposed to "horizontal" processes occurring on surfaces of uniform depth.

The degree to which the above assumption is valid cannot be stated quantitatively. If there were no diffusion or mixing in the ocean, this approximation would necessarily be an exact statement, since the potential steric anomaly of a fluid element is defined by its salinity and potential temperature, which are conservative properties in the sense stated previously. It does seem reasonable to assume that in a stratified system (such as the ocean) fluid elements are constrained somewhat to flow along, rather than across, surfaces of uniform potential steric anomaly. Ultimately, however, use of the assumption rests on empirical grounds (*e.g.*, Reid, 1965, Figure 3) and on the proven value of this model.

As a consequence of the third assumption, vertical advection is no longer a separate term in the diffusion equation, having been absorbed in the lateral advection terms. At this stage the model has been reduced to a balance between lateral advection and diffusion. In the large-scale physical processes of the ocean, molecular diffusion is negligible compared with turbulent diffusion, or mixing, which represents the gross effect of the fluctuating advective terms on the mean field. Turbulent mixing is customarily decomposed into vertical and lateral components.

In studies like the present one it is often assumed (at least tacitly) that vertical mixing is of secondary importance compared

with lateral mixing. This assumption is probably due to the heavy emphasis placed on lateral mixing by Rossby (1936, 1937), Montgomery (1938), and others who developed the method used here. In most cases, such an assumption is not inconsistent with the distributions of properties in the open ocean. On the other hand, even in those studies where lateral mixing is assumed to predominate there may be regions where the observed patterns can be explained only in terms of vertical mixing. That is, on the particular surface in question, there is no source of water with the characteristics necessary to produce the observed distributions.

Theoretical studies are of little assistance in deciding whether lateral or vertical mixing should predominate. The large-scale oceanic distributions are matched equally well by models containing (1) only vertical mixing (Robinson and Stommel, 1959), (2) only lateral mixing (Sverdrup, 1939), or (3) no mixing at all (Welander, 1959). Some of the confusion is no doubt due to our imperfect understanding of the mechanisms involved in turbulent mixing, and the consequent use of rather arbitrary mathematical functions to represent the mixing terms. In the present work I am not concerned with the analytical form of the mixing terms but only with the qualitative effects of mixing. The relative importance of vertical and lateral mixing is determined from the observed distributions. Except in a few cases where vertical mixing is clearly important, the distributions are assumed to represent a balance between lateral mixing and lateral advection,

with the mean flow taking place along the isopleths.

Three sets of maps have been drawn for this study. The first two sets show the salinity, concentration of dissolved oxygen, and depth of the surfaces where potential steric anomaly equals 50 and 30 centiliters per ton[3] (abbreviated cl/t). Potential steric anomaly, δ_θ, is defined by the following equation:

(1) $$\delta_\theta = \alpha_{s,\theta,0} - \alpha_{35,0,0}$$

where $\alpha_{s,\theta,0}$ = specific volume of sea water of salinity s, potential temperature θ, at sea pressure 0 db; potential temperature is the temperature a sea water sample would have after being raised adiabatically to the naviface (p = 0);

and $\alpha_{35,0,0}$ = specific volume of sea water of salinity 35‰, potential temperature 0°C, sea pressure 0 db,

= 0.97264 ml/g.

Surfaces of uniform potential steric anomaly will be called isanosteric surfaces.

C.-G. Rossby appears to have been the first to use the distribution of a conservative property along a surface of uniform potential density to deduce geophysical circulation patterns.

---

[3] These surfaces correspond to potential density surfaces σ_θ = 27.60 and 27.81 g/l, respectively.

The method was applied to the atmosphere by Rossby and collaborators (1937), who used specific humidity as a tracer on surfaces of constant potential temperature (isentropic surfaces).

Because of the transient nature of even the large-scale atmospheric motion, isentropic analysis, as it was called, has not found much application in synoptic meteorology. However, the concept has proven valuable in studies of the ocean, where, as I noted earlier, the large-scale circulation is reasonably steady.

The earliest oceanographic applications of Rossby's technique were by Parr (1938) and Montgomery (1938). Parr discussed the distribution of salinity on several surfaces of uniform σ_t ($\sim$ potential density) south of Newfoundland. Montgomery made a detailed study of the circulation in the tropical North Atlantic using the distributions of salinity and dissolved oxygen on six σ_t-surfaces. Montgomery chose to call the method isentropic analysis in conformity with meteorological usage. This terminology is still commonly seen. In view of the fact that isanosteric surfaces (or surfaces of uniform σ_t) are not in general isentropic surfaces, the expression "isanosteric analysis" suggested by Tsuchiya (1968) may be more appropriate.

Notable applications of isanosteric analysis have been made in recent years by Taft (1963), whose maps of salinity and dissolved oxygen at intermediate depths cover the southern hemisphere; Reid (1965), who examined the intermediate waters of the Pacific; Tsuchiya (1968), who studied the tropical Pacific; and Barkley

(1968), who has prepared an atlas of the Pacific Ocean.

All the above studies have used isanosteric surfaces which are confined to the shallow and intermediate layers of the ocean. When surfaces which extend to great depth (as in the present work) are used, an additional complication is introduced. The problem is caused by a rather subtle effect pointed out by Montgomery (1937) some time ago, but generally ignored until quite recently (Lynn and Reid, 1968). The compressibility of sea water is a function of its temperature, cold water being more compressible than warm. As a consequence, two fluid elements of equal steric anomaly, but different temperatures, at the naviface will have different steric anomalies if both are moved adiabatically to some depth, say 2000 m. In other words, fluid elements which could mix laterally at the naviface could not do so at 2000 m. The implication is that a single isanosteric surface does not define a surface of lateral advection and mixing at all depths.

Necessary conditions for the above effect to be important are that the temperature range on the isanosteric surface be significant (2-3°C) and that the isanosteric surface undergo large variations in depth (> 2000 m). In the case of the 30-cl/t surface, the depth range is large ($\sim$ 2500 m), but the temperature range is small (< 1°C) over the region where most of the variation in depth occurs. The largest temperature gradients are found near Antarctica, where the 30-cl/t surface is shallow and pressure effects are not significant. Similar conditions obtain on the 50-cl/t surface. It therefore appears that

the errors introduced by using a single isanosteric surface to represent a surface of lateral advection and mixing are not serious in this particular study.

In the antarctic, the water below the 30-cl/t surface is extremely uniform with respect to density. Small measurement errors or interpolation errors lead to substantial errors in computing the characteristics of deeper isanosteric surfaces. Therefore, isanosteric analysis is not useful for studying the water near the bottom.

The third set of maps prepared for this paper shows the distributions of potential temperature, salinity, and dissolved oxygen near the sea floor. Data were plotted only in regions where the depth of water exceeds 3500 m. With few exceptions the samples are within 300 m of the bottom; the great majority are within 200 m of the bottom.

Deacon (1937) and Wüst (1938) have prepared circumpolar maps of bottom potential temperature in depths greater than 4000 m. These maps were based on a much sparser data grid than is now available. Gordon (1966) plotted maps of bottom potential temperature and dissolved oxygen in depths greater than 3000 m for the sector 20°W to 170°W. The bottom salinity and dissolved oxygen maps presented in the present paper are the first such maps to be drawn for the entire circumpolar zone.

I.D. Data Processing and Quality Control

The bulk of the data used in this study was acquired from the

National Oceanographic Data Center (NODC), Washington, D. C. Additional data have been acquired from various sources shown in Table 1, which lists the data by ship in chronological order. Over three-quarters of the stations were taken by three ships: *Eltanin* (41%), *Discovery* (27%), and *Ob'* (9%). All but three of the stations are Nansen casts, the exceptions being *Eltanin* S-T-D stations.

Figure 2 shows the geographical distribution of stations for the isanosteric maps, and Figure 9 shows the distribution of stations for the bottom maps. Most, but not all, of the bottom stations were used in the isanosteric maps too. Note the rather sparse coverage of the central Indian Ocean.

Approximately 75% of the stations were occupied during the six months November-April, with 50% of the total being occupied in the three months January-March, the austral summer.

The hydrographic data were processed on The Johns Hopkins University Computing Center IBM 7094. Potential temperature and potential steric anomaly were computed using equations from Fofonoff (1962a). Linear interpolation was used to determine the values of parameters on the 50- and 30-cl/t surfaces. All data were plotted and contoured by hand on polar sterographic maps of scale $1:15 \times 10^6$. Bottom topography, Figure 1, was taken from U. S. Naval Hydrographic Office charts H.O. 16, 892-1 (1959) and H.O. 1262A and from the Soviet Atlas Antarktiki (Tolstikov, 1966). In order to avoid crowding on the smaller-scale maps

TABLE 1. Sources of data.

SHIP	NATION	YEARS	TOTAL STATS.	BOTTOM STATS.	DATA SOURCE
Meteor	Germany	1925-26	32	11	1
Discovery	Gt. Brit.	1931-39 1951	240	39	1
Thorshaven	Norway	1934	1	0	1
Galathea	Sweden	1952	1	1	1
Ob'	USSR	1956-63 1965-66	78	8	1
Capitan Canepa	Argen.	1957-59 1962	10	4	1
Horizon	US	1957	5	1	1
San Martin	Argen.	1958	1	0	1
Operation Deep Freeze: various Navy & Coast Guard icebrkrs	US	1957-61 1964 1967	22	0	1
Atlantis	US	1959	6	4	2
Vema	US	1959-60	6	3	1
Argo	US	1960-61 1962	5	4	1
Diamantina	Austral.	1960-62	15	4	1
Gascoyne	Austral.	1961	6	0	1
Umitaka-Maru	Japan	1961-62	21	0	1
Africana II	S. Africa	1962-64	8	0	1
Eltanin	US	1962-67 1967 1968 1970	362	208	1 3 4 5

TABLE 1. (continued)

SHIP	NATION	YEARS	TOTAL STATS.	BOTTOM STATS.	DATA SOURCE
Anton Bruun	US	1964	2	0	1
Glacier (IWSOE)	US	1968-69	22	5	6
Hakuho-Maru	Japan	1969	18	14	7
T. Washington	US	1969	21	14	8
			882	320	

1. National Oceanographic Data Center
2. Fuglister (1960)
3. Cruises 28, 29 (Scorpio Expedition): SIO/WHOI (1969)
4. Cruises 32-36: Jacobs *et al.* (1970)
5. Cruise 41: author (unpublished data)
6. International Weddell Sea Oceanographic Expedition: Hufford & Tennyson (1970)
7. Tokyo University Ocean Research Inst. (1970)
8. Piquero Expedition: SIO (unpublished data)

presented here, only station positions have been plotted.

Data quality and quality control are extremely important considerations in a study of this type, for they determine the resolution and reliability of the contours. The precision of routine shipboard temperature and salinity measurements has been well established by accumulated experience and by statistical analyses of results (see, for example, Wooster and Taft, 1958). Reversing-thermometer measurements are accurate to better than 0.02°C. Salinities determined by chlorinity titration are generally good to within 0.02 ‰, although greater precision can be achieved by taking special precautions, as in the case of *Meteor* salinities. Salinities measured with electrical conductivity salinometers[4] are significantly more accurate than those done by titration. Cox (1965) states a precision of 0.002 ‰ for these instruments. In routine use the reliability is probably somewhat less, perhaps 0.004 ‰.

The reliability of the dissolved-oxygen determinations is difficult to estimate. Nearly all methods for determining the concentration of dissolved oxygen in sea water are based on the Winkler method. Under optimum conditions this method may achieve an accuracy of 0.1% (Carpenter, 1965). However, as Carritt and Carpenter (1966) have demonstrated, numerous variations in analytical technique among oceanographic institutions and individual chemists make it impossible to establish the routine reliability

---

[4] Virtually all the salinity data since 1962 (about half of the total) were measured by this method.

of oxygen data. Wide variations in quality may be expected.

Of particular significance to this study are the oxygen measurements made during the *Discovery* cruises. Several authors (Wooster and Volkmann, 1960; Gordon, 1966; Carritt and Carpenter, 1966) have noted that these measurements are consistently lower than those made by other ships in the same vicinity. The discrepancy has been reported to be on the order of -0.5 ml/l by Gordon (1966) and Carritt and Carpenter (1966).

The present author has made numerous comparisons between the *Discovery* dissolved-oxygen data and those of other ships at the same depth and approximate geographical location. The consistent difference observed by others was confirmed. The possibility of a long-term increase in dissolved-oxygen concentration was ruled out by the fact that *Discovery* values were also lower than *Meteor* (1925-26) data, and that no trend in oxygen concentration was observed in the *Discovery* data, which were taken over a ten-year period.

Unfortunately, the raw *Discovery* data were destroyed in World War II, and it is not possible to determine and correct the error properly. I decided to devise a correction curve by comparing the measured navifacial oxygen concentration with the saturation value appropriate to the measured navifacial temperature and salinity. The resulting linear best-fit shown in Figure 32 was used to correct all *Discovery* oxygen data. The correction is proportional to the dissolved oxygen concentration, ranging from + 0.2 ml/l at a measured value of 4.0 ml/l to + 0.4 ml/l at 7.0 ml/l.

A similar trend (increasing error with concentration) was observed from the comparison of deep *Discovery* oxygen measurements with those of other ships. However, the corrections derived by extrapolating those comparisons are somewhat larger than those found from the navifacial-concentration/saturation-value method. The differences between the two methods might be partly accounted for by the fact that antarctic navifacial waters are commonly supersaturated (Jacobs and Amos, 1967), leading to an underestimate of the naviface-measurement error. On the whole, it was felt that the naviface-comparison method was a more reliable correction procedure, since it was based on a wider range of data points. It is likely, however, that the corrected *Discovery* oxygen data are still, on the average, lower than neighboring points from other ships.

Aside from the systematic correction applied to all *Discovery* dissolved-oxygen data, no corrections were made to the original data. Questionable points were evaluated, and occasionally eliminated, on the basis of the following objective and subjective criteria:

(1) agreement with neighboring points on the same surface, and consistency of vertical profile;

(2) method of making measurement;

(3) general reliability of data from the particular ship or cruise in question.

The "general reliability" test was based on repeated comparisons of stations from several ships in close proximity to each

other. As a rule, these comparisons showed good agreement among the data of different ships. The notable exception (in addition to the *Discovery* oxygens) was the *Ob'* salinity measurements, which contain more scatter than those of other ships. Since most of the *Ob'* stations used are close to the Antarctic continent, where the lateral gradients are relatively strong, this scatter is not serious.

II. THE 50-cl/t SURFACE

The 50-cl/t isanosteric surface was chosen for analysis because it forms what might be considered the upper boundary of the deep water mass being studied here. It is recognized that the definition of such a boundary must be somewhat arbitrary, being based on gradients in the characteristics which distinguish each water mass.

Perhaps the most fundamental and unambiguous of these characteristics is salinity. South of about 55°S, the 50-cl/t surface lies within the sharp halocline which marks the transition from the fresh upper waters of the antarctic to the more saline deep water. North of about 50°S (the "Antarctic Convergence"), the 50-cl/t surface is found between the salinity minimum (Antarctic Intermediate Water) at 80 cl/t and the deep salinity maximum (Circumpolar Deep Water) at 30 cl/t (see Figures 18, 20).

Over much of the antarctic region (indeed, over a large part of the southern hemisphere), the 50-cl/t surface coincides with the vertical minimum of dissolved oxygen (see Figures 16, 19, 21). This relationship persists from the subtropics to about 60°S, except in the eastern South Atlantic, where the two coincide between roughly 30°S and 50°S. In this respect the 50-cl/t surface again provides a convenient boundary between the upper and intermediate waters and the deep water, all of which have higher dissolved-oxygen concentrations.

II.A. Depth

The depth of the 50-cl/t surface (Figure 3) ranges from less than 100 m near Antarctica to more than 1600 m at about 40°S. During the summer season, this isanosteric surface lies below the naviface everywhere except in some parts of the Ross and Weddell seas. The data used in this study show the 50-cl/t surface intersecting the naviface at several stations along the western side of the Ross Sea and at two stations very close to the western and southern boundaries of the Weddell Sea. Only two years' (1968, 1969) summer data are available for the Weddell Sea, and it is not known how representative they are of general conditions there. In the Ross Sea, on the other hand, numerous stations have been occupied by U. S. icebreakers over the past fifteen years. These data show that navifacial steric anomaly values less than 50 cl/t are not uncommon in the southeastern and western portions of the Ross Sea. It appears that the 50-cl/t surface frequently intersects the naviface in the interior of the Ross Sea during summer. In view of the similarity of climatic conditions in the Ross and Weddell seas, it is not unlikely that this situation occurs intermittently in the extreme reaches of the Weddell Sea too.

The only winter observations from either of these areas were taken by the *Deutschland* in the Weddell Sea in 1912. These stations show navifacial steric anomaly values well below 50 cl/t (but above 30 cl/t) occurring throughout the central Weddell Sea.

Indirect evidence of winter conditions is provided by the very cold water (Winter Water, Mosby, 1934) which is observed just below the thin navifacial mixed layer near the Antarctic continent in summer. This water, which is the remnant of the homogeneous navifacial layer formed in winter, has the following characteristics: $\theta < -1.0°C$, $S \geq 34.3$ ‰, $\delta_\theta < 50$ cl/t. Therefore, it is highly probable that in winter the 50-cl/t surface intersects the naviface several degrees from the coast all around Antarctica.

The depth contours of an isanosteric surface provide a qualitative representation of the large-scale geostrophic circulation. The dominant pattern evident in the contours of the 50-cl/t surface is the quasi-zonal, eastward-flowing Antarctic Circumpolar Current. In most longitudes the zonal flow occupies a band of latitude some 10° - 15° in width, as defined by the distance between the 200-m contour and the 1400-m contour in the Atlantic and the 1600-m contour in the Indian and Pacific oceans. However, in several places the flow constricts tightly to a width of about 5°, indicating significantly increased velocities in these areas. Such constrictions occur in Drake Passage, across the Macquarie Rise, and north of the Ross Sea at 145°W.

The first two of these constrictions are obviously forced by contractions of the lateral boundaries of the flow, but the constriction north of the Ross Sea cannot be explained in terms of lateral boundary effects. Gordon (1967b) has stated that the flow pattern here is caused by the "channelling" effect of the

fracture zone (called by Gordon the USARP fracture zone) which cuts across the Pacific-Antarctic Ridge at 140°W. Although the fracture zone may play some part in constricting and turning the flow north of the Ross Sea, it is difficult to believe that such a striking change in the flow could be caused by this relatively small topographic feature.

In all of the places where constrictions of the flow occur, and over the Scotia Ridge too, wave-like distortions of the zonal flow are observed. These features are in approximately the same positions as those noted by Sverdrup *et al.* (1942).

Close to the antarctic coast there is a tendency for the 50-cl/t surface to deepen slightly toward the south. The reverse slope, which is most pronounced from 0° to 140°E, is indicative of westward flow along the coast. Deacon (1937) gave the name "East Wind Drift" to the shallow coastal current. The name suggests the probable cause of the westward flow near the coast: easterly winds prevail south of about 65°S. Barcilon (1966) has shown that such a current might be driven by the discharge of melt water from the antarctic ice cap. Even if this is not the case, significant seasonal variations in the coastal current due to changes in the sea-ice cover and melt-water runoff might be expected. For obvious reasons there are no observations to support or contradict such conjecture.

North of the eastward Circumpolar Current there is evidence of the anticyclonic subtropical gyres which dominate the low- and

middle-latitude circulation. The gyre stands out particularly well in the western South Pacific, where the 50-cl/t surface reaches its maximum depth of nearly 2000 m. The trough which marks the axis of the gyre runs along 49°S approximately. Strong southward flow along the eastern edge of the New Zealand Plateau closes the gyre to the west.

At shallower depths, the structure of the South Pacific gyre is rather different from that on the 50-cl/t surface. On Reid's (1965) map of the 125-cl/t surface (depth 500-700 m) the gyre encompasses a much larger area, and its axis lies to the north along 23°S. The western boundary of the gyre is found along the coast of Australia (the East Australian Current), and there is only a slight indication of southerly flow along the east coast of New Zealand. On Reid's 80-cl/t map the axis of the gyre has shifted south to about 40°S. At the depth of this isanosteric surface (1000-1200 m), New Zealand and the shallow plateau surrounding it form a major obstacle to the flow, and the subtropical gyre begins to divide into two gyres, one in the Tasman Sea and a larger one in the western South Pacific. A poleward boundary current is now clearly present east of New Zealand. Presumably, the ridges north of New Zealand serve to separate the two gyres even more at greater depths, leading to the well-defined closed gyre observed in the western South Pacific on the 50-cl/t surface.

In the Indian Ocean, only the western tip of the subtropical anticyclone appears on this map (near 35°S, 40°E). Associated

with the anticyclonic gyre is a complex eddy-like feature to the southwest. This appears to be produced by the shear between the intense westward Agulhas Current and the eastward Circumpolar Current. In the Atlantic Ocean too the map does not extend far enough north to show much of the subtropical gyre. However, the poleward western boundary current can be seen along the east coast of South America between 35°S and 42°S.

In addition to the anticyclonic gyres normally associated with low- and middle-latitude wind-driven circulation in the oceans, there is also a somewhat anomalous gyre south of Australia. North of the elongated trough centered on roughly 45°S, the 50-cl/t surface shoals, indicating a return flow to the west. Although this feature is evident even in the earliest antarctic sections (*e.g.*, Deacon, 1937, PL. XIX), there is no mention of it in the literature.

Systematic hydrographic work in the Australian Bight has only recently been started, and data are still rather sparse. Bye (1968) has discussed some of the characteristics of the westward flow, which he called the Flinders Current. According to Bye, the average westward transport of the Flinders Current is $20 - 30 \times 10^6$ m^3/s. Most of this water comes around the southern tip of Tasmania, Bass Strait being too shallow to permit a significant flux. The water transported to the west must represent a mixture of water brought from the north by the East Australian Current and antarctic water deflected north by the New Zealand Plateau.

The circulation in the Australian Bight is complex. Prominent meanders are present at 132°E and 115°E. In Bye's report, these areas are marked by large-scale eddies. More data will be required to resolve the structure of the circulation in this region.

II.B. Salinity

Salinity on the 50-cl/t isanosteric surface (Figure 4) ranges from 34.28 ‰ to 34.62 ‰ , a difference of 0.34 ‰ . The range of potential temperatures which corresponds to the salinity range for δ_θ = 50 cl/t is -1.2°C to 3.1°C. At the melting point, water of δ_θ = 50 cl/t has the characteristics θ = -1.86°C, S = 34.26 ‰ .

The salinity distribution, like the flow, is predominantly zonal, with values increasing from south to north. Perhaps the most striking aspect of the circumpolar salinity distribution is its separation into two distinct bands, a southern one in which the salinity gradient is comparatively steep, and a northern one in which the gradient is much smaller. Roughly speaking, the 34.52- ‰ isohaline marks the boundary between the two zones. In the Atlantic and western Indian oceans this isohaline follows the 50°S parallel. Continuing around Antarctica toward the east, the 34.52- ‰ isohaline shifts toward the south, eventually reaching about 60°S in the eastern South Pacific.

The steep salinity gradient is found south of the 34.52- ‰ isohaline. The gradient is generally confined to a narrow band approximately 5° of latitude in width. Except in the Ross and

Weddell seas, where large areas of uniformly low-salinity water occur, the gradient is contiguous to the antarctic coast.

Near the coast, the 50-cl/t surface lies just below the shallow layer of fresh, warm water which forms as the sea ice recedes in summer. Vertical mixing with the navifacial layer provides low-salinity ($\sim$ 33.9 ‰) water which mixes along the 50-cl/t surface with more saline water from the north, producing the observed gradient. In winter, the character of the salinity gradient is probably not significantly altered, for the 50-cl/t surface intersects the naviface where salinities are less than 34.0 ‰ (Gordon and Goldberg, 1970, PL. 3).

Relatively fresh water formed at the naviface in summer flows out of the Weddell Sea toward the north and east. Northward flow occurs east of the South Orkney Islands and along the western side of the South Sandwich Islands. These two outflows combine to form the low-salinity tongue surrounding South Georgia.

The cyclonic Weddell Sea gyre is evidenced by the low-salinity tongue projecting toward the east along roughly 62°S. Return flow near the coast is indicated by the westward penetration of more saline water. The anomalously diffuse appearance of the salinity gradient to the east of the Weddell Sea is probably due to the gyral circulation.

A second major source of low-salinity water along the antarctic coast is found in the eastern Ross Sea. This water propagates toward the northwest, splitting into two branches near 70°S, 180° . One branch continues toward the northwest, extending past the

Balleny Islands as far as 57°S, 145°E. The other tongue of low-salinity water flows northeast parallel to the Pacific-Antarctic Ridge.

The sharp bend in the isohalines at 55°S, 145°W coincides with the abrupt change in direction of the circumpolar flow noted on the depth map. After crossing over the Pacific-Antarctic Ridge, the Circumpolar Current flows east toward Drake Passage. There is a tendency for some of the water to recirculate into the Ross Sea, although the gyre is not as well developed as in the Weddell Sea.

Somewhat higher salinities (> 34.32 ‰ , reaching 34.34 ‰) than those found in the eastern sector of the Ross Sea are present in the central and western sectors. This is true throughout the water column (Countryman and Gsell, 1966, Figure 17), not just at 50 cl/t. The higher salinities must be the result of local processes taking place within the Ross Sea, since the water flowing into the Sea is of lower salinity.

The low-salinity tongue extending northward to the east of the Kerguelen Ridge appears to indicate outflow from MacKenzie Bay and the Davis Sea.

The abrupt transition from the high-gradient to the low-gradient band is explained by noting that the 34.52- ‰ isohaline generally lies just to the south of the steepest slope of the 50-cl/t surface. According to the geostrophic relation, the steep slope marks the high-velocity core of the Antarctic Circumpolar Current. The increased lateral shear and zonal transport associated with the velocity core quickly smear out the lateral

salinity gradient, leading to a uniform salinity distribution to the north.

Within the uniform circumpolar band, salinities range from 34.52 ‰ to about 34.58 ‰. The high-salinity water required to maintain these values comes from two principal sources: the western South Atlantic and the western Indian oceans. The first source shows clearly as a tongue of high salinity extending poleward along the east coast of South America. Near 40°S, the high-salinity water mixes with lower-salinity water which flows northward around the east coast of the Falkland Islands. The resulting mixture ($S \sim 34.56$ ‰) then flows east in the Circumpolar Current.

The Indian Ocean source is inferred from (1) the saline water to the south and southeast of Africa, (2) the salinity distribution on Taft's (1963) 60-cl/t map, and (3) the very high salinity values found on the 50-cl/t isanostere in the western Indian Ocean section of Clowes and Deacon (1935). The high-salinity water is evidently derived from North Indian Deep Water which flows south in the western Indian Ocean.

Salinity in the Pacific Ocean north of 60°S is exceedingly uniform. Fortunately, all the data plotted in this region were taken by electrical salinometer. Therefore, the small variations that are observed may be used with confidence to trace the circulation. The anticyclonic flow around the subtropical gyre is marked by a broad northward displacement of the 34.56- ‰ isohaline centered on 120°W. Further to the east, salinity increases slightly, suggesting slow poleward flow along the west coast of South

America. A similar trend (although less well defined because of the lower precision of the data) is evident on Taft's (1963) 60-cl/t map.

A distinct tongue of low-salinity water can be seen entering the eastern Tasman Sea from the south and then curving in an anticyclonic sense. This pattern is consistent with the deflection of the Circumpolar Current indicated by the 50-cl/t depth map.

The salinity distribution in the Australian Bight is confusing. High-salinity water is present at either end of the continent, but the two regions are separated by a well-defined zone of slightly lower salinity between 130°E and 135°E. This is the region where a large cyclonic meander appears on the depth map. There are insufficient data in the northern half of the Bight to be conclusive, but one possible interpretation is that the circulation consists of two large eddies, a cyclonic one to the west of Tasmania and an anticyclonic one near 120°E. These eddies would transport low-salinity water north into the center of the Bight.

II.C. Dissolved Oxygen

The dissolved oxygen distribution on the 50-cl/t surface (Figure 5) is remarkably consistent with the salinity distribution. In particular, the division into two distinct gradient bands observed in the salinity map also occurs in the oxygen distribution. The 4.5-ml/l oxypleth will be taken as the approximate boundary between the two bands.

South of the 4.5-ml/l oxypleth, the dissolved oxygen concentration increases rapidly. Values exceeding 7.5 ml/l are found nearly everywhere along the coast, except to the west of the Antarctic Peninsula, where the dissolved-oxygen concentration does not reach 6.0 ml/l.[5] Maximum values (> 8.0 ml/l) are found in the southwestern corner of the Ross Sea. Typically, the high-gradient zone is 5° in width, although it is substantially broader east of the Weddell and Ross seas.

In the Indian and Pacific oceans, the dissolved-oxygen values decrease monotonically toward the north away from the high-gradient band. Concentrations of less than 4.0 ml/l are observed along the northern limit of the maps in both oceans. In the Atlantic Ocean, the concentration of dissolved oxygen reaches a minimum of about 4.0 ml/l along 45°S, then increases toward the north.

Earlier it was pointed out that the 50-cl/t surface coincides with the vertical minimum of dissolved oxygen over much of the antarctic. Gordon (1967b) also noted the widespread oxygen minimum, which he identified with the upper Circumpolar Deep Water. Gordon attributed the minimum to depletion by biological activity in low latitudes of the oxygen-rich North Atlantic Deep Water. However, it is clear from Figure 5 that the water flowing south along the east coast of South America is substantially richer in dissolved oxygen than the water in the lateral minimum. The min-

---

[5] This may be due partly to the scarcity of data in this region, especially in the Bellingshausen Sea, where heavy ice is always encountered.

imum cannot be due to the gradual consumption of oxygen in the North Atlantic Deep Water as suggested by Gordon. The source of the oxygen minimum is the oxygen-poor water (< 3.2 ml/l) found along the west coast of South America (see Barkley, 1968, Figure 106). This water flows south and mixes with the circumpolar water in Drake Passage. The low-oxygen water flowing eastward out of Drake Passage stands out as a lateral minimum across the South Atlantic on the 50-cl/t surface and also in the Drake Passage and Greenwich Meridian oxygen sections, Figures 14, 16. Minimum values in the low-oxygen core in the South Atlantic are: Drake Passage - 3.87 ml/l, 45°W - 3.84 ml/l, Greenwich Meridian - 3.90 ml/l.

Off the tip of South Africa additional oxygen-poor water mixes with the eastward-flowing Circumpolar Current. The low-oxygen water which appears as a tongue along 20° - 25°E originates in the North Indian Ocean (Clowes and Deacon, 1935). This water is transported southward along the east coast of Africa, and it feeds the circumpolar flow via the complex eddy observed on the depth map. The effect of this water is offset by mixing with water from the Weddell Sea gyre, which transports high-oxygen water eastward along 60°S. As a result, oxygen values in the uniform circumpolar belt do not change significantly south of Africa.

High-oxygen water from the Weddell Sea can be seen flowing north into the Scotia Sea along the same paths followed by the low-salinity water. Once again these tongues merge to form a

prominent tongue which extends past South Georgia.

A high-oxygen tongue along 90°E marks the outflow from MacKenzie Bay and the Davis Sea. MacKenzie Bay is the third largest indentation in the antarctic coast, so it is not surprising to find it acting as a source of oxygen-rich, low-salinity water similar to that originating in the Ross and Weddell seas.

In the Ross Sea, the dual tongues of low salinity are matched by a divided tongue of high-oxygen water. High values extend northwest past the Balleny Islands and northeast along the Pacific-Antarctic Ridge. The weak cyclonic gyre north of the Ross Sea is again evident.

The anticyclonic gyre in the Pacific may be discerned in the northward penetration of relatively high-oxygen water along 120°W. The southward dip of the oxypleths adjacent to the eastern edge of the New Zealand Plateau represents poleward transport in the western boundary current.

The deflection of part of the Circumpolar Current into the Tasman Sea shows up in the high-oxygen tongue reaching as far as 42°S. Oxygen values in the Australian Bight are very uniform. Those in the eastern end off Tasmania tend to be slightly higher than those in the west. However, the differences are too small to allow any conclusions to be drawn regarding the flow.

III. THE 30-cl/t SURFACE

In the Antarctic Ocean the 30-cl/t isanosteric surface lies within the deep salinity-maximum layer nearly everywhere (see Figures 13, 17, 18, 20). The principal exceptions are the areas surrounding the Ross and Weddell seas, where the salinity maximum is 400-600 m deeper than the 30-cl/t surface. This is to be expected, since both regions are sources of dense, low-salinity water [6] which alters to a significant degree the distributions around them. As the Ross and Weddell sea waters mix with the saline water from the north, the salinity maximum is eroded and forced to greater depth.

The deep salinity maximum is a wide-spread feature of the world ocean. Originating in the North Atlantic, the highly saline deep water can be traced through the South Atlantic, across the Indian Ocean south of about 30°S, and into the Pacific Ocean as far as 40°S. The fact that the salinity maximum coincides with the 30-cl/t surface over such a large area of the ocean makes this isanosteric surface of particular interest. At the same time it provides support for the original assumptions upon which this analysis is founded.

III.A. Depth

The 30-cl/t surface ranges in depth from about 200 m in the Ross and Weddell seas to more than 3500 m in the central South Pacific

---

[6] The high-salinity Ross Bottom Water is much denser than 30 cl/t and does not mix with the deep water. See Figure 33.

(Figure 6). In the Atlantic and Indian oceans, the maximum depth of the 30-cl/t surface is slightly over 2500 m. At none of the stations used in this study does the 30-cl/t surface intersect the naviface. It was pointed out earlier that the *Deutschland* Weddell Sea stations show navifacial steric anomalies greater than 30 cl/t even in mid-winter. It is probable that this isanosteric surface lies below the naviface throughout the year, although it may be shallower in winter than in summer.

In addition to the shallow plateaus surrounding New Zealand and the Falkland Islands, there are several mid-ocean regions where the entire water column has a potential steric anomaly greater than 30 cl/t. In such places the 30-cl/t surface intersects the sea floor, which acts as a barrier to flow along the surface.

In high latitudes there is a close resemblance between the flow on the 30- and 50-cl/t surfaces. The large-scale deflections of the zonal circumpolar flow associated with topographic features are found in the same places on both surfaces. Weak cyclonic gyres in the Ross and Weddell seas are evident in the topography of the 50-cl/t surfaces and to an even greater degree in the 30-cl/t surface.

One high-latitude feature which stands out on the 50-cl/t surface but can not be seen on the 30-cl/t surface is the antarctic coastal countercurrent (East Wind Drift). This fact provides an indication of how shallow the countercurrent is, since the 30-cl/t surface is only 300 m below the naviface near the coast.

A narrow trough in the 30-cl/t surface runs along roughly 43°S south of Australia. While the topography of the isanosteric surface indicates anticyclonic relative motion, the absolute sense of flow can not be determined from this evidence alone. This question will be resolved by examining the distributions of properties.

The small cyclonic eddy south of Africa appears, like its counterpart on the 50-cl/t surface, to be related to the shear between the westward-flowing Agulhas Current and the eastward Circumpolar Current.

In lower latitudes the topographies of the 30- and 50-cl/t surfaces do not match as well as they do in the circumpolar belt. The subtropical anticyclone in the South Pacific, which is so clearly defined on 50 cl/t, is completely absent on 30 cl/t. In view of the great depth of the 30-cl/t surface in this region, it is not surprising that the subtropical gyre is not evident.

While the subtropical gyre is not present, there is an indication of a boundary current along the New Zealand Plateau. Stommel and Arons (1960) have predicted from a model of the abyssal circulation that a northward-flowing deep boundary current exists in the western South Pacific Ocean. Recent field work (Reid *et al.*, 1968) has confirmed the existence of the current and suggests a transport of $8 - 12 \times 10^6$ m^3/s. In the present work, the deep current is reflected not only in the slope of the 30-cl/t surface but also in the distributions of salt and oxygen on that surface and in the distributions in the bottom layer.

There is no indication of the subtropical gyre in the Indian Ocean south of 35°S. However, the data are scarce, and the gyre may still persist at this depth. In the Atlantic, the gyre does show up as a narrow trough centered on 40°S.

III.B. Salinity

The total range of salinity on the 30-cl/t isanosteric surface is from 34.56 ‰ in the Ross and Weddell seas to 34.92 ‰ in the western South Atlantic Ocean (Figure 7). Over most of the map, however, the salinity range is much smaller, about 34.68 - 34.80 ‰ , a difference of only 0.12 ‰ . Potential temperature on this surface decreases from 3.4°C in the north to -0.8°C near the Antarctic continent. Over most of the antarctic region, the meridional change in potential temperature is about 2°C. At the melting point, water with δ_θ = 30 cl/t has the characteristics θ = -1.87°C, S = 34.52 ‰ .

Three water masses with distinctly different salinities converge in the western South Atlantic Ocean. Extremely uniform Circumpolar Deep Water enters through Drake Passage in the west. The salinity of this water varies from 34.71 ‰ along the northern side of the Passage to 34.73 ‰ along the Antarctic Peninsula. After flowing through Drake Passage, the Circumpolar Deep Water continues east until it impinges on the Scotia Ridge, where it is forced to divide. Part of the water flows north out of the Scotia Sea through the passage between the Falkland Islands and

South Georgia, while the remainder flows east around the southern end of South Georgia. Low-salinity water from the former branch can be seen extending along the continental-shelf of Argentina and along the northern side of the Scotia Ridge.

Water of salinity lower than that of Circumpolar Deep Water enters the South Atlantic from the Weddell Sea. The outflow is marked by a tongue of fresh water ($S < 34.68$ ‰) centered on the South Sandwich Islands. The effects of this water on the salinity distribution can be detected as far north as 47°S.

In sharp contrast to the two water types flowing into the South Atlantic from the west and from the south is the highly saline North Atlantic Deep Water. In the tropics, water with salinity exceeding 34.90 ‰ is found between 2000 and 3000 m across the entire South Atlantic (see Fuglister, 1960, p. 61). Maximum salinities in the western trough are slightly higher (~ 0.02 ‰) than those in the eastern trough. Maximum salinities on both sides of the South Atlantic decrease toward the south, but those on the eastern side decrease more than those on the western side. At 32°S, the maximum in the western high-salinity core is about 0.06 ‰ greater than that in the eastern core (Fuglister, 1960, p. 57).

Near 35°S the western high-salinity core, which in lower latitudes is pressed against the east coast of South America, separates from the boundary. It mixes with the lower-salinity water from the south and joins the general eastward flow across

the South Atlantic along roughly 40°S. As it approaches the African coast, part of the deep water turns north in the subtropical gyre. The northward flow of this slightly diluted deep water (S = 34.80 - 34.84 ‰) probably accounts for the greater poleward decrease in salinity in the eastern South Atlantic relative to the western South Atlantic.

The deep water which does not turn north in the subtropical gyre continues east past the tip of Africa. This salty water shows up clearly in the northern end of the 20°E vertical section, Figure 17. Near 40°E the 34.80- ‰ isohaline turns abruptly to the north, indicating that the high-salinity water is flowing along the east coast of Africa. The abyssal model of Stommel and Arons (1960) predicts a northward-flowing deep boundary current in the western South Indian Ocean as well as in the South Pacific. At present the hydrographic coverage of this region is regrettably sparse, and the prediction of Stommel and Arons remains untested. The present map, however, suggests that such a current does exist.

Across the Indian sector of the antarctic the 34.76- ‰ isohaline marks the boundary between the salty deep water originating in the North Atlantic and the less saline Circumpolar Deep Water which flows through Drake Passage. Near 110°E the salty deep water shifts several degrees to the south before continuing eastward in a broad band across the Indian-Antarctic Basin. In this region, the vertical salinity maximum associated with the

30-cl/t surface develops into a lateral maximum which can be traced around the circumpolar belt as far as Drake Passage (see Figures 18, 20, 13). Maximum values in the high-salinity core are: 132°E - 34.755 ‰ , 170°W - 34.743 ‰ , Drake Passage - 34.739 ‰ , which represents a decrease of less than 0.02 ‰ in about 10,000 km.

The fact that a tongue develops in the salinity distribution south of Australia is due to the presence of relatively low-salinity water (< 34.74 ‰) in the South Australian Basin north of 40°S. The Tasman Sea is the only source of such water on this map. Thus, it appears that the deep flow in the South Australian Basin is westward, and the large gyre along 43°S is in fact anticyclonic. Transport calculations to be discussed in Section V indicate that the westward flow is extremely weak in the deep layers.

The northward loop in the 34.74- ‰ isohaline west of New Zealand indicates deflection of some of the circumpolar flow into the Tasman Basin. The rest of the Circumpolar Deep Water flows into the South Pacific and divides into two branches. A portion ($8 - 12 \times 10^6$ m^3/s, Reid *et al.*, 1968) turns to the north along the eastern edge of the New Zealand Plateau. This tongue of relatively high-salinity water marks the beginning of the deep western boundary current which was mentioned earlier. The deep water which flows north in the boundary current fills the entire deep Pacific, there being no sources of deep water in the North Pacific.

A northward transport of 10×10^6 m^3/s in the boundary current implies a residence time of about 10^3 years for water in the layer below 2000 m in the Pacific.

The bulk of the deep water flows eastward across the Pacific in the Circumpolar Current. This flow is marked by a thin, meandering tongue defined by the 34.74- ‰ isohaline. In the eastern South Pacific, water of salinity less than 34.70 ‰ moves southward along the coast of South America. Mixing between this water and Circumpolar Water produces the uniform deep water which enters Drake Passage and flows into the western South Atlantic.

Near the antarctic coast, the salinity distribution on 30 cl/t is much like that on 50 cl/t. Low-salinity water originating in the southwestern part of the Weddell Sea moves north along the Antarctic Peninsula and then east parallel to the South Orkney Islands. The very distinct tongue along 55° - 60°S shows that this water continues east as far as 20°E before turning south in the cyclonic Weddell Sea gyre.

Just to the east of Kerguelen Ridge low-salinity water extends northward from MacKenzie Bay and Davis Sea. In the Ross Sea two tongues of low salinity are again evident, one extending northwestward in the direction of Macquarie Island, the other eastward along the southern flank of the Pacific-Antarctic Ridge. The southward extension of the 34.74- ‰ isohaline along 135°E and the indentation of the 34.72- ‰ isohaline along 73°S provide further evidence of a weak cyclonic gyre in the Ross Sea similar

to that in the Weddell Sea. This feature stands out in the meridional salinity and dissolved-oxygen sections along 170°W, Figures 20, 21. The high-salinity, low-oxygen water between 500 and 1000 m near 73°S marks the westward return flow into the Ross Sea. (The return flow into the Weddell Sea is evident in the Greenwich Meridian potential-temperature section, Figure 15. Note the relatively warm water near 400 m at 65°S.)

III.C. Dissolved Oxygen

In the Atlantic and Indian sectors of the antarctic the distribution of dissolved oxygen (Figure 8) is distinguished by a lateral minimum (< 4.5 ml/l). This feature, like its counterpart on the 50-cl/t surface, originates in the eastern South Pacific, where low-oxygen water (< 4.2 ml/l) from the north mixes with higher-oxygen water (> 4.5 ml/l) in the circumpolar zone. The resulting mixture (4.3 ml/l < O_2 < 4.5 ml/l) flows into the western South Atlantic between oxygen-rich North Atlantic Deep Water and Weddell Sea water, both of which have concentrations well over 5.0 ml/l. The flow of Circumpolar Deep Water north into the Argentine Basin is indicated by the northward displacement of the oxypleths in this region.

As with salinity, the Circumpolar Deep Water and the North Atlantic Deep Water can be distinguished by their oxygen concentration across the Atlantic and Indian sectors. The difference in concentration weakens gradually toward the east. South of

Australia, the lateral minimum associated with the Circumpolar Deep Water and the weak maximum associated with the North Atlantic Deep Water merge into a broad belt of very uniform oxygen concentration.

Further evidence of westward flow in the South Australian Basin is provided by the oxygen-poor water (O_2 < 4.2 ml/l) north of 45°S. Low concentrations are also found in the Tasman Basin. The northward extension of the 4.5-ml/l oxypleth along 160°E is consistent with the deflection of part of the Circumpolar Current into the Tasman Sea.

In the Pacific Ocean, the oxygen concentration decreases monotonically from south to north. Northward flow along the western boundary of the South Pacific is indicated by the prominent tongue of relatively high-oxygen water along 165°W.

Dissolved-oxygen concentrations exceeding 5.0 ml/l occur along the antarctic coast from the Weddell Sea eastward to the Ross Sea. Maximum concentrations (> 7.0 ml/l) are found in the southwestern corners of the Ross and Weddell seas and in MacKenzie Bay. High-oxygen tongues extend from the Ross and Weddell seas along the paths followed by low-salinity water originating in these seas. However, the water in MacKenzie Bay has a rather modest influence on the oxygen distribution outside the Bay compared with the strong effect on the salinity distribution noted in the previous section.

IV. THE BOTTOM WATER

Because of the vertical homogeneity of deep antarctic waters, it is not possible to use isanosteric analysis below the 30-cl/t surface. However, it is possible to observe the circulation of abyssal waters in the horizontal distributions of sea-water properties near the ocean floor. The distributions of three such properties--potential temperature, salinity, and dissolved oxygen --have been mapped for this report. Approximately 320 data points were plotted for each map (see Figure 9 for station positions). All sample points are from depths greater than 3500 m, and all but a few are within 300 m of the ocean floor.

IV.A. Potential Temperature

The most commonly measured and mapped bottom-water characteristic is its temperature, or rather its potential temperature. I have already noted that maps of bottom potential-temperature, covering part or all of the circumpolar zone, have been prepared by Wüst (1933, 1938), Deacon (1937), and Gordon (1966). However, it seemed worthwhile to prepare a new bottom potential-temperature map both for the sake of completeness in this report and because the previous maps either were based on rather poor data grids (Wüst, Deacon) or covered only part of the antarctic region.

Before examining the map of potential temperature, the effect of geothermal heating on the temperature structure of the bottom water will be considered. Heat generated in the earth's

crust is conducted into the water layer above the sea floor. The geothermal flux has been measured at a number of locations in the Atlantic and Pacific oceans. Except over ocean ridges, where it may be somewhat larger, the flux F is uniform and of the order 10^{-6} cal/cm^{2}s (Bullard, 1963). To find out if this rate of heating will alter to an appreciable degree the thermal structure of near-bottom waters, a simple model of the circulation near the sea floor will be constructed.

Assume that a thin, vertically homogeneous layer of water ("bottom water") of thickness H flows over the floor of an ocean basin at a uniform speed U. Assume further that the vertical uniformity of the water is due to convective overturning caused by heating from below, and that no mixing occurs between the bottom water and water above it. What temperature change, ΔT, will occur as a water parcel moves along the basin floor?

The heat Q added to each water column of unit area as it moves a distance L is

$$Q = \frac{LF}{U} \quad .$$

Therefore, the downstream temperature gradient due to geothermal heating is

(2) $$\Delta T/L = \frac{Q/L}{\rho c H} = \frac{F}{\rho c U H} \quad ,$$

where ρ = density of sea water

c = specific heat.

The most difficult to determine of the above parameters is the homogeneous bottom-layer thickness, H (not to be confused with the Ekman boundary layer at the bottom). Few hydrographic stations with closely-spaced bottles near the bottom are available. Fortunately, some of the stations occupied during *Eltanin* cruises in the South Pacific Ocean (Cruise 28) and eastern Indian Ocean (Cruises 32 and 41) do have several bottles at 50 - 100 m intervals near the bottom. These indicate that the bottom few hundred meters of water are extremely uniform. A choice of 100 m, which is typical of the sampling level of the data used in this study, for H would appear to be conservative. The remaining parameters will be given the following values:

$$F = 10^{-6} \text{ cal/cm}^2\text{s}$$

$$U = 1 \text{ cm/s}$$

$$c = 1 \text{ cal/cm}^3 \text{ °C} .$$

From (2) the horizontal potential-temperature gradient due to geothermal heating is found to be 0.01°C/1000 km. Observed gradients (from Figure 10) are much larger: Atlantic-Antarctic Basin, 0.08°C/1000 km; Southwestern Pacific Basin, 0.14°C/1000 km; Pacific-Antarctic Basin, 0.27°C/1000 km. It appears that the geothermal flux does not significantly alter the distribution of potential temperature in the bottom water.

In the present map of potential temperature (Figure 10), as in the earlier ones by Wüst and Deacon, the most striking feature

is the extremely cold water (< -0.8°C) in the Weddell Sea. This water, which will be called Weddell Bottom Water, originates along the western shelf of the Sea, then flows east in a narrow tongue along the southern flank of the Scotia Ridge. Some of the Weddell Bottom Water enters the Argentine Basin through the deep South Sandwich Trench. This water continues to flow north along the western boundary of the Basin. According to Wüst (1933), antarctic deep water (Weddell Bottom Water) can be detected in the western trough of the Atlantic as far north as 40°N.

Some cold bottom water from the Weddell Sea also enters the Scotia Sea, probably through a passage (sill depth 3000 - 3500 m) near 61°S, 40°W (Gordon, 1966). A sharp horizontal gradient of potential temperature is found in the Scotia Sea. Reid and Nowlin (1971) suggest that the gradient is caused by the shielding effect of the ridge along 60°W, which allows Weddell Bottom Water to collect in the southwestern Scotia Sea. The strong flow of warm deep and bottom water in the Circumpolar Current is deflected northward by the ridge and is confined to the northern half of Drake Passage. The sharp potential-temperature gradient marks the boundary between the warm water from the Pacific Ocean and the cold water from the Weddell Sea.

It is evident from the distribution of potential temperature that a substantial part of the bottom water produced in the Weddell Sea continues to flow east along roughly 60°S. Water colder than -0.4°C fills the entire Atlantic-Antarctic Basin. The temperature

increases steadily from -0.8°C in the Weddell Sea to about -0.5°C along the western flank of Kerguelen Ridge. Mixing with warmer deep water accounts for most of the increase in temperature.

Although the flow of bottom water in the Atlantic-Antarctic Basin is primarily zonal, there is some northward flow through gaps in the mid-ocean ridge system. A major break in the ridge occurs near 50°S, 30°E, connecting the Atlantic-Antarctic and Agulhas basins. Wüst (1933, 1938) and Deacon (1937) showed water colder than 0°C penetrating past 40°S, whereas on the present map the 0°C-isotherm reaches only as far as 47°S. Generally speaking, the bottom water in the Agulhas Basin seems to be somewhat warmer than Wüst and Deacon indicated. The distribution of potential temperature in the Agulhas Basin shown in Figure 10 suggests a weaker antarctic influence than would be inferred from the earlier maps.

The Kerguelen Ridge, which separates the Atlantic-Antarctic Basin from the Indian-Antarctic Basin, is very shallow. From 47°S to 62°S the sill depth is less than 2000 m. The only notable passage through which bottom water from the Weddell Sea can flow is at 64°S, where the sill is at 3000 - 3500 m.

East of Kerguelen Ridge, the bottom-water temperature continues to rise slowly as far as 110°E, where it is slightly less than -0.4°C. Beyond that point, the potential temperature drops to nearly -0.6°C. The decrease in potential temperature, along with changes in the other properties to be examined later, is evidence

of a second source of bottom water in this region. It will become evident that the second source is the Ross Sea.

Bottom water from the Indian-Antarctic Basin flows into the South Australian Basin through the gap in the Indian-Antarctic Ridge at 120°E. As a result, the potential temperature in the center of the South Australian Basin is slightly lower than it is to the east and west.

Some bottom water also flows out of the Indian-Antarctic Basin through the narrow passage at 59°S, 146°E. Part of this water moves north into the Tasman Basin while the remainder flows into the Southwestern Pacific Basin over the narrow sill at 59°S, 160°E. Having entered the Southwestern Pacific Basin, the bottom water flows northeast along the New Zealand Plateau in the deep western boundary current and spreads into the central South Pacific.

The bottom water south of the Pacific-Antarctic Ridge is significantly colder than that north of the Ridge. Part of the water in the western end of the Pacific-Antarctic Basin originates in the Ross Sea. The salinity data show that there is also a strong contribution from the Weddell Bottom Water west of the Macquarie Rise.

The moderate temperature gradient along the southern flank of the Pacific-Antarctic Ridge indicates zonal flow from about 140°W to 100°W. The warmer water observed in the northern Pacific-Antarctic Basin probably comes from the Southwestern Pacific Basin. According to Gordon (1966), the warmer bottom water crosses the

Pacific-Antarctic Ridge through the complex fracture zone located at 130°W.

IV.B. Salinity

The map of bottom-water salinity included in this paper (Figure 11) is the first to be constructed for the entire circumpolar region. Previously, the salinity distribution in the Indian and Pacific sectors was regarded as being too homogeneous to provide useful information. However, even the small salinity differences which are observed in this region provide information about the bottom circulation which cannot be derived from the temperature and dissolved oxygen distributions.

The bottom salinity has been mapped before in the Atlantic sector of the Antarctic Ocean. A comparison of the old map (Wüst, 1933) with the present map reveals one significant difference, a difference which led Wüst to draw erroneous conclusions regarding the formation and circulation of bottom water in the Atlantic Ocean.

On Wüst's map and the present one, low-salinity water ($< 34.65\,‰$) is found along the southwestern margin of the Weddell Sea, a region where bottom water is formed. Both maps also show a tongue of low-salinity water extending along the western side of the Argentine Basin. However, whereas the present map shows the salinity increasing steadily from the Weddell Sea source to the Argentine Basin, Wüst's does not. On Wüst's map a

large region of slightly higher salinity separates the low-salinity water in the Weddell Sea from that in the Argentine Basin. This distribution led Wüst to conclude that the fresh, cold water in the Argentine Basin derives from a source other than the Weddell Sea. He hypothesized that the bottom water which spreads northward in the western trough of the Atlantic (which he called antarctic deep water A_I) forms near the pack-ice boundary in autumn and winter, while the bottom water which forms over the Weddell Sea shelf (which he called antarctic bottom water, A_{II}) remains trapped in the western Atlantic-Antarctic Basin.

I have already stated in Section I.B that the mechanism proposed by Wüst for the formation of A_I-type water is highly improbable. Oceanographers have for some time accepted the notion that the bottom water which propagates along the western Atlantic trough originates in the Weddell Sea. It is reassuring to find that the salinity distribution is in fact consistent with this view.

The salinity distribution helps define the path taken by Weddell Bottom Water as it enters the Argentine Basin. It is clear that the Weddell Bottom Water passes through the South Sandwich Trench, not along the channel east of the Trench (Gordon, 1966).

The salinity distribution in the Scotia Sea, like the distribution of potential temperature, reveals an influx of Weddell Bottom Water. The salinity increases rapidly toward the west owing

to the influx of more saline Pacific water through Drake Passage. Examination of several *Eltanin* stations along the Scotia Ridge between the Falkland Islands and South Georgia showed no bottom water of salinity less than 34.72 ‰ passing over the Ridge into the Argentine Basin. The Weddell Bottom Water which enters the Scotia Sea must be thoroughly mixed with Pacific water before it flows into the Argentine Basin.

The bottom-water salinity in the Atlantic-Antarctic Basin is highly uniform. Only in the extreme western and eastern ends of the Basin does the salinity differ from 34.66 ‰ . (The apparent uniformity of the bottom water in this basin is partly due to the fact that all the data were taken by chlorinity titration. Salinometer measurements will undoubtedly reveal some variations in the salinity distribution.) Low salinities in the southern Agulhas and Crozet basins are indicative of Weddell Bottom Water flowing north through the gaps at 30°E and 60°E. The relatively high salinities found in the northern Agulhas Basin reflect eastward flow around the tip of Africa of water from the South Atlantic.

Across the Kerguelen Ridge the salinity of the bottom water increases from 34.66 ‰ to 34.68 ‰ . Unfortunately, there are no salinometer measurements in the vicinity of the Ridge, and the salinity structure over the Ridge cannot be properly investigated. It is reasonable to assume that in passing over the Ridge the bottom water mixes with the Circumpolar Deep Water, causing an increase in salinity near the bottom.

The slight salinity minima in the South Australian and Tasman basins mark the flow of bottom water into these basins. Recall that weak temperature minima were observed in these basins, also.

In the South Pacific Ocean, the bottom-water salinity distribution is more complex and its interpretation less obvious than in the South Atlantic and Indian sectors. Low-salinity water which crosses the sill near 59°S, 160°E spreads north into the Southwestern Pacific Basin. The tongue of low salinity along the New Zealand Plateau is another manifestation of the deep western boundary current.

In the central Southwestern Pacific Basin salinity at first increases slowly, reaching a maximum of about 34.715 ‰ near 40°S. Beyond this point, salinity decreases slowly, dropping below 34.70‰ at 30°S. The change in sign of the meridional bottom-water salinity gradient is related to changes in the salinity of the deep water. As deep and bottom water flow north after entering the South Pacific, the deep salinity maximum is gradually eroded by mixing. As a result, the salinity of the bottom water increases slightly. North of about 40°S, where the deep salinity maximum disappears in the central South Pacific, salinity decreases monotonically from the ocean floor to the Intermediate Water. Further vertical mixing tends to decrease the salinity at the bottom.

The value of the bottom-water salinity map is well demonstrated in considering the Pacific-Antarctic Basin. The range of salinity in the Basin is very small, and no doubt some of the

detail shown in the isohalines is due to observation error. However, I am confident that the pattern shown in the salinity map does reflect real differences in the bottom water. The data grid is denser than in any other part of the antarctic, and the major features have been observed on several different cruises.

The essential features of the salinity distribution in the bottom water of the Pacific-Antarctic Basin are: saline water (> 34.71 ‰) north of 60°S and in the extreme western end of the Basin, with a band of slightly less saline water (< 34.70 ‰) extending along roughly 65°S.

I have already stated on the basis of the potential-temperature distribution that the bottom water found in the northern part of the Pacific-Antarctic Basin probably comes from the Southwestern Pacific Basin. The salinity distribution is consistent with this view. With respect to salinity, the water in the northern Pacific-Antarctic Basin is indistinguishable from that in the central Southwestern Pacific Basin.

The small region of relatively high salinity in the western end of the Pacific-Antarctic Basin is the result of outflow from the Ross Sea. For reasons which are not clear, the bottom water formed in the western Ross Sea is much more saline than that in the Weddell Sea. Whereas the cold shelf water of the Weddell Sea has a maximum salinity of less than 34.70 ‰ , that of the Ross Sea has a maximum salinity of more than 34.85 ‰ . Typical station curves for the southwestern reaches of both seas are shown in Figure 33.

Finding "... no stream of cold poorly saline bottom water sinking from the Ross Sea," Deacon (1937, p. 115) concluded that the Ross Sea had little or no influence on the bottom water outside the Sea. Probably Deacon was looking for water like that produced in the Weddell Sea, on the assumption that the similar climatology of the two regions would produce similar water types. Deacon went on to conclude that any bottom water which is formed within the Ross Sea must be trapped by the shallow ridge which runs across the mouth. This thesis has been generally accepted by oceanographers for many years.

Recent topographic maps of the Ross Sea (*e.g.*, Countryman and Gsell, 1966) indicate that the barrier across the outer shelf is broken by several shallow troughs which extend into the interior of the Sea. These provide paths for Ross Bottom Water to escape. Gordon (1966, 1970) has shown from the distributions of properties outside the Sea that some bottom water does indeed flow out of the Ross Sea. It would appear, however, that he has overestimated the effect of the Ross Bottom Water, particularly in the western Pacific-Antarctic Basin. He implied that the cold bottom water found there is supplied by the Ross Sea alone. It will be seen that this is clearly not the case. Also, his assertion that the bottom water which flows into the South Australian Basin is a mixture of Ross Bottom Water and a "locally-produced water" seems unlikely. If the Ross Sea were contributing large amounts of bottom water, salinities in the eastern Indian-Antarc-

tic Basin would be much higher than those observed there.

The conclusion that the bottom water found in the western Pacific-Antarctic Basin is not solely from the Ross Sea is related to the salinity minimum which extends across the Basin at 65°S. Figure 20, which is a salinity section along 170°W, shows high-salinity Ross Bottom Water in the deep basin south of the Pacific-Antarctic Ridge and less saline water (< 34.70 ‰) over the crest of the Ridge. Figure 22, which is a salinity section along roughly 65°S from 140°E to 150°W, demonstrates that the low-salinity water comes from the west. The low-salinity water represents the last traces of Weddell Bottom Water, which flows up the western flank of the Macquarie Rise, along the Pacific-Antarctic Ridge, and then into the western end of the Pacific-Antarctic Basin. Ross Bottom Water can be observed beneath the Weddell Bottom Water at 160° - 170°E, suggesting that the outflow takes place along the western boundary of the Ross Sea. The fact that the salinity minimum persists past 90°W indicates that the flow of Weddell Bottom Water across the Macquarie Rise must be strong relative to the flux of Ross Bottom Water into the Pacific-Antarctic Basin.

IV.C. Dissolved Oxygen

The map of dissolved-oxygen concentration for the bottom water (Figure 12) is strikingly similar to the potential temperature and salinity maps. The latter two distributions and the circulation patterns they reveal have been discussed in great detail in the

preceding sections. To avoid unnecessary repetition, only the most significant aspects of the dissolved-oxygen distribution will be described.

The highest concentrations of dissolved oxygen (> 6.0 ml/l) on this map are found along the western and northern margins of the Weddell Sea. Eastward flow out of the Sea is marked by a tongue of high-oxygen water which is pressed against the southern arc of the Scotia Ridge. Overflow of Weddell Bottom Water into the Scotia Sea is evident in the high oxygen values east of Drake Passage. Oxygen-rich water is also observed in the Argentine Basin. It is clear from the oxygen distribution that the high-oxygen water in the Argentine Basin is derived from the tongue extending northward along the South Sandwich Trench. No such water was found to be crossing the ridge separating the Scotia Sea and the Argentine Basin.

As Weddell Bottom Water moves east in the Atlantic-Antarctic Basin, the dissolved-oxygen concentration falls from 6.0 to 5.4 ml/l. In the western Indian-Antarctic Basin the oxygen concentration remains at about 5.4 ml/l, but in the eastern end of the Basin the concentration increases to over 5.6 ml/l. This increase, like the small changes in potential temperature and salinity observed in this region, is a result of the influx of Ross Bottom Water from the east.

In the Macquarie Rise sector, the oxygen distribution shows bottom water flowing out of the Indian Ocean via three paths: north into the Tasman Basin; across the Macquarie Rise at 59°S and

into the Southwestern Pacific Basin; across the Macquarie Rise along 65°S and into the Pacific-Antarctic Basin. The flow into the Southwestern Pacific Basin continues east along the Pacific-Antarctic Ridge and then turns north to feed the deep western boundary current along 160°W. The eastward flow of bottom water across the Macquarie Rise and Pacific-Antarctic Ridge shows up clearly in the oxygen sections along 65°S (Figure 23) and 170°W (Figure 21). A large proportion of this water is Weddell Bottom Water. Ross Bottom Water, with a somewhat higher oxygen concentration (> 5.3 ml/l), can be seen beneath the Weddell Bottom Water in both sections.

In the Pacific-Antarctic Basin, the large region with oxygen concentrations greater than 5.0 ml/l represents both Weddell and Ross bottom waters and their mixtures. The lower oxygen values in the northern Pacific-Antarctic Basin are evidence of the influx of bottom water from the Southwestern Pacific Basin and of mixing with oxygen-poor water along the Chile coast.

V. FLUX AND VELOCITY STRUCTURE OF THE ANTARCTIC CIRCUMPOLAR CURRENT

A shortcoming of the method used in the previous sections is that it provides only a qualitative view of the circulation. In this section the structure of the circumpolar flow, particularly that of the Antarctic Circumpolar Current, will be examined by more quantitative means. This will be done principally in terms of the relative geostrophic velocity field computed for several meridional hydrographic sections around Antarctica. Deep current-meter measurements taken along 132°E south of Australia will be used to compute the "absolute" net flux in the circumpolar zone, and the result compared with a similar computation of the Drake Passage transport.

The mass transport of the Antarctic Circumpolar Current has been estimated by numerous investigators using the dynamic, or geostrophic, method. These calculations have been carried out most frequently for the Drake Passage section, which is considerably shorter than any other section across the Circumpolar Current. Clowes (1933) was the first to compute the zonal flux through Drake Passage, which he determined to be 110×10^6 m^3/s relative to 3500 db. Later estimates, which range from 90 to 218×10^6 m^3/s (excluding the unrealistically low results of Ostapoff, 1961) have been reviewed by Gordon (1967a) and will not be discussed here.

Sverdrup (1940), using BANZARE stations along 145°E, has estimated the net eastward flux from the naviface to the bottom

between Australia and Antarctica at 150 × 10^6 m^3/s. Kort (1963) computed the eastward flux in the same sector (165°E) to be 189 × 10^6 m^3/s from data taken by the *Ob'* in March 1958. Both Sverdrup and Kort calculated the transport relative to 3000 db at 144 × 10^6 m^3/s.

Kort (1963) has also computed the net eastward transport between South Africa and Antarctica. From hydrographic stations occupied by the *Ob'* in February-March 1957 he calculated 150 × 10^6 m^3/s relative to 3000 db and 198 × 10^6 m^3/s relative to the bottom[7]. From *Discovery* data taken along 20°E in April 1938 Kort computed the transport relative to 3000 db to be 205 × 10^6 m^3/s.

While the zonal fluxes computed from the Australian and South African sections are in reasonable agreement, the flux computed for Drake Passage is significantly smaller than the other two sections. Obviously there has been no gain or loss of water in the Atlantic, Pacific, and Indian oceans, since mean sea level has remained constant for many years. Simple water budget calculations will show that the mean transports across the Drake Passage, South African, and Australian sections must in fact be very nearly equal.

In comparison with the zonal water transport of the Antarctic Circumpolar Current, the average annual difference between evaporation and precipitation-plus-runoff makes a small net contribution

---

[7] The substantial increases in transport between 3000 m and the bottom which Kort reported seem unrealistically large in view of the very small relative velocities which are observed below 3000 m.

to the water budgets of the Atlantic, Indian, and Pacific oceans. For example, an average difference of 1 m/yr between evaporation and precipitation over the entire Pacific Ocean would represent a flux of only 5×10^6 m^3/s. The actual average difference, although not well known for the oceanic areas, is probably somewhat less than 1 m/yr (see Dietrich, 1963, Figure 75).

Aside from the circumpolar zone, the only direct communication among the oceans is through Bering Strait and the East Indian Archipelago. Numerous current measurements have been made in Bering Strait. The mean transport through the Strait is known to be $1.0 - 1.5 \times 10^6$ m^3/s toward the north (see Coachman and Aagaard, 1966, for a summary of Bering Strait transport calculations). The net flux through the East Indian Archipelago has not been determined as precisely as the Bering Strait flux. The only significant passage through the islands is between Timor and Australia. Wyrtki (1961) has estimated the transport of upper water in the Timor Current at $1.0 - 1.5 \times 10^6$ m^3/s toward the west. It is clear from the deep water in the Timor Trench that the deep flow must be in the opposite direction to the surface current (Sverdrup *et al.*, 1942, p. 739). It is unlikely that the net transport through the East Indian Archipelago exceeds 5×10^6 m^3/s.

The fact that the net transport figures cited earlier do not agree either for a given section or among sections might be interpreted as evidence of seasonal or longer-term transient motions in the circumpolar circulation. Kort (1963), Deacon (1963), and Gordon (1967a) have suggested that transient motions are significant

in the Antarctic Circumpolar Current. Recent studies indicate, however, that this is not the case. Bowen and Stommel (1968) analyzed sixteen sections along 20°E taken by the *Discovery* during the period April 1938 to March 1939. No seasonal variations in the temperature (hence mass) distribution were observed. Reid and Nowlin (1971) have computed the transport relative to the bottom through Drake Passage using four hydrographic sections made by different ships between 1930 and 1969. The range of the transports was 92 - 117 × 10^6 m^3/s; three of the four were from 113 - 117 × 10^6 m^3/s.

The author has computed the transport relative to the bottom across two sections south of Australia: 115°E (*Discovery*, December 1937 - January 1938) and 132°E (*Eltanin*, December 1969 - January 1970). The net eastward flux through these sections was 149 × 10^6 m^3/s and 156 × 10^6 m^3/s, respectively. The results compare well with Sverdrup's (1940) estimate of 150 × 10^6 m^3/s at 145°E.

It would appear that the net relative transport across any section is reasonably steady, at least with respect to seasonal and longer-period fluctuations. A more likely explanation for the variations in computed transport among the sections is that these calculations determine only part of the flux. The total transport consists of the relative component plus the "barotropic" component (Fofonoff, 1962b), which corrects for any difference between the true velocity and the assumed velocity at the reference level. For a deep reference level the velocity difference is usually small,

resulting in relatively minor changes in the computed velocity field. However, a small correction to the velocity field may have an appreciable effect on the transport. A barotropic correction of 1 cm/s between two stations 250 km apart in 4 km of water represents an increment of 10×10^6 m^3/s in the transport.

In order to determine the absolute transport, current measurements must be taken along with the hydrographic stations from which the relative transport is to be computed. Over the past two austral summers two such sections have been made in the antarctic, the first in Drake Passage (January 1969) and the second along 132°E between Australia and Antarctica (December 1969 - January 1970). The results of these cruises will be discussed in order to demonstrate the magnitude of the barotropic correction and to estimate the total mean transport.

The instruments and techniques used to measure deep currents in the antarctic have been developed at the Scripps Institution of Oceanography. (See Isaacs *et al.*, 1966, for a detailed description of the current-meter system.) The current meter is tethered to an anchor on the sea floor for a preset period. At the end of the period, the meter automatically breaks its mooring and ascends to the naviface where it is recovered. If the current measurements are to be used to compute absolute geostrophic transports, as in the present case, the instrument is tethered at or above the level of the deepest bottle on the hydrographic casts on either side of it. In the antarctic experiments, the

meters were usually set 300 - 500 m off the bottom, although two were as much as 900 m off the bottom.

Output from the current meter consists of a continuous trace indicating current direction (magnetic) and a record of the number of revolutions made by the Savonius rotor per unit time. The practical threshold of the rotor is 0.5 cm/s. Tests off the California coast have shown good reproducibility between adjacent meters (Isaacs *et al.*, 1966).

For the present purposes the raw data were reduced to hourly-mean speeds and directions. Semi-diurnal, diurnal, and daily-mean velocity components were derived by computer from the reduced data. In all cases the records were at least one lunar day (25 hours) long.

The barotropic velocity component was determined by taking the difference between the measured mean speed normal to the section and the geostrophically-computed speed at the same depth. For those station pairs with no current meter between them, the barotropic component was determined by linear interpolation between the values on either side.

Results of the Drake Passage cruise are discussed in detail by Reid and Nowlin (1971) and will only be summarized here. Five complete current-meter records of 25 - 99 hours' duration were obtained. At all current-meter stations the daily mean current was toward the east. Overall mean speeds ranged from about 3 cm/s at the northern end to nearly 9 cm/s at the southern end of the sec-

tion. The geostrophic transport relative to the deepest common level of each station pair was found to be 113 × 10^6 m^3/s. The barotropic transport was 124 × 10^6 m^3/s, giving a total eastward flux of 237 × 10^6 m^3/s. This estimate does not include any correction for the small area outside the sampling grid, *i.e.*, between the continents and the current meters at the ends of the section, or between the sea floor and the reference level.

The section along 132°E between Australia and the antarctic continental shelf was made during *Eltanin* Cruise 41. Twenty-one deep hydrographic stations were occupied along the section, and five complete current-meter records were obtained. The current-meter results are summarized in Table 2. On the whole, the mean speeds were somewhat smaller than those measured in Drake Passage, as might be expected in the wider section.

From the hydrographic data, the geostrophic transport relative to the deepest common level of each station pair was found to be 156 × 10^6 m^3/s. The barotropic component, which was determined in the same manner as for the Drake Passage section, was 77 × 10^6 m^3/s, giving a net transport of 233 × 10^6 m^3/s. Figures 24 and 25 show the relative and absolute velocity and transport fields.

It is evident from these calculations that the barotropic component is a significant part of the total transport in the circumpolar belt. In Drake Passage the barotropic component accounted for 52% of the total, while at 132°E it represented 33% of the total flux.

TABLE 2. Summary of current-meter measurements along 132°E, in order from north to south.

CURRENT-METER NUMBER	DATE/TIME (LOCAL) OF RECORD	POSITION	DEPTH OF BOTTOM (m)	DEPTH OF METER (m)	MEAN SPEED/DIRECTION (cm/s; °T)	MEAN ZONAL COMPONENT* (cm/s; + EAST)
1	27 XII/0850- 29 XII/1620	40°02'S 131°56'E	5530	5070	3.56/080°	3.51
7	19 I/2100- 21 I/0730	44°59'S 131°55'E	4575	3825	0.94/097°	0.93
2	1 I/0645- 3 I/0900	50°00'S 132°01'E	3365	2905	** / ~240°	**
4	3 I/1720- 5 I/1730	50°03'S 132°17'E	3359	2900	7.56/231°	-5.90
6	14 I/1215- 16 I/1230	55°02'S 132°04'E	4230	3315	4.54/052°	3.58
5	10 I/1400- 11 I/1745	63°05'S 132°06'E	4270	3355	4.64/022°	1.72

*Second decimal probably not significant. Speeds rounded to tenths before computing barotropic transports.

**No speed record. Direction ranged from 220° to 260°.

The close agreement between the net transports through the Australian and Drake Passage sections is remarkable in view of the uncertainties inherent in the method used to compute them. Although the Pacific Ocean water budget indicates that the two should agree to within, say, 5×10^6 m^3/s, it would be unrealistic to conclude that the circumpolar flux has been measured to that precision.

Two major potential errors stand out: (1) The unmeasured barotropic flux through the side and bottom areas might make a significant contribution (say, ± 10%) to the total. (2) The limited number of short-term current measurements upon which these calculations are based may not be representative of the long-term average flow. These limitations are particularly evident in the Australian section, where the meter spacing was much larger, the gaps in the current-meter coverage (*viz*, north of 40°S) greater, and the record lengths shorter than for the Drake Passage section.

In spite of these shortcomings, the fact that the two transport calculations do agree so well gives some encouragement that the method provides a reasonable estimate of the mean net circumpolar flux. Probably the above estimate is low, since extrapolation of the measured currents into the side and bottom boundaries results in an increase in the net flux. Assuming an increase of 10%, a reasonable estimate of the net circumpolar flux would be 250×10^6 m^3/s.

The transport of the Antarctic Circumpolar Current alone varies with longitude. In Drake Passage the eastward Circumpolar Current occupies the full width of the section and has a transport equal to the net zonal flux. South of Africa and Australia, on the other hand, westward currents are found along the continental boundaries, and the transport of the Circumpolar Current must be slightly greater ($\sim$ 20 - 30 $\times$ 10^6 m^3/s) than the net flux through the section.

Whereas the averaged deep currents measured in Drake Passage were consistently toward the east, those south of Australia were not. The record of current meter No. 4 (record length 47 hrs) gave a strong mean component toward the west. Even with the oscillatory component included, the current direction was always between 210° and 260°T. Current meter No. 2, dropped at the same position two days earlier, provided further evidence of westward flow. This meter (record length 45 hrs) gave no speed record, but the direction trace indicated that the velocity vector was steady within the arc 220° - 260°T.

Current meters Nos. 2 and 4 were positioned over the crest of the Indian-Antarctic Ridge. Figure 24 shows that over the Ridge crest the relative geostrophic flow dropped to effectively zero. As a result the absolute flow over the ridge was toward the west throughout the water column (Figure 25).

Without the appropriate current measurements it is not possible to determine if the current structure observed at 132°E

exists elsewhere in the antarctic. However, there are remarkable similarities between the relative geostrophic velocity field at 132°E and at a number of other meridional sections across the Antarctic Circumpolar Current in the Australian sector.

Five additional meridional sections between 115°E and 146°E have been worked up. The data were taken over a span of thirty years. Two of the sections were made by the *Discovery* (1936, 1938), three by the *Eltanin* (1968). All the sections cross the Indian-Antarctic Ridge, which runs nearly east-west along 50°S in this region. (See Figures 26 - 30.)

At the northern end of each section, weak westward flow is observed. This, of course, is the westward Flinders Current, which was discussed in previous sections. Strong eastward flow with maximum navifacial velocities of 15 - 25 cm/s is concentrated in a narrow band north of the Ridge, over the South Australian Basin. In the Indian-Antarctic Basin, the flow is also eastward but slower (5 - 10 cm/s) and more uniform than in the north. Just south of the Ridge crest the relative velocities drop sharply, and the vertical shear practically vanishes. In one instance (117°E) the maximum velocity over the Ridge is 1 cm/s eastward. In all other cases it is weakly westward.

If the absolute flow field is qualitatively similar to the relative flow field (as it was at 132°E), velocity sections south of Australia indicate that westward flow along the crest of the Indian-Antarctic Ridge is a common feature of the circulation in this re-

gion. Generalizing further, it might be inferred that the current reversal is in some way caused by the bottom topography. Certainly there is little doubt that major topographic features do influence the structure of the Circumpolar Current, as shown by the large-scale meanders noted previously.

The sector south of Africa is topographically similar to the Australian sector. Deep basins in the north and south are separated by an east-west ridge along roughly 50°S. A *Discovery* (1939) section along 20°E was worked up in order to examine the structure of the velocity field with respect to the ridge. Here, too, maximum eastward navifacial velocities ($\sim$ 15 cm/s) are present over the northern flank of the ridge and weak westward velocities over the southern flank. However, in this section the velocities south of the ridge are in general very weak, and the current reversal over the ridge is not as distinct as in the Australian sections. On the other hand, Kort's (1963) velocity section along 20°E, Figure 31, does resemble closely the situation south of Australia.

The limited observations available indicate that a weak countercurrent exists over the mid-ocean ridge in those areas of the antarctic where both the Circumpolar Current and the mid-ocean ridge have an east-west orientation. The evidence supporting this conclusion is summarized in Table 3, which suggests that the magnitude of the current reversal increases with the slope of the southern flank of the ridge. (This table includes only the six Australian sections; Kort's section did not show the individual data points necessary to determine the maximum speed over the ridge.)

TABLE 3. Maximum westward relative velocities over the Indian-Antarctic Ridge.

SECTION	MAXIMUM SPEED OVER RIDGE (cm/s, + east)	TOTAL ELEVATION OF SOUTHERN FLANK (m)	SLOPE OF SOUTHERN FLANK ($\times 10^{-3}$)
117°E	+ 1.4	900	1.5
132°E	0	1300	1.6
115°E	- 0.3	1100	1.7
146°E	- 1.4	1100	1.8
128°E	- 2.0	1300	2.2
140°E	- 5.0	2000	4.2

Although the observations suggest that the countercurrent is the result of bottom-topography effects, the dynamical explanation for such a relationship is not apparent. Since the flow in the regions of interest is zonal, fluid elements do not experience a change in the Coriolis parameter. Therefore, the simple qualitative arguments based on conservation of potential vorticity, which have been used to explain the meanders of the Circumpolar Current, are not applicable. If a more complete vorticity balance is considered, then the production of relative vorticity by the wind stress must be included. It is perhaps significant that the maximum westerly winds in the southern hemisphere occur at roughly 50°S (von Arx, 1957). The sense of the wind-produced relative vorticity changes from anticyclonic to cyclonic in about the same latitude in which the countercurrent occurs. It is not clear how the wind stress distribution and bottom topography might interact to produce the observed current structure.

VI. CONCLUSIONS AND REMARKS

In analyzing the distributions of heat, salt, and dissolved oxygen in abyssal antarctic waters, I have pointed out certain characteristics of the antarctic and sub-antarctic circulation. Some of these features have been noted by other workers, in which case the present discussion represents an extension or modification of previously-held ideas. Other aspects of the circulation which are discussed here are new. All are summarized below. Those items which are new are marked with an asterisk.

(1)* The upper deep water of the antarctic is characterized by a vertical minimum of dissolved oxygen. The minimum originates in the eastern South Pacific Ocean, where oxygen-poor water flows south and mixes into the circumpolar flow. The resulting low-oxygen mixture is transported eastward in the Circumpolar Current, forming a lateral as well as vertical oxygen minimum across the South Atlantic. Additional low-oxygen water, flowing poleward from the North Indian Ocean, feeds into the Circumpolar Current south of Africa. Through lateral mixing, the oxygen-poor water from these two sources spreads over much of the antarctic region.

The distributions of salt and dissolved oxygen in the upper deep water (50 cl/t) are markedly zonal. A narrow belt with sharp meridional salinity and dissolved-oxygen gradients is found adjacent to the Antarctic continent. North of these gradients the distributions are relatively uniform. The transition from high-

to low-gradient zones occurs south of the high-velocity core of the Circumpolar Current.

(2) Circumpolar Deep Water is also characterized by a vertical salinity maximum, which is found below the oxygen minimum. North Atlantic Deep Water, the source of the high-salinity water, flows south along the western Atlantic trough and joins the circumpolar flow near 40°S. The saline water is confined to the northern part of the Antarctic Ocean in the Atlantic and western Indian sectors. Only in the eastern Indian Ocean south of Australia does the North Atlantic component become fully integrated into the Circumpolar Current. In the South Pacific Ocean, Circumpolar Deep Water is marked by a lateral salinity maximum, which is slowly eroded as the water flows east, finally disappearing west of Drake Passage.

In the Pacific and Indian oceans, high-salinity deep water is observed flowing north along the western boundary. This distribution is consistent with the theoretical abyssal circulation model of Stommel and Arons (1960) and with recent field observations in the South Pacific.

(3)* West of the Macquarie Rise-New Zealand Plateau, deep and bottom water in the Antarctic Circumpolar Current is deflected northward into the Tasman Sea. This water feeds a westward countercurrent which flows south of Tasmania and across the Australian Bight to at least 115°E. The uniformity of the water in the Australian Bight makes it impossible to discuss in detail the flow in this region.

(4)* The structure of the wind-driven anticyclonic circulation in the South Pacific Ocean changes dramatically with depth. In the upper layers the gyre is closed by a western boundary current along the east coast of Australia. At greater depths, the ridge system running north from New Zealand acts as a barrier to the circulation, and a poleward western boundary current develops along the east coast of New Zealand. At a depth of about 1800 m, a well-defined closed gyre is present in the western South Pacific.

Along the eastern margin of the South Pacific, poleward flow is evident beneath the Antarctic Intermediate Water. This flow is less intense than that along the New Zealand Plateau, but the low-oxygen, low-salinity water it transports to the south has a much stronger influence on the distributions of properties in the antarctic.

(5)* A detailed examination of the velocity field in the Australian-New Zealand sector has revealed the following:

a. The net eastward geostrophic transport relative to the bottom is reasonably uniform with longitude and has a magnitude of about 150×10^6 m^3/s.

b. The "absolute" net geostrophic transport is approximately 230×10^6 m^3/s, which agrees well with the net transport computed for Drake Passage.

c. The relative geostrophic velocity field consists of weak westward flow in the Australian Bight (40° - 45°S), strong eastward flow concentrated in a narrow zone over the northern flank

of the Indian-Antarctic Ridge, weak westward flow just south of the crest of the Ridge, and moderate eastward flow over the Indian-Antarctic Basin. A similar regime exists in the topographically-similar region south of Africa.

d. Deep current measurements made along 132°E confirm the structure of the velocity field presented above. In particular, steady westward flow along the Indian-Antarctic Ridge was detected by two meters positioned on the Ridge crest. The westward transport over the Ridge reduced the net eastward flux through the section by about 10%.

(6) On these maps, a westward current along the antarctic coast (East Wind Drift) is observed only at shallow depths (< 300 m) and in the sector from the Greenwich Meridian to 140°E. Large cyclonic gyres in the Weddell and Ross seas cause westward flow along the coast in both seas. The Weddell gyre is stronger and more clearly defined than the Ross gyre.

(7) Ross Bottom Water, which is characterized by its high salinity (∿ 34.71 ‰), does flow out of the western Ross Sea in small quantities. Part of the Ross Bottom Water moves west along the antarctic coast and into the eastern Indian-Antarctic Basin, while the remainder flows northeast into the western Pacific-Antarctic Basin.

The Weddell Sea is a much stronger source of bottom water than is the Ross Sea. Even in the Pacific-Antarctic Basin, immediately to the north of the Ross Sea, the influx of Ross Bottom

Water causes only slight changes in the bottom-water characteristics which were originally established in the Weddell Sea, some 15,000 km distant.

Aside from the Weddell and Ross seas, there are no significant sources of bottom water along the coast of Antarctica. Specifically, there is no evidence of water from the Davis Sea-MacKenzie Bay region in the bottom layer.

(8)* The Weddell Bottom Water which flows north into the Argentine Basin (and eventually into the northern hemisphere) does so via the South Sandwich Trench. Weddell Bottom Water does spill into the Scotia Basin, but there is no indication that any of this water crosses the northern arc of the Scotia Ridge and flows into the Argentine Basin.

I began this paper by stating that understanding the antarctic circulation is an important part of understanding the general circulation of the world ocean. This study has attempted to refine our understanding of the antarctic circulation and to quantify some aspects of that flow. However, at best the conclusions reached here are only tentative answers to some very significant problems. I will close by briefly reviewing these problems and discussing how they might be approached in the future.

(1) Hydrographic coverage of the Antarctic Ocean. The hydrographic coverage of the Pacific, eastern Indian and western Atlantic sectors of the antarctic is quite good. The only area where the coverage is inadequate is the central Indian sector. This region

includes the Kerguelen Ridge, where modern salinity and oxygen measurements would be extremely useful, especially for investigating the flow of bottom water over the Ridge.

Repeated, systematic hydrographic stations in the Weddell Sea would be of great interest. Summer stations could be taken by a specially-equipped icebreaker, for example, the *Glacier*. Winter data might be taken by an unmanned station set on the bottom or on the ice. Observations of winter conditions over the continental shelf of the Weddell Sea would be particularly valuable.

(2) Zonal flux in the Antarctic Ocean. The transport calculations presented in this report are only a first approximation. However, the work carried out during *Eltanin* Cruise 41 and the Piquero Expedition has at least demonstrated the feasibility of measuring the flux. Future experiments should be carried out to determine:

a. the optimum horizontal spacing of current meters;

b. the short term (< 1 month) variability of the Circumpolar Current;

c. the transports of the westward boundary currents (Flinders Current, Agulhas Current, East Wind Drift) associated with the Circumpolar Current;

d. whether westward flow is a common feature over the crests of the Atlantic-Indian and Indian-Antarctic ridges.

Once the zonal velocity field is known in greater detail than it is at present, long-term experiments ($\sim$ 1 year) can be designed to examine the seasonal variability of the circumpolar flow. The

relative flow appears to be steady, but there might be significant seasonal fluctuations in the barotropic component. (Note that the two sets of current measurements reported in this paper were both made during austral summer.) Also, the magnitude of the meridional transport of the deep western boundary currents could be determined by measuring the zonal circumpolar flux upstream and downstream of the regions where these boundary currents originate.

(3) Formation of bottom water. This study did not address the problem of bottom-water formation, but it is clearly an important problem in physical oceanography. The most pressing need, in the context of the general circulation, is to determine the annual rate of production of Weddell Bottom Water, which is the predominant constituent of antarctic bottom water. From repeated hydrographic stations taken in the Weddell Sea and current measurements taken at key locations, *e.g.*, the Scotia Ridge, South Sandwich Trench, and western Atlantic-Antarctic Basin, a quantitative assessment of the Weddell Sea source could be made. These data would indicate whether there is a marked winter peak in the rate of bottom-water production, as Brennecke's model suggests, or if formation of bottom water continues through the summer, as predicted by the recent theories of Gill and Turner (1969) and Seabrooke *et al.*, (1971). Investigations of this sort could eventually lead to an understanding of the mechanism(s) involved in the production of bottom water in the antarctic.

MAPS (FIGURES 1 - 12)

Figures 2 and 9 show the distributions of stations for the isanosteric and bottom maps, respectively. The key given below identifies the ship symbols. To avoid crowding, only the last two digits of station numbers are shown on some meridional sections. Those stations for which there was no originator station-number in the NODC files are designated by the year the data were taken, enclosed by parenthesis.

On the isanosteric maps, areas in which the entire water column is less dense than 50 or 30 cl/t are hatched. On the bottom maps, areas less than 3500 m deep are hatched.

Key

Eltanin ◇

Cruises 28 & 29 (Scorpio Expedition): ◇ S

Cruise 41: ◇ E

Discovery ●

Ob' ▲

Meteor +

Operation Deep Freeze □

Atka: AK *Northwind:* NW

Edisto: ED *Staten Island:* SI

Glacier: GL *Westwind:* WE

Glacier (IWSOE-1968 & 1969) ■

Hakuho-Maru ◆

Thomas Washington ▲

Umitako Maru ✳

All others ○

Anton Bruun: AB

Africana II: AF

Argo: AR

Atlantis: AT

Capitan Canepa: CC

Diamantina: D

Gascoyne: G

Galathea: GA

Horizon: HO

San Martin: SM

Thorshaven: TH

Vema: V

William Scoresby: WS

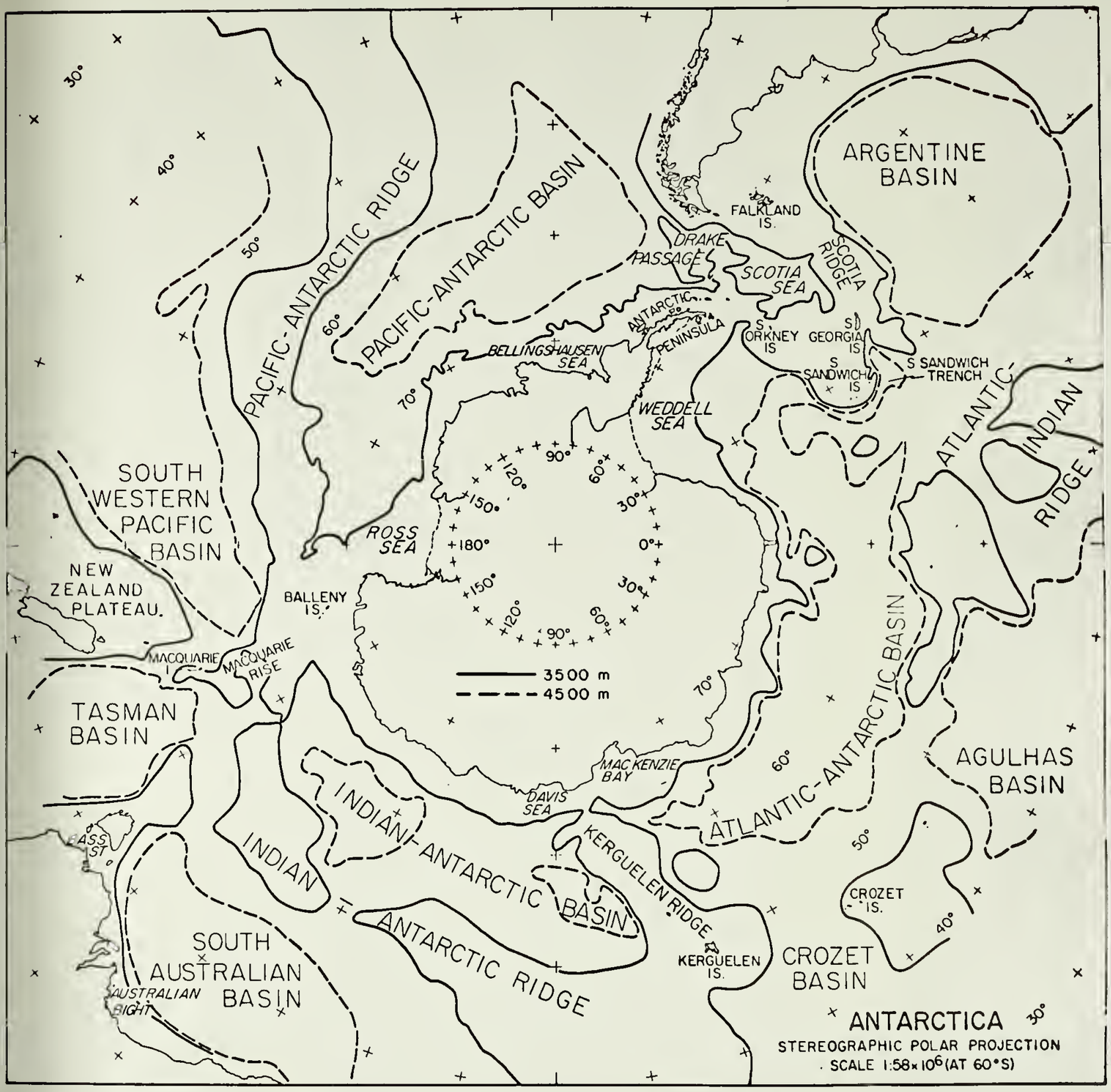

Figure 1. Major topographic features of the Antarctic Ocean

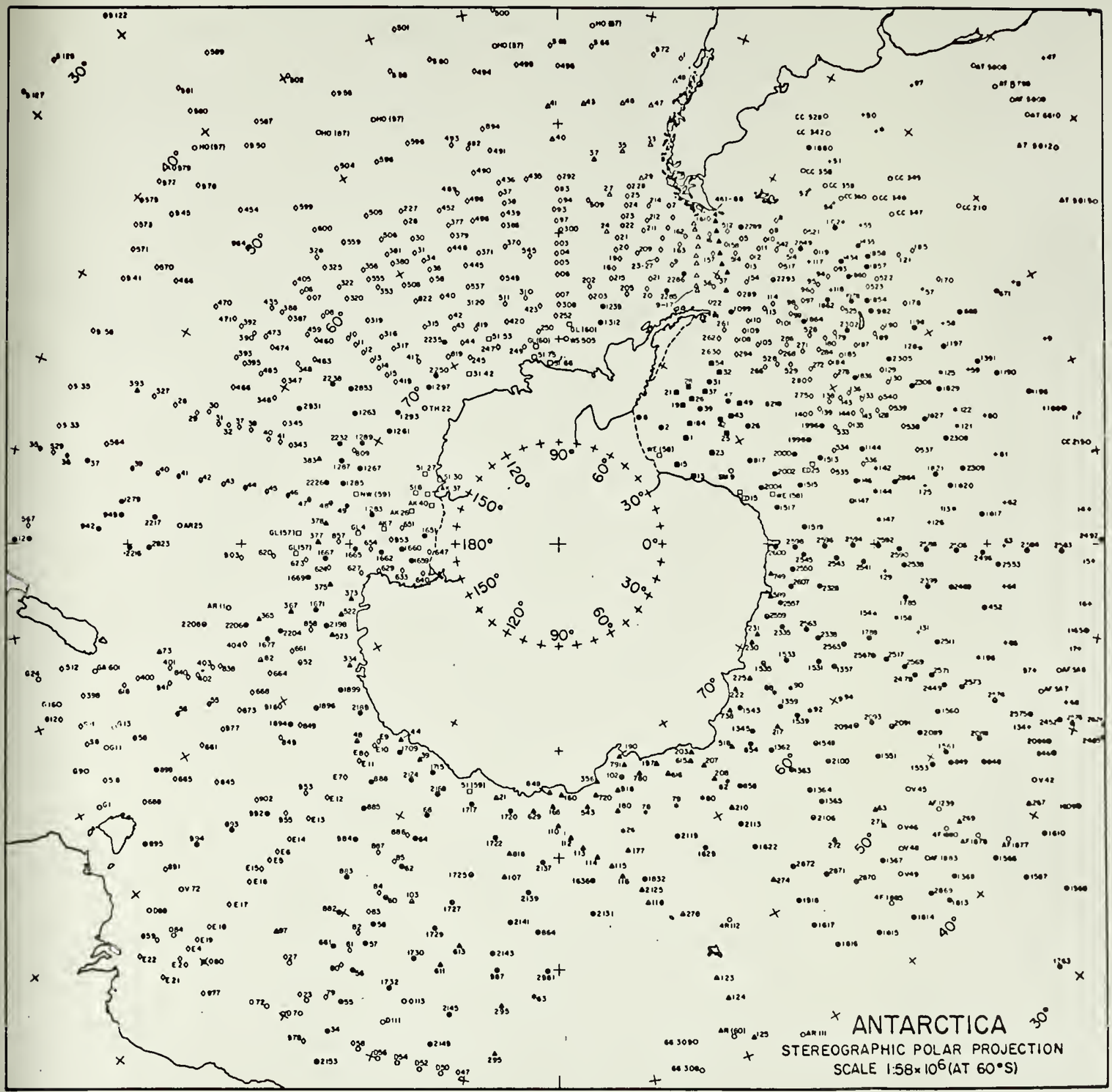

Figure 2. Stations for the 50- and 30-cl/t maps

Figure 3. The 50-cl/t surface: depth

Figure 4. The 50-cl/t surface: salinity

Figure 5. The 50-cl/t surface: dissolved oxygen

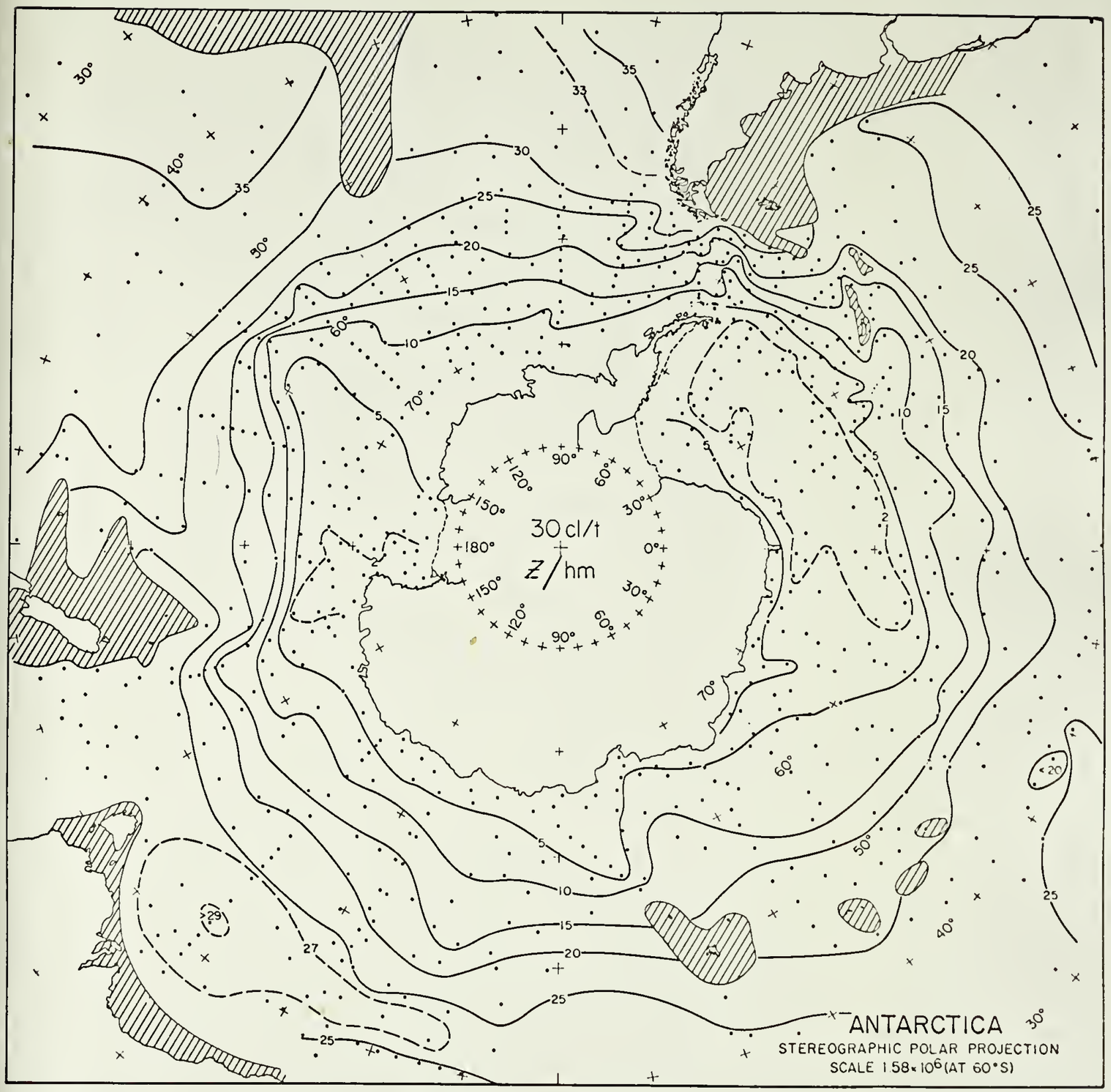

Figure 6. The 30-cl/t surface: depth

Figure 7. The 30-cl/t surface: salinity

Figure 8. The 30-cl/t surface: dissolved oxygen

Figure 9. Stations for the bottom-water maps

Figure 10. The bottom water: potential temperature

Figure 11. The bottom water: salinity (- 34.00 ‰)

Figure 12. The bottom water: dissolved oxygen

SECTIONS (FIGURES 13 - 31)

The vertical exaggeration for all sections (except Figure 31) is 500. In the meridional sections of θ, S, and O_2, the 50- and 30-cl/t isanosteres are shown by heavy dashed lines. At each station in the meridional salinity sections, the highest value within the deep salinity maximum is enclosed by parentheses. At each station in the meridional dissolved-oxygen sections, the minimum value is enclosed by parentheses. Station numbers are given along the bottom of each section. If data from more than one cruise have been plotted in a section, the following abbreviations have been used to identify the data source: *Atka*, AK; *Discovery*, DS; *Eltanin*, ET; *Hakuho Maru*, HM.

In the zonal-velocity sections, the heavy dashed line represents the reference level for computing geostrophic speeds. The units are cm/s, positive east. The numbers just below the reference level give the net flux (positive east) for each station pair, in millions of cubic meters per second.

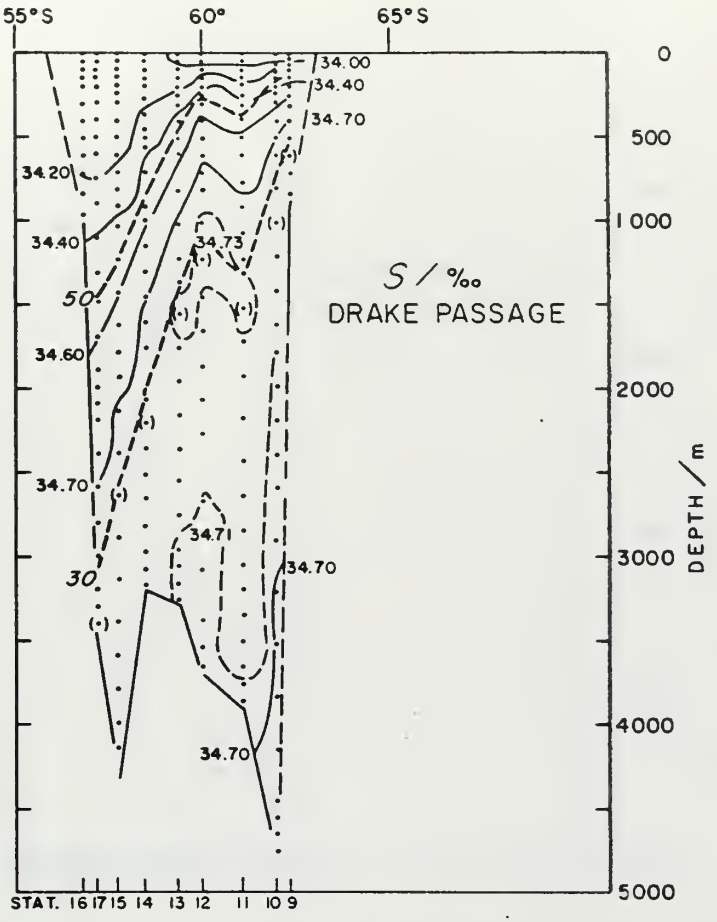

Figure 13. Drake Passage: salinity section. Data from Piquero III Cruise of the *Thomas Washington*, 21-27 January 1969.

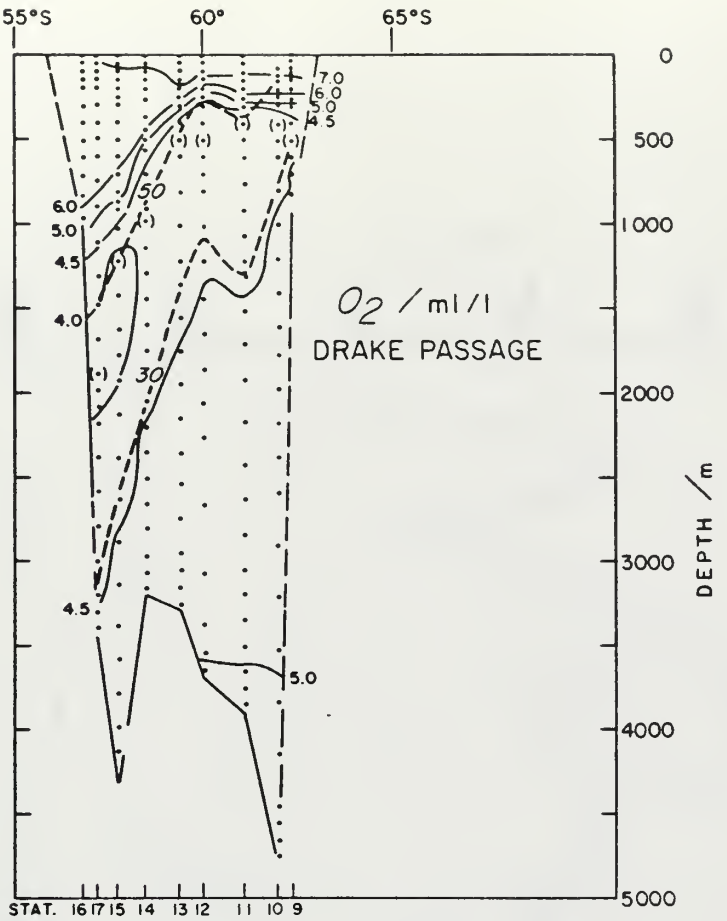

Figure 14. Drake Passage: dissolved-oxygen section. Data source same as Figure 13.

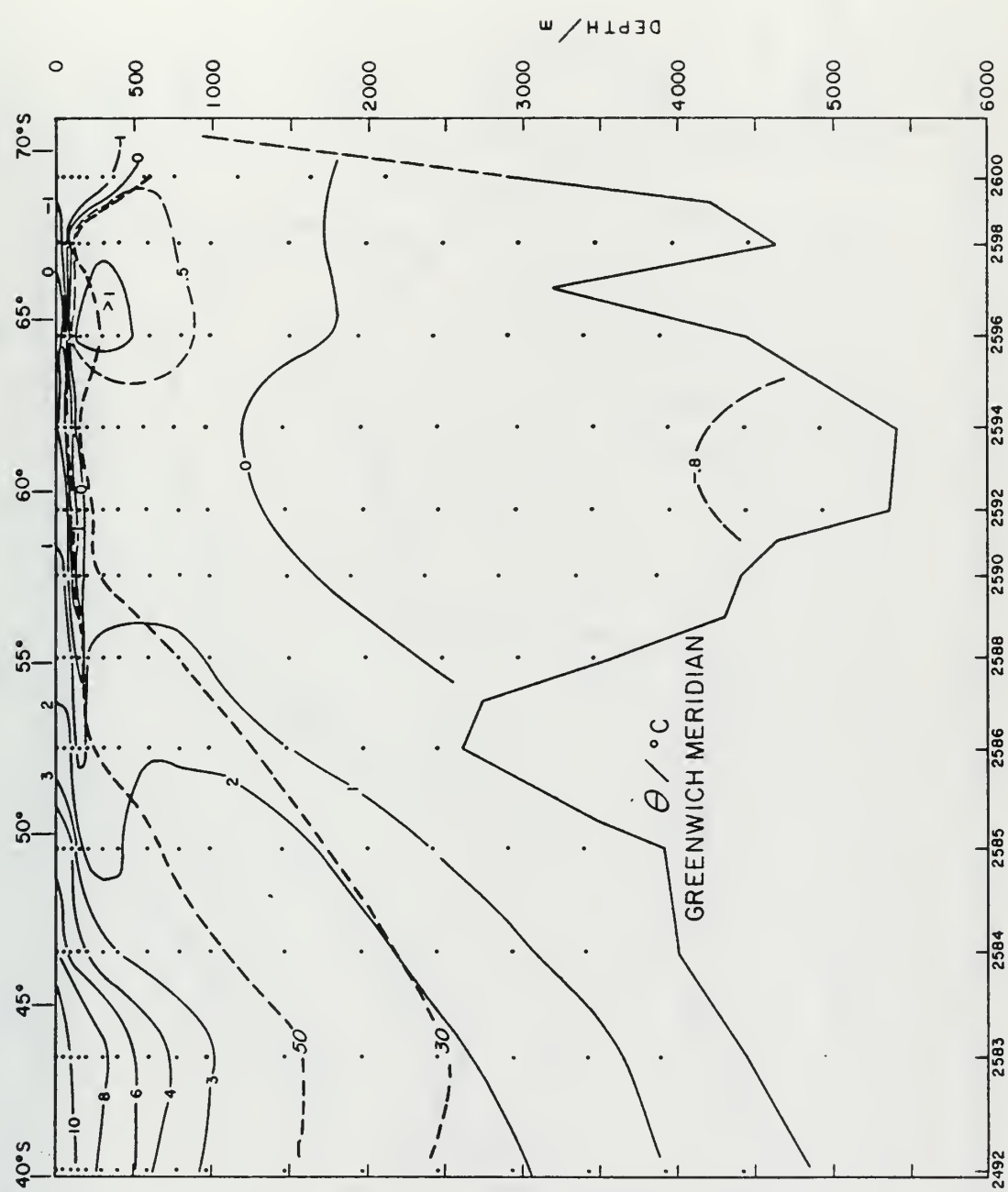

Figure 15. Greenwich Meridian: potential-temperature section. Data from *Discovery II*, 21 February - 3 March 1939; DS 2492 occupied 28 November 1938.

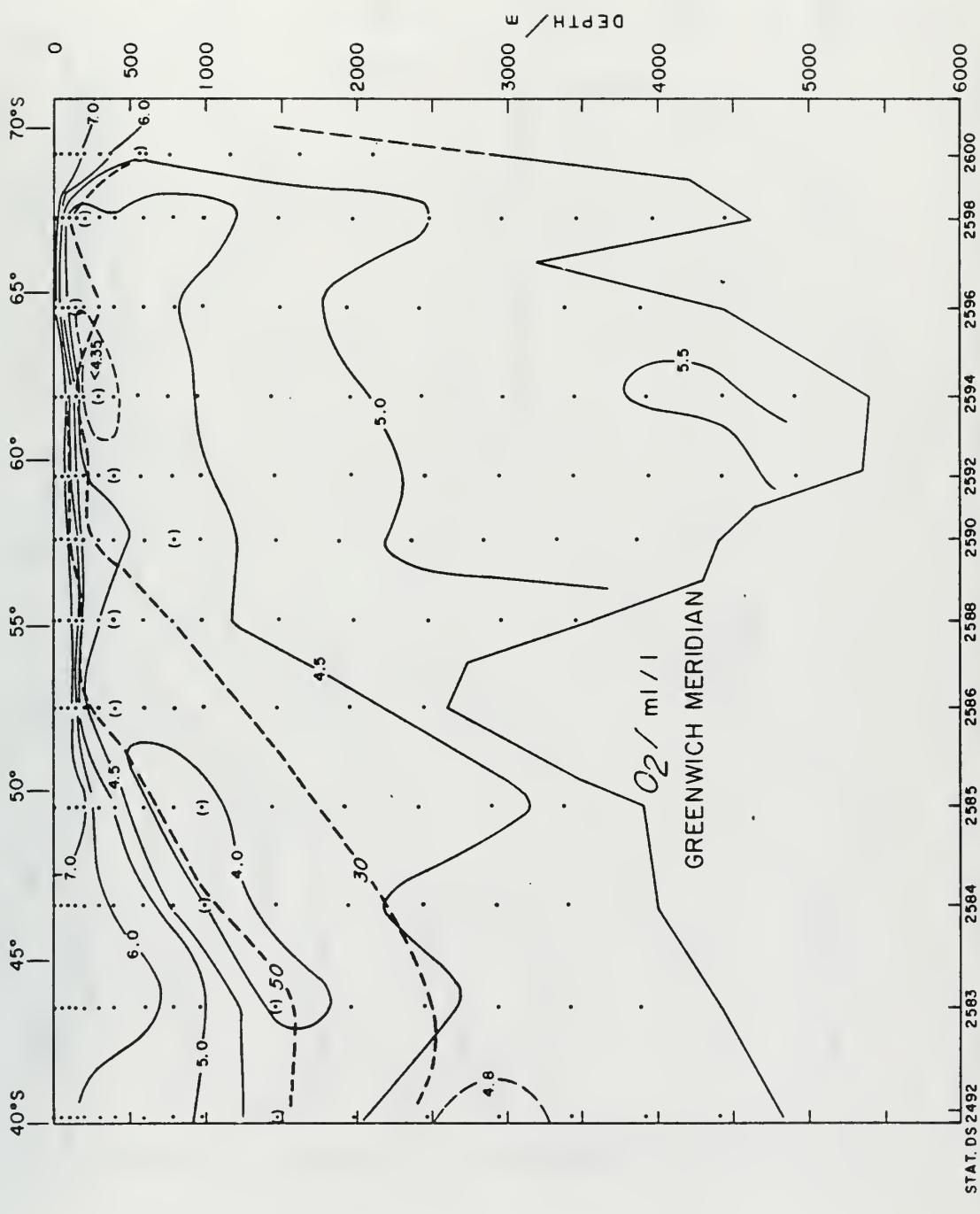

Figure 16. Greenwich Meridian: dissolved-oxygen section. Data source same as Figure 15.

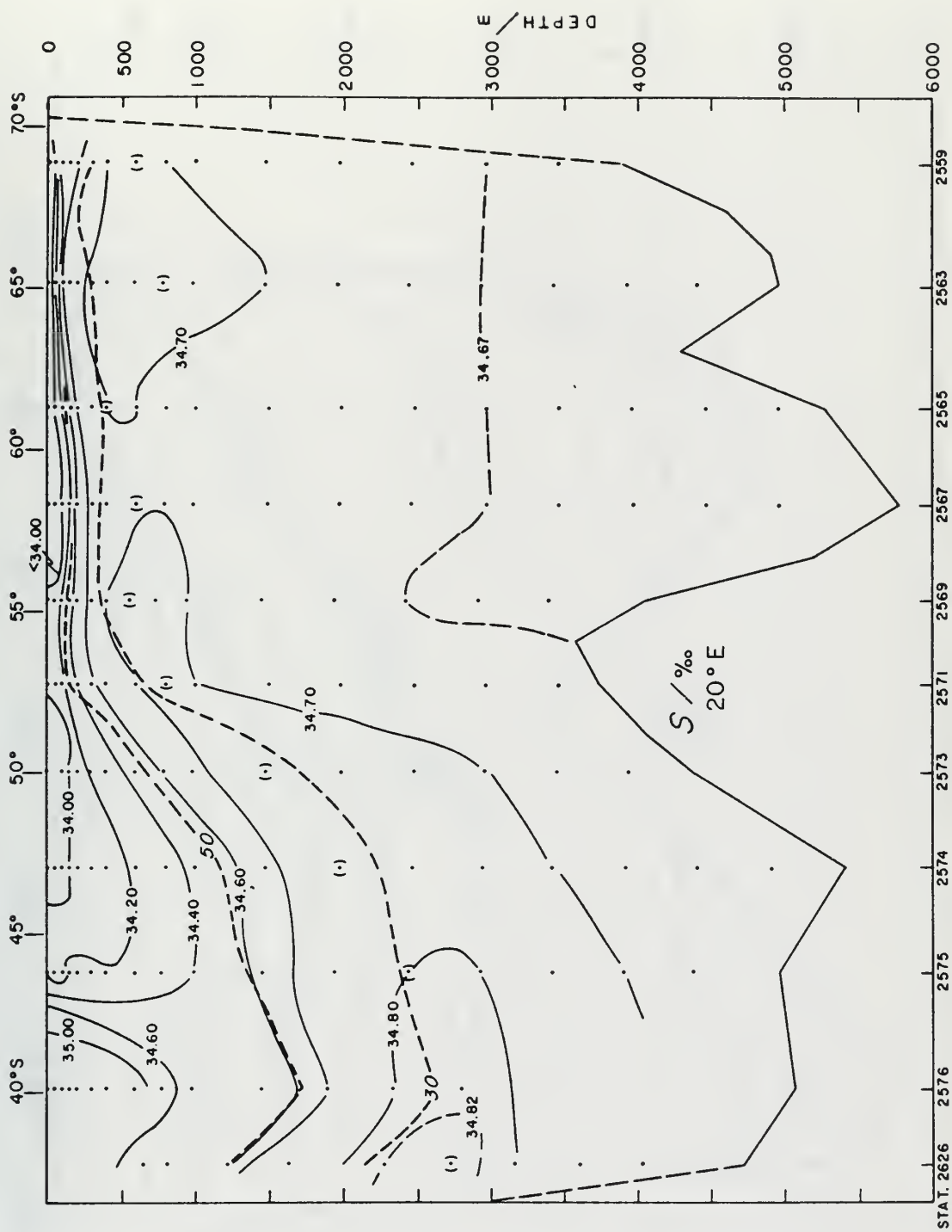

Figure 17. 20°E: salinity section. Data from *Discovery II*, 27 January - 5 February 1939; DS 2626 occupied 18 March 1939.

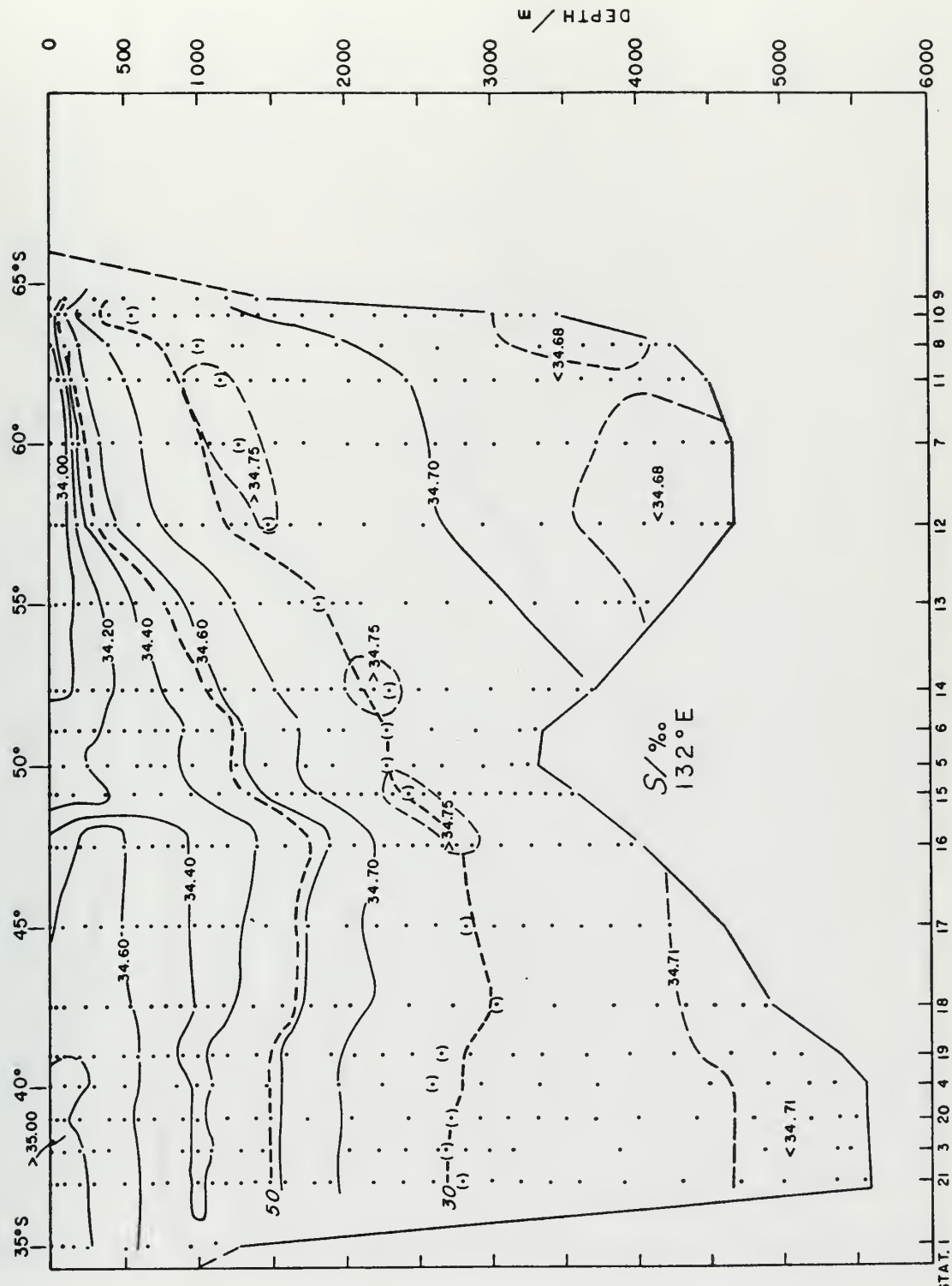

Figure 18. 132°E: salinity section. Data from *Eltanin* Cruise 41, 22 December 1969 - 24 January 1970.

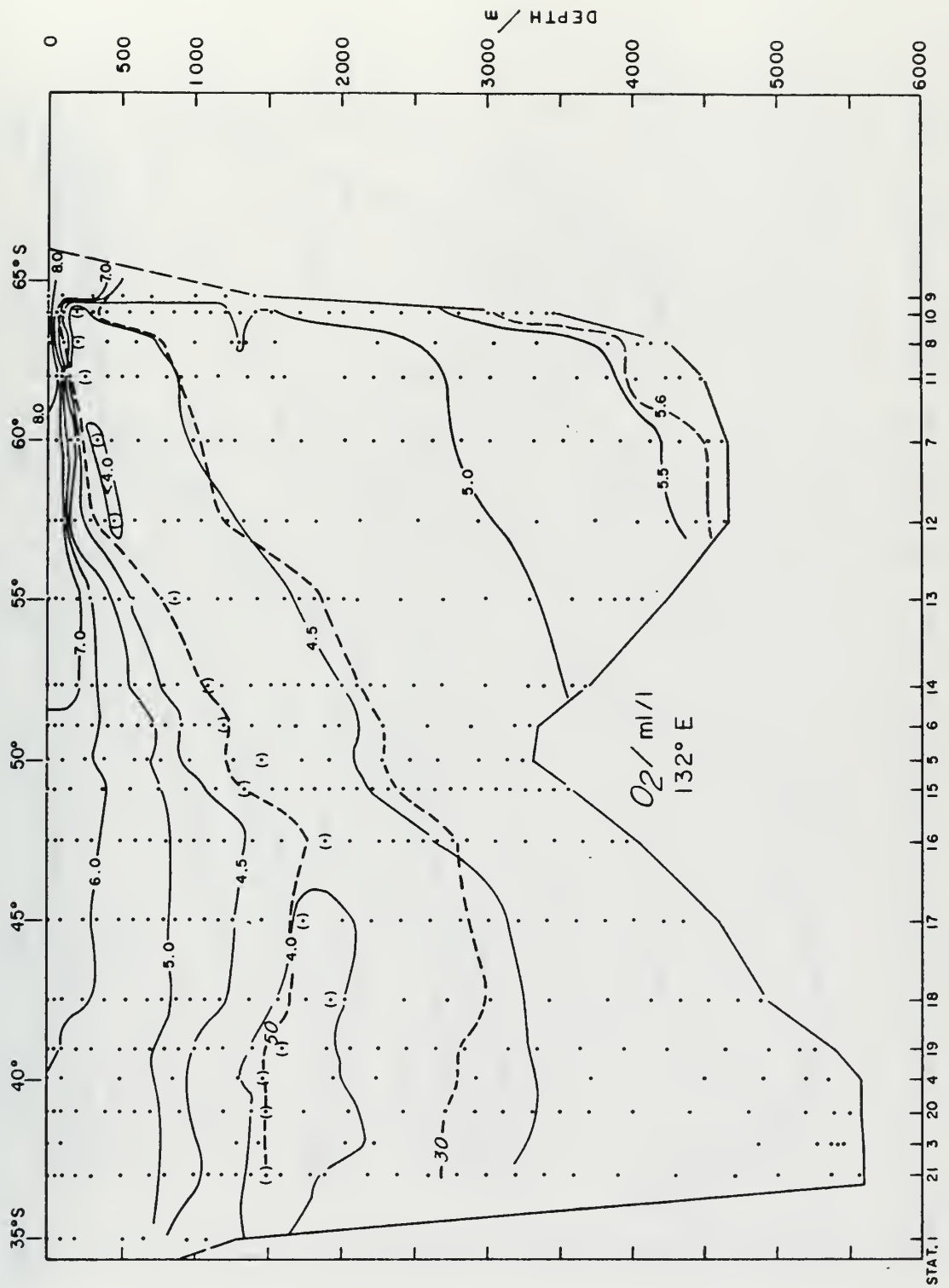

Figure 19. 132°E: dissolved-oxygen section. Data source same as Figure 18.

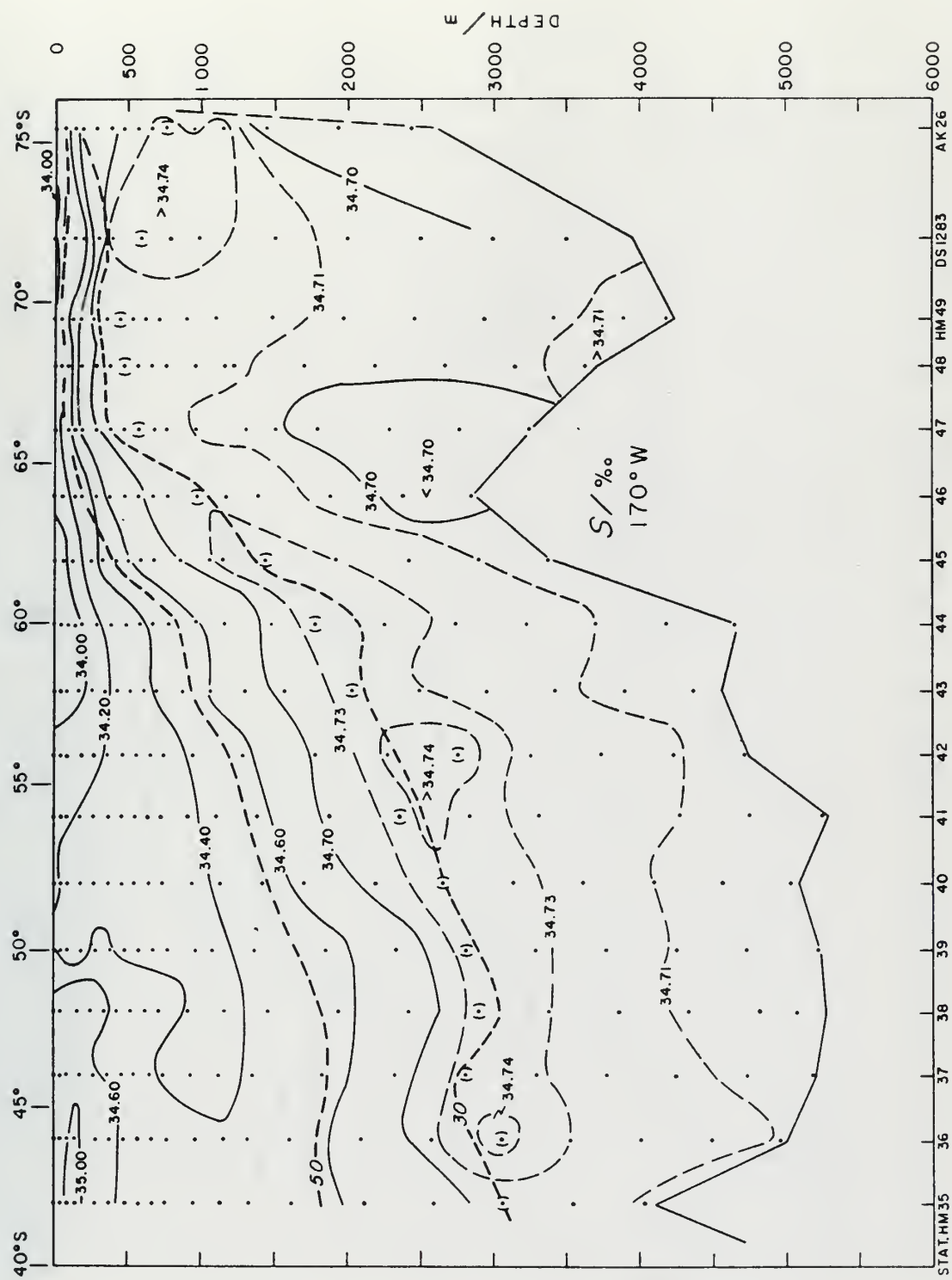

Figure 20. 170°W: salinity section. Data from Southern Cross Cruise of the *Hakuho Maru*, 27 December 1968 - 19 January 1969; DS 1283 occupied 23 February 1934, AK 26 occupied 17 February 1964.

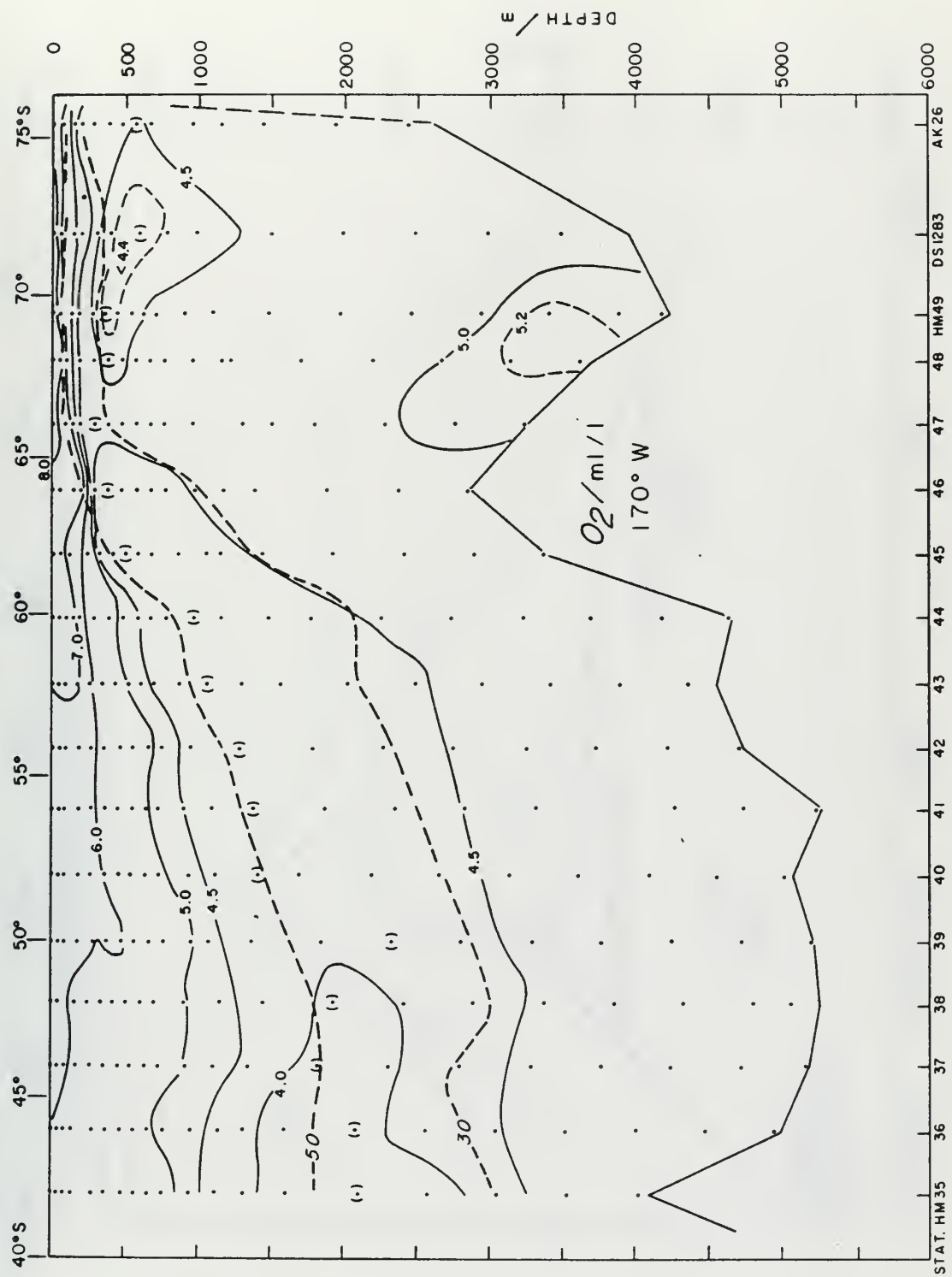

Figure 21. 170°W: dissolved-oxygen section. Data source same as Figure 20.

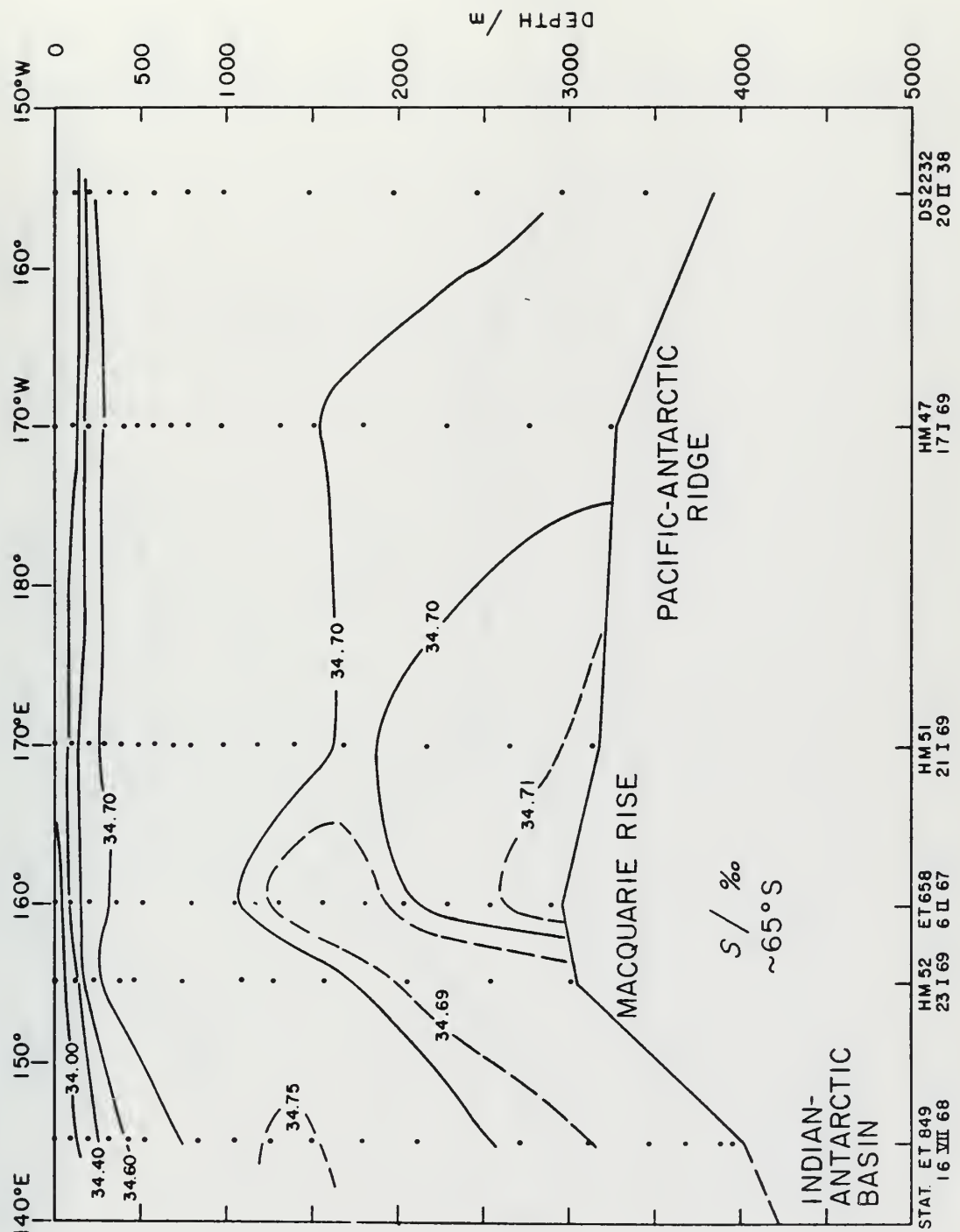

Figure 22. 65°S: salinity section. Data sources shown beneath section.

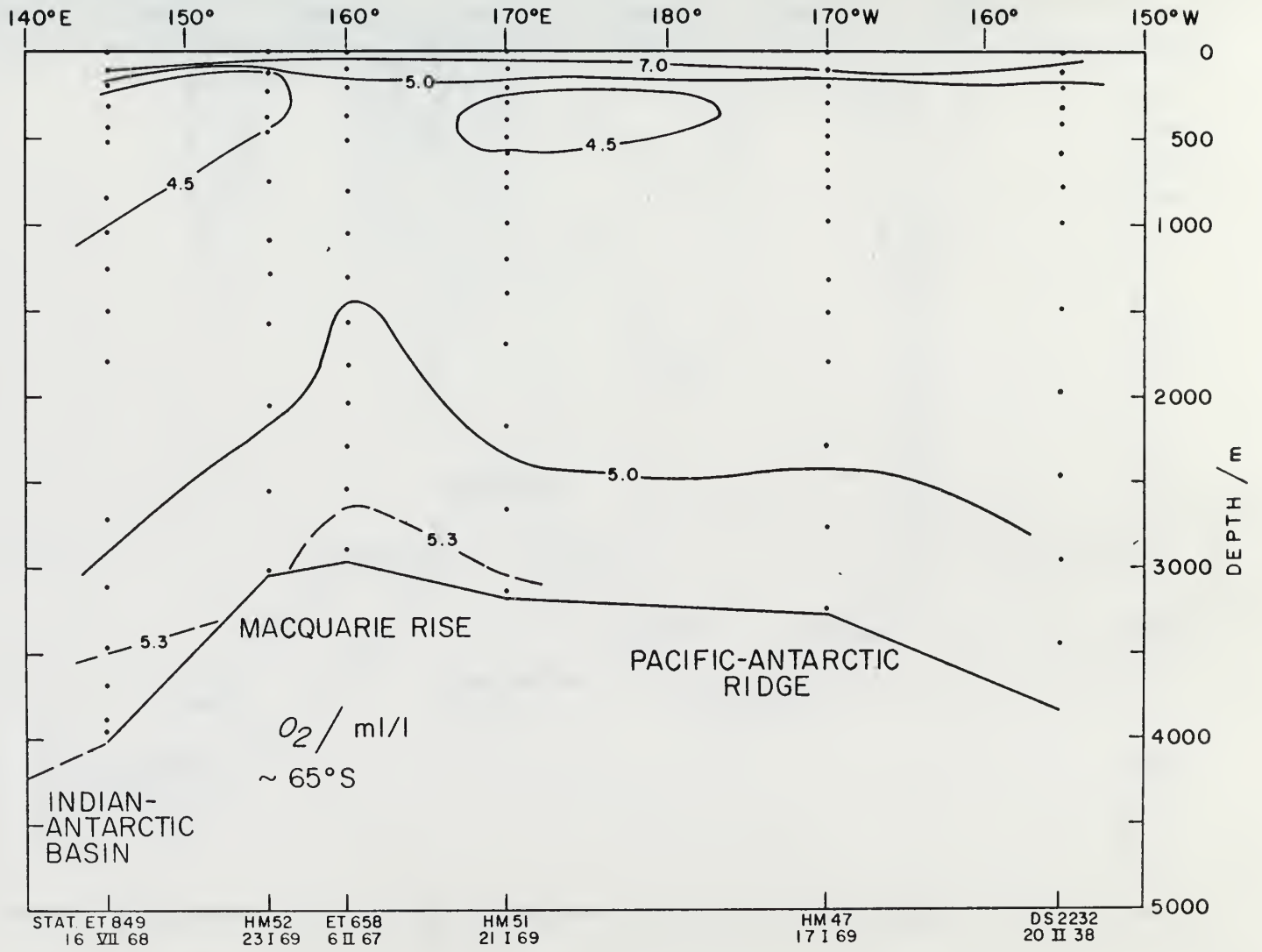

Fig. 22. [illegible] dissolved-oxygen section. Data sources shown be[illegible] section.

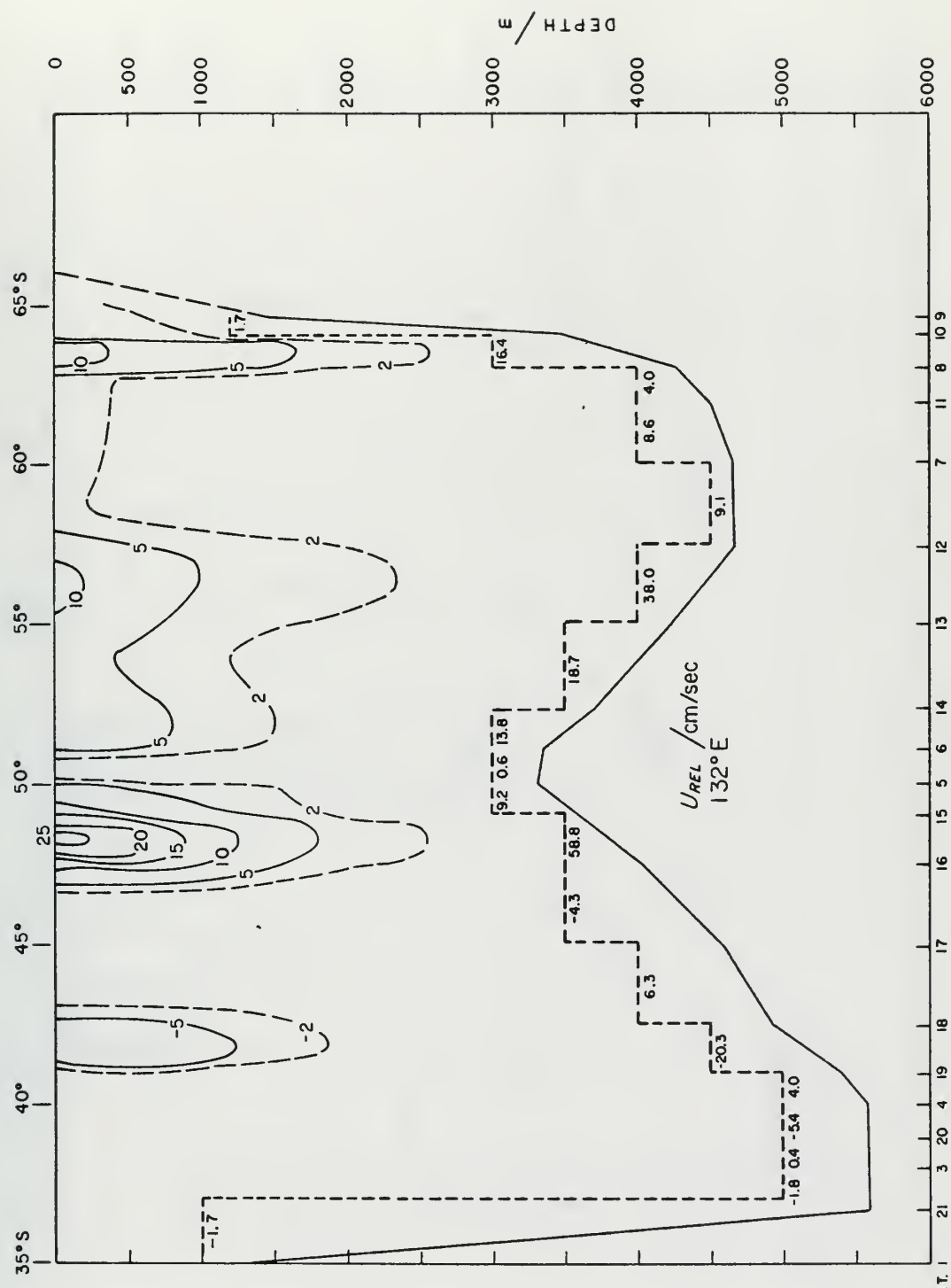

Figure 24. 132°E: zonal component of relative geostrophic velocity (positive east). Data source same as Figure 18. Net transport (35° - 65°S) equals 156 × 10^6 m^3/s.

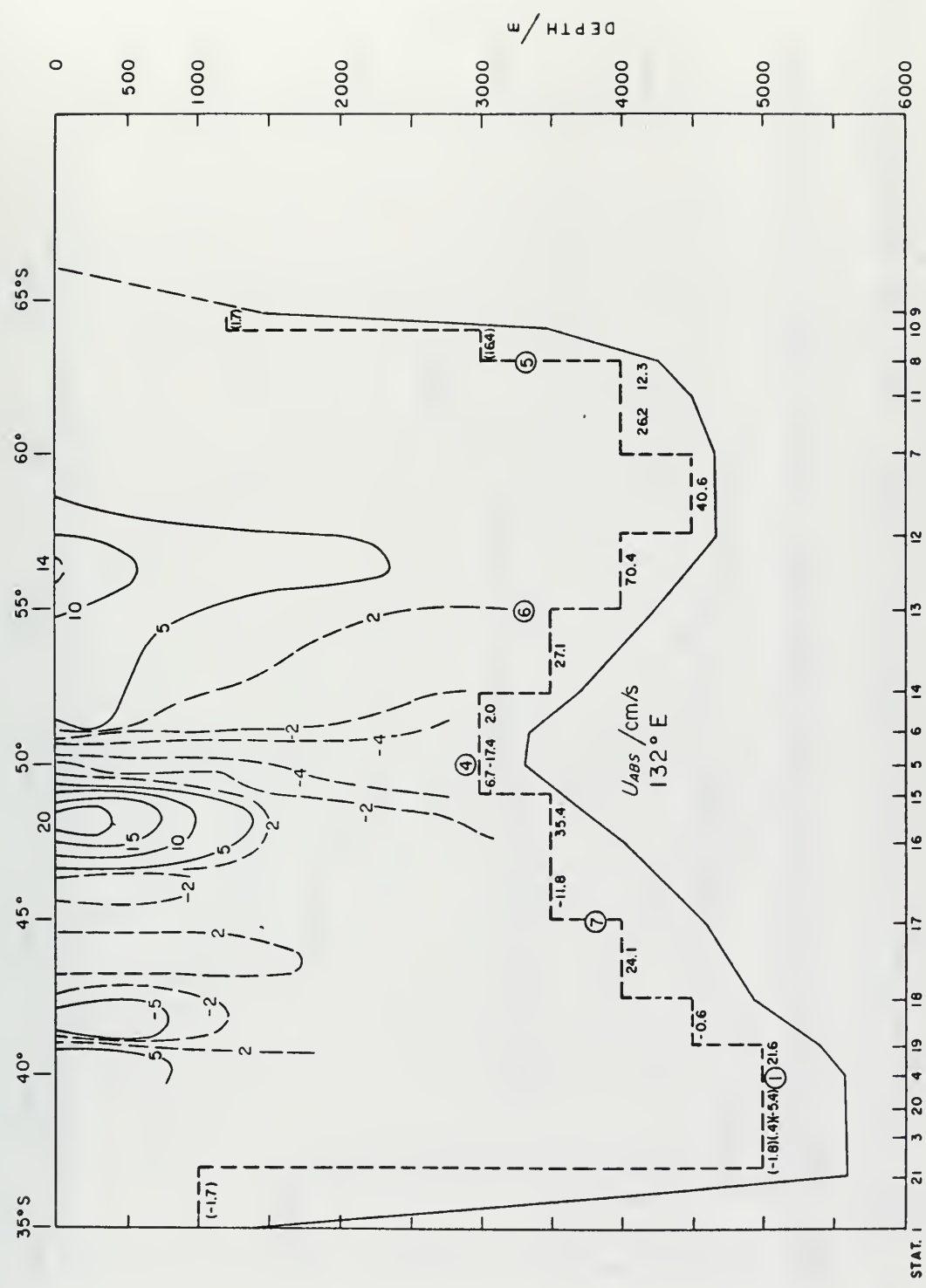

Figure 25. 132°E: zonal component of absolute geostrophic velocity. Data source same as Figure 18. Numbered circles represent current-meter positions. Transports enclosed by parentheses do not include barotropic correction. Net transport (35° - 65°S) equals 233 × 10^6 m^3/s.

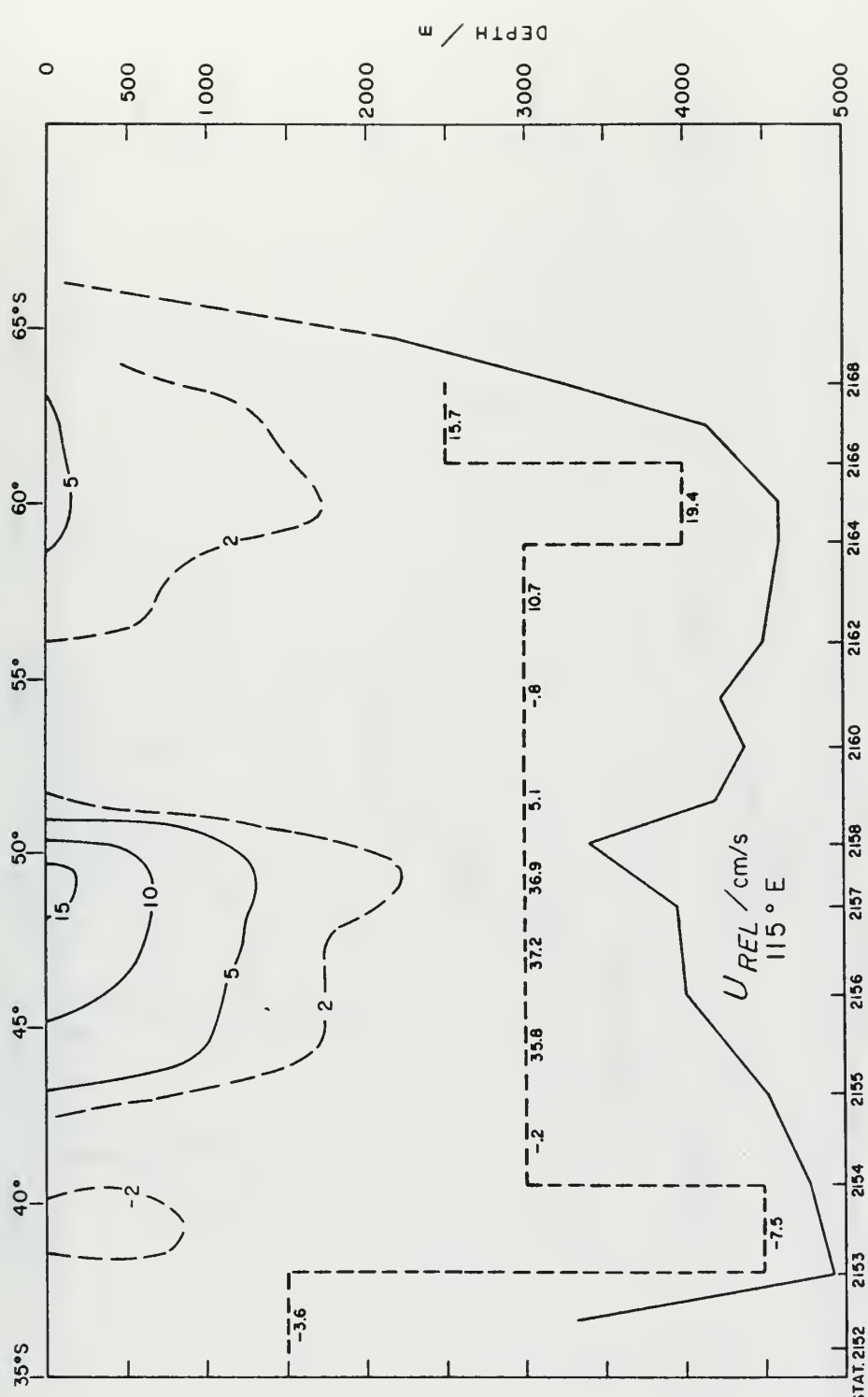

Figure 26. 115°E: zonal component of relative geostrophic velocity. Data from *Discovery II*, 30 December 1937 - 10 January 1938. Net transport (35° - 63°S) equals 149 × 10^6 m^3/s.

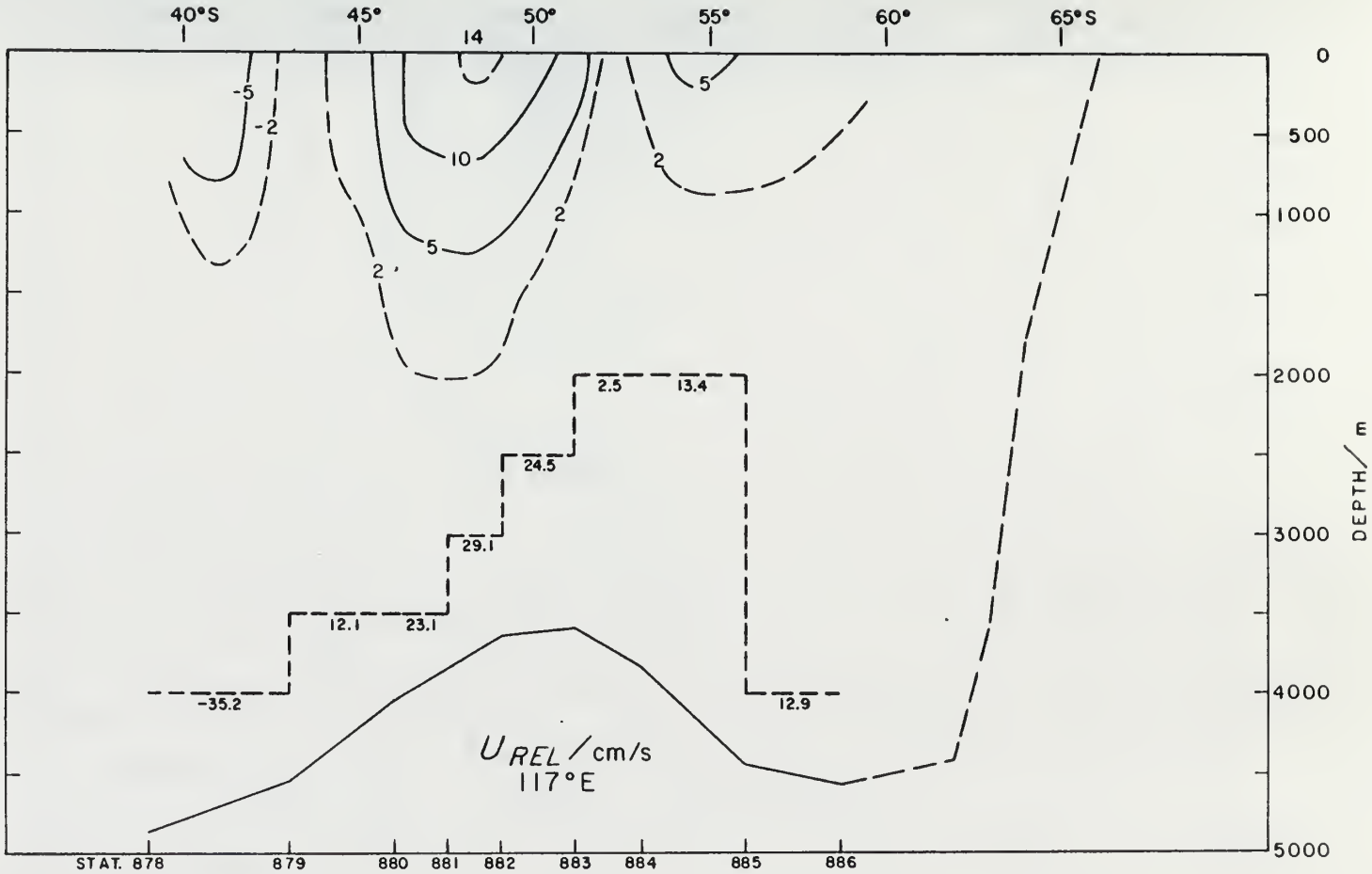

Figure 27. 117°E: zonal component of relative geostrophic velocity. Data from *Eltanin* Cruise 35, 13 - 25 September 1968. Net transport (40° - 60°S) equals 83 × 10^6 m^3/s.

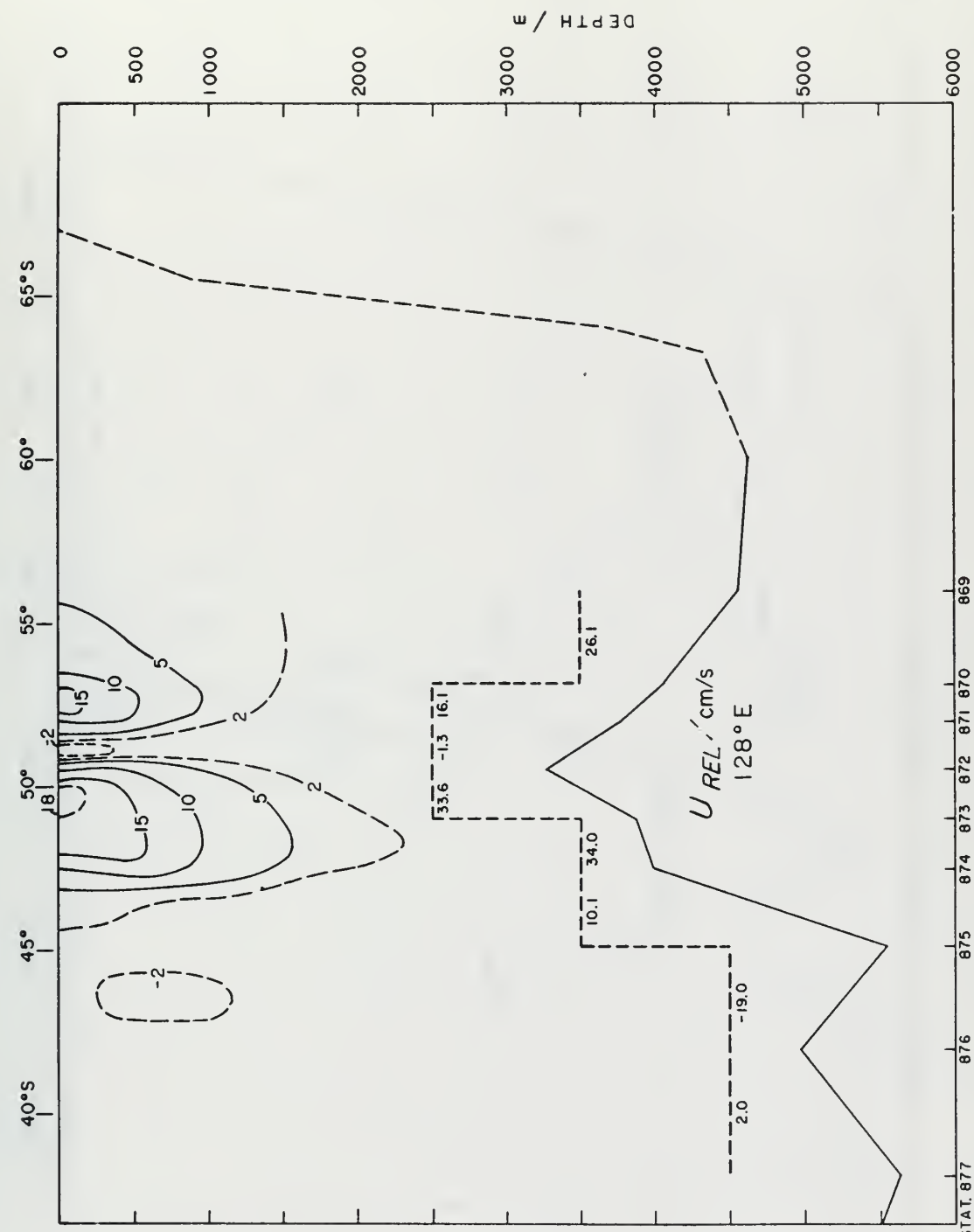

Figure 28. 128°E: zonal component of relative geostrophic velocity. Data from *Eltanin* Cruise 35, 26 August-6 September 1968. Net transport (40° - 55°S) equals 102 × 10^6 m^3/s.

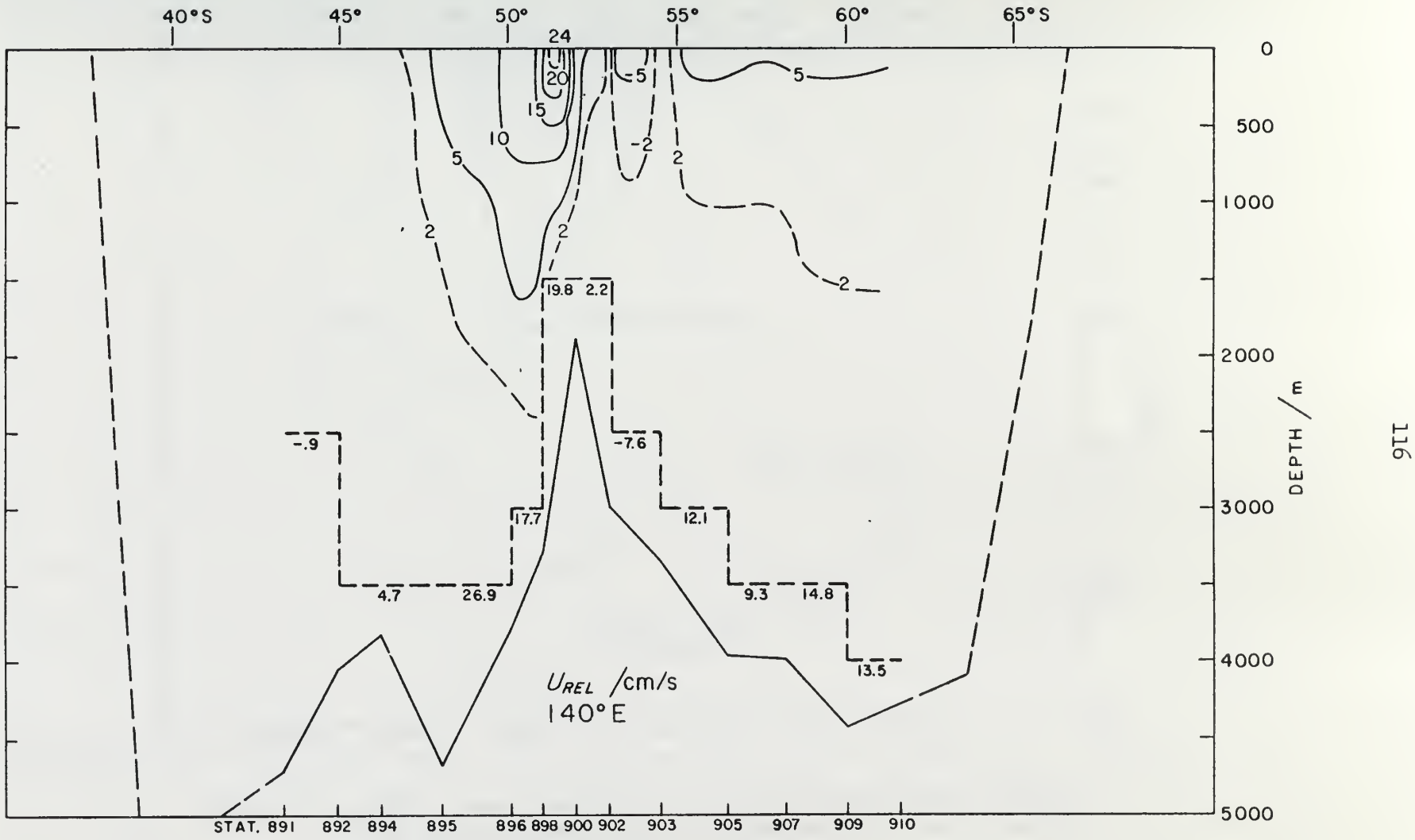

Figure 29. 140°E: zonal component of relative geostrophic velocity. Data from *Eltanin* Cruise 36, 22 October-3 November 1968. Net transport (43° - 62°S) equals 112 × 10^6 m^3/s.

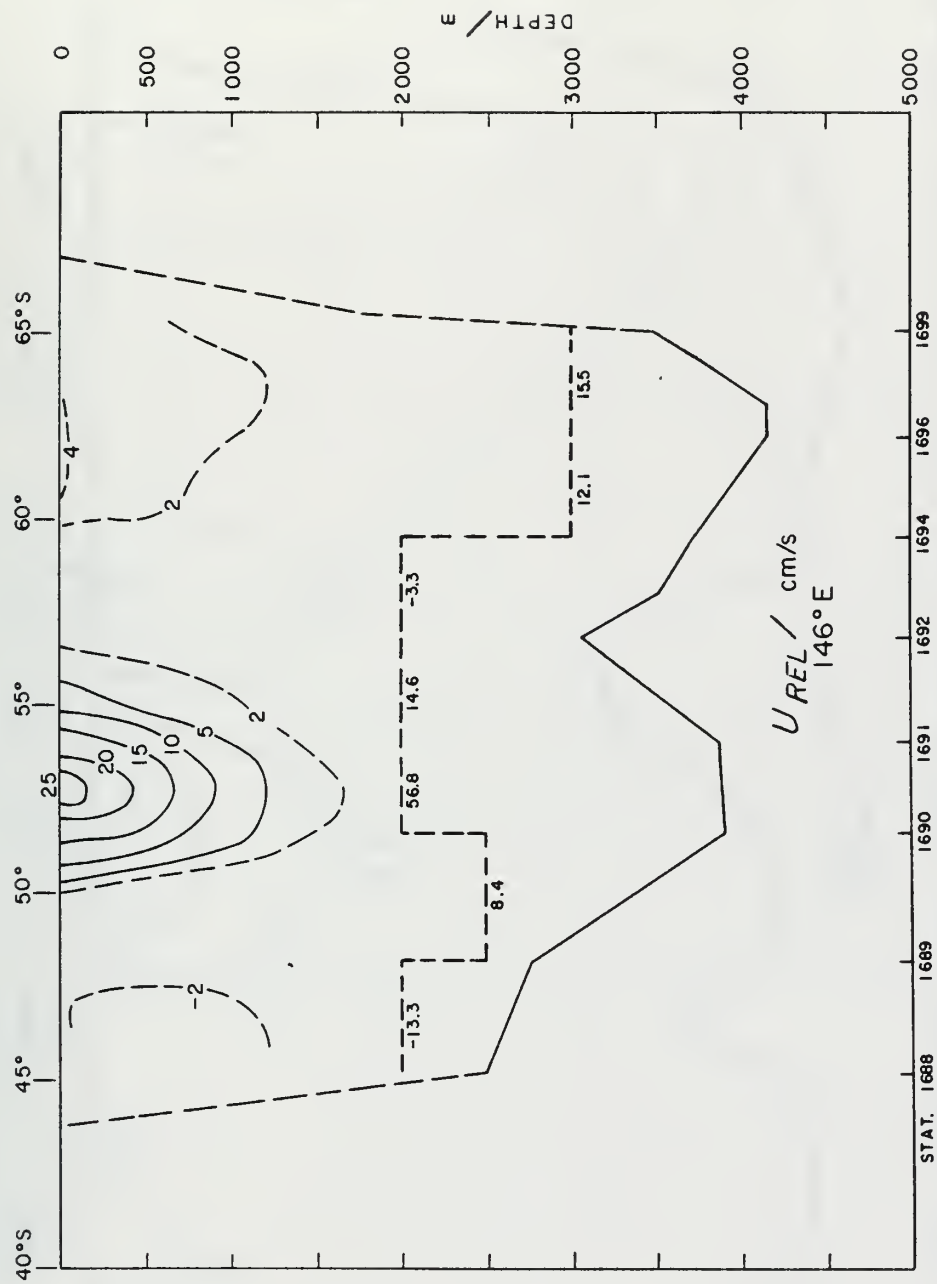

Figure 30. 146°E: zonal component of relative geostrophic velocity. Data from *Discovery II*, 6 - 15 March 1936. Net transport (45° - 65°S) equals 90 × 10^6 m^3/s.

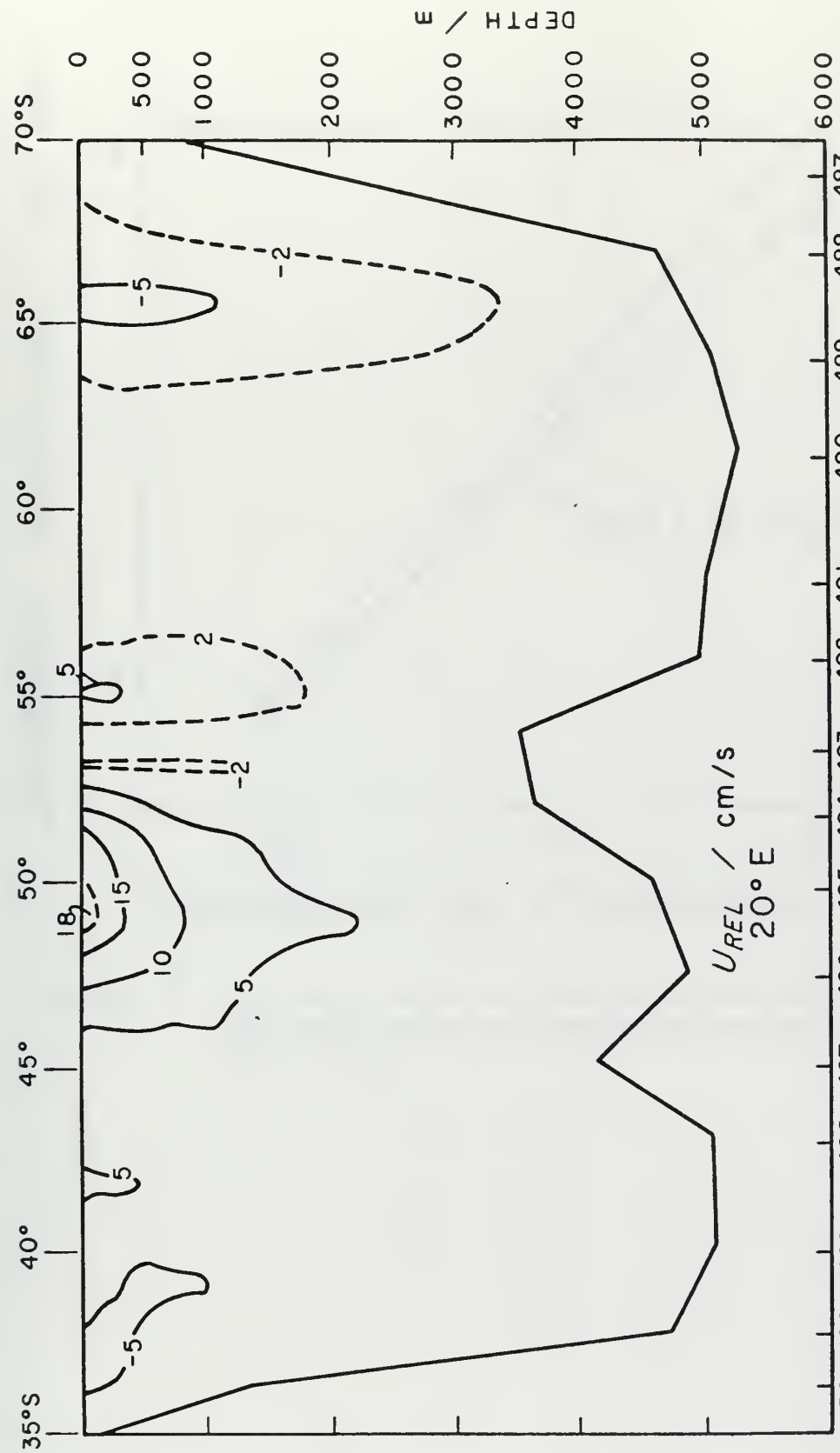

Figure 31. 20°E: zonal component of relative geostrophic velocity. Data from *Ob'* Cruise 4, 9 - 22 March 1959. Vertical exaggeration is 370. (After Kort, 1963).

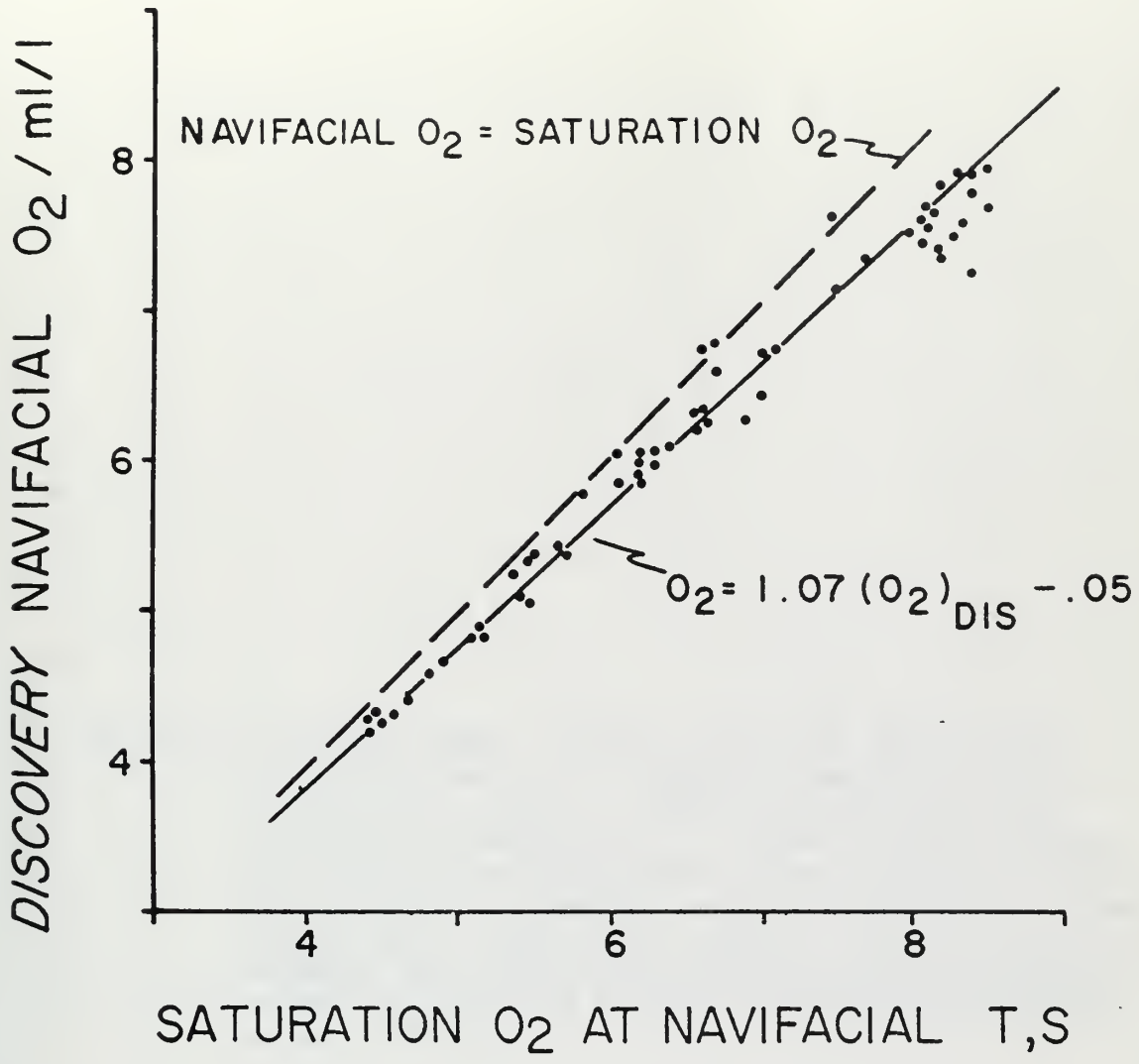

Figure 32. Correction curve for *Discovery* dissolved-oxygen data. Data points taken from various cruises over the period 1931 - 1939.

Figure 33 (following page): Station curves for the Ross Sea (lower) and Weddell Sea (upper). Station positions are marked on Figure 2. The abscissa of each plot is potential temperature (°C). The left-hand ordinate is depth (m); the right-hand ordinate is salinity (‰). The potential-temperature profile is defined by circles; the potential temperature, salinity curve is defined by squares. The slightly-curved lines running diagonally across the plots are lines of uniform potential steric anomaly (cl/t).

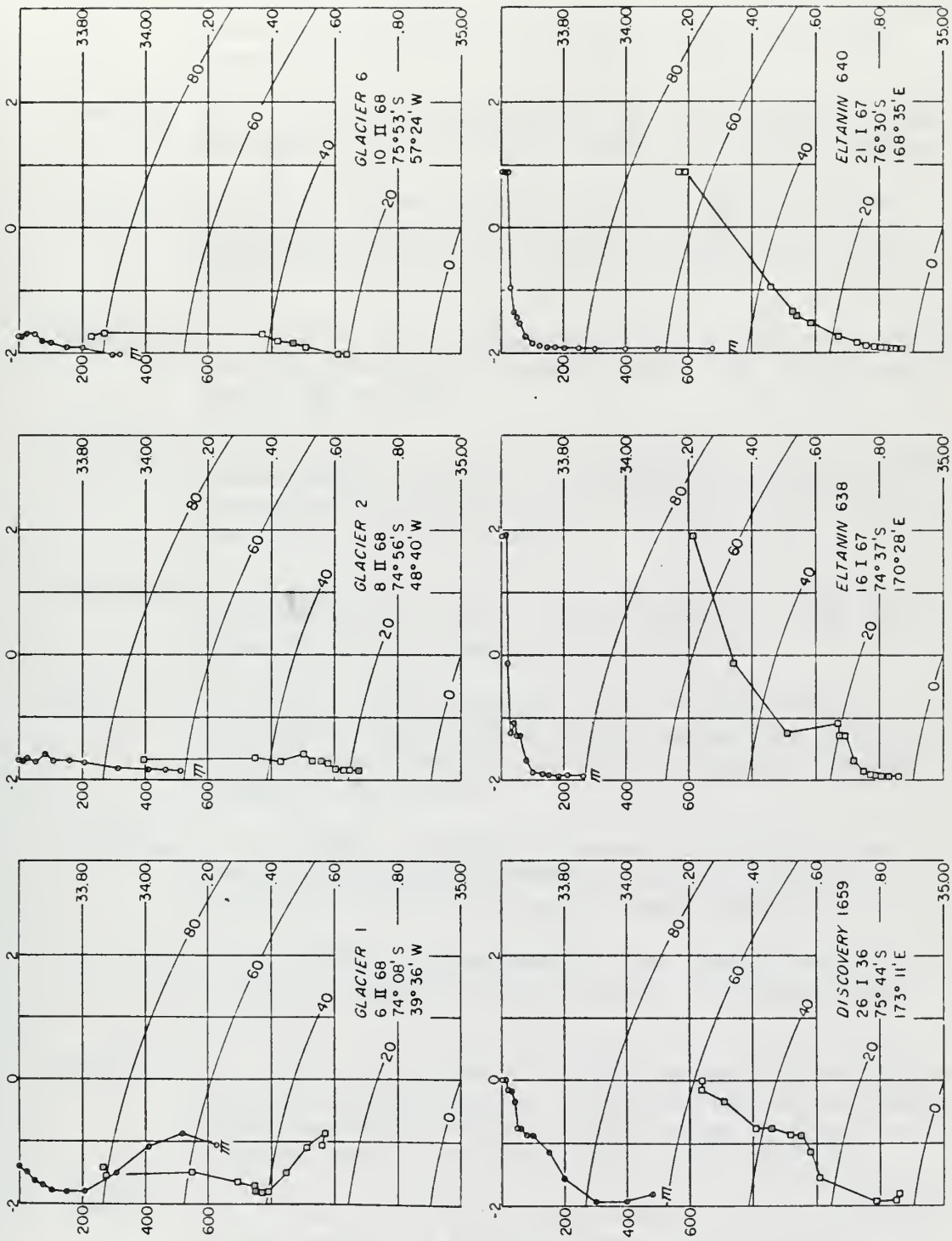
GLACIER 1
6 II 68
74° 08' S
39° 36' W
GLACIER 2
8 II 68
74° 56' S
48° 40' W
GLACIER 6
10 II 68
75° 53' S
57° 24' W
DISCOVERY 1659
26 I 36
75° 44' S
173° 11' E
ELTANIN 638
16 I 67
74° 37' S
170° 28' E
ELTANIN 640
21 I 67
76° 30' S
168° 35' E
m
.20
.40
.60
.80
3380
3400
3500
200
400
600
-2
0
2
20

REFERENCES

Barcilon, V. (1966) On the influence of the peripheral Antarctic water discharge on the dynamics of the Circumpolar Current. Jour. Mar. Res., 24: 269-275.

Barkley, R. A. (1968) Oceanographic Atlas of the Pacific Ocean. Honolulu: Univ. of Hawaii Press, 20 pp., 156 figures.

Bowen, J. L. and H. Stommel (1968) On the steadiness of the Antarctic Circumpolar Current. Am. Assoc. Adv. Sci. Symposium on Antarctic Research, Dallas, Texas, Dec., 1968.

Brennecke, W. (1921) Die ozeanographischen Arbeiten der deutschen Antarktischen Expedition 1911-1912. Aus. d.Arch. Dtsch. Seew., 39, 215 pp.

Buchan, A. (1895) Report on oceanic circulation, based on observations made on board H.M.S. *Challenger*, and other observations. *Challenger* Reports, Physics and Chemistry, Part VIII, 38 pp., 16 maps.

Bullard, E. C. (1963) The flow of heat through the floor of the ocean *in* The Sea, Vol. 3 (M. N. Hill, ed). New York: Interscience Publishers, pp. 281-296.

Bye, J. A. T. (1968) The hydrology of the Southern Ocean. 1. The Australian section - north. Horace Lamb Centre, The Flinders University of South Australia. Research Paper No. 26, 44 pp.

Callahan, J. E. (1968) A survey of theoretical models of the Antarctic Circumpolar Current. The Johns Hopkins University, M.A. Dissertation (unpublished).

Carpenter, J. H. (1965) The accuracy of the Winkler method for dissolved oxygen analysis. Limnol. & Oceanog., 10: 135-140.

Carritt, D. E. and J. H. Carpenter (1966) Comparison and evaluation of currently employed modifications of the Winkler method for determining dissolved oxygen in sea water; a NASCO report. Jour. Mar. Res., 24: 286-318.

Clowes, A. J. (1933) Influence of the Pacific on the circulation in the south-west Atlantic Ocean. Nature, 131: 189.

Clowes, A. J. and G. E. R. Deacon (1935) The deep-water circulation of the Indian Ocean. Nature, 136: 936-938.

REFERENCES (continued)

Coachman, L. K. and K. Aagaard (1966) On the water exchange through Bering Strait. Limol. & Oceanog., 11: 44-59.

Countryman, K. A. and W. L. Gsell (1966) Operations Deep Freeze 63 and 64: summer oceanographic features of the Ross Sea. U.S. Naval Oceanographic Office Tech. Rep. TR-190, 193 pp.

Cox, R. A. (1965) The physical properties of sea water *in* Chemical Oceanography, Vol. 1 (J. P. Riley and G. Skirrow, eds). New York: Academic Press, pp. 73-120.

Craig, H. and R. F. Weiss (1970) The GEOSECS 1969 intercalibration station: introduction, hydrographic features, and total CO_2-O_2 relationships. Jour. Geophys. Res., 75: 7641-7647.

Deacon, G. E. R. (1933) A general account of the hydrology of the Southern Ocean. *Discovery* Rep., 7: 171-238.

Deacon, G. E. R. (1937) The hydrology of the Southern Ocean. *Discovery* Rep., 15: 1-124.

Deacon, G. E. R. (1963) The Southern Ocean *in* The Sea, Vol. 2 (M. N. Hill, ed). New York: Interscience Publishers, pp. 281-296.

Dietrich, G. (1963) General Oceanography (translated by F. Ostapoff). New York: Interscience Publishers, 588 pp.

Fofonoff, N. P. (1956) Some properties of sea water influencing the formation of Antarctic bottom water. Deep-Sea Res., 4: 32-35.

Fofonoff, N. P. (1962a) Physical properties of sea water *in* The Sea, Vol. 1 (M. N. Hill, ed). New York: Interscience Publishers, pp. 3-30.

Fofonoff, N. P. (1962b) Dynamics of ocean currents *in* The Sea, Vol. 1 (M. N. Hill, ed). New York: Interscience Publishers, pp. 323-395.

Fuglister, F. C. (1960) Atlantic Ocean Atlas. The Woods Hole Oceanographic Institution Atlas Series, Vol. 1, 209 pp.

Gill, A. E. and J. S. Turner (1969) Some new ideas about the formation of antarctic bottom water. Nature, 224: 1287-1288.

REFERENCES (continued)

Gordon, A. L. (1966) Potential temperature, oxygen and circulation of bottom water in the Southern Ocean. Deep-Sea Res., 13: 1125-1138.

Gordon, A. L. (1967a) Geostrophic transport through the Drake Passage. Science, 156: 1732-1734.

Gordon, A. L. (1967b) Structure of antarctic waters between 20°W and 170°W. Am. Geogr. Soc. Antarctic Map Folio Series, Folio 6, 10 pp., 14 pls.

Gordon, A. L. (1970) Bottom circulation of antarctic waters south of Australia and New Zealand (abstract). Trans. Am. Geophys. Union, 51: 321.

Gordon, A. L. and R. D. Goldberg (1970) Circumpolar characteristics of antarctic waters. Am. Geogr. Soc. Antarctic Map Folio Series, Folio 13, 5 pp. 18 pls.

Hufford, G. L. and E. J. Tennyson, Jr. (1970) Distribution of nutrients in the Weddell Sea, February-March 1968, February-March 1969. U.S. Coast Guard Oceanographic Rep. No. 33 (CG 373-33), 106 pp.

Isaacs, J. D., J. L. Reid, Jr., G. B. Schick, and R. A. Schwartzlose (1966) Near-bottom currents measured in 4 kilometers depth off the Baja California coast. Jour. Geophys. Res., 71: 4297-4303.

Ishino, M. (1963) Studies on the oceanography of the antarctic circumpolar waters. Jour. Tokyo Univ. Fisheries, 49: 73-181.

Jacobs, S. S. and A. F. Amos (1967) Physical and chemical oceanographic observations in the Southern Oceans, USNS *Eltanin* Cruises 22-27. Lamont Geological Observatory Tech. Rep. No. 1-CU-1-67, 287 pp.

Jacobs, S. S., P. M. Bruchhausen, and E. B. Bauer (1970) *Eltanin* Reports, Cruises 32-36. Lamont-Doherty Geological Observatory, 460 pp.

Kort, V. G. (1963) The water transport of the Southern Ocean (in Russian). Okean. Issledovaniya, No. 8: 1-16. Moscow: Acad. Sci. USSR.

REFERENCES (continued)

Lynn, R. J. and J. L. Reid, Jr. (1968) Characteristics and circulation of deep and abyssal waters. Deep-Sea Res., 15: 577-598.

Montgomery, R. B. (1937) A suggested method for representing gradient flow in insentropic surfaces. Bull. Am. Met. Soc., 18: 210-212.

Montgomery, R. B. (1938) Circulation in the upper layers of the southern North Atlantic deduced with use of isentropic analysis. Pap. Phys. Oceanog. & Met., 6, 55 pp.

Montgomery, R. B. (1958) Water characteristics of Atlantic Ocean and of world ocean. Deep-Sea Res., 5: 134-148.

Montgomery, R. B. (1969) The words naviface and oxyty. Jour. Mar. Res., 27: 161-162.

Mosby, H. (1934) The waters of the Atlantic Antarctic Ocean. Sci. Res. Norwegian Ant. Exped., 1927-1928 *et seqq.*, No. 11, 131 pp.

Ostapoff, F. (1961) A contribution to the problem of the Drake Passage circulation. Deep-Sea Res., 8: 111-120.

Parr, A. E. (1938) Isopycnic analysis of current flow by means of identifying properties. Jour. Mar. Res., 1: 133-154.

Reid, J. L., Jr. (1965) Intermediate waters of the Pacific Ocean. The Johns Hopkins Oceanog. Studies, No. 2. Baltimore: The Johns Hopkins Univ. Press, 85 pp.

Reid, J. L., Jr., H. Stommel, E. D. Stroup, and B. A. Warren (1968) Detection of a deep boundary current in the western South Pacific. Nature, 217: 937.

Reid, J. L., Jr. and W. D. Nowlin, Jr. (1971) Transport of water through the Drake Passage. Deep-Sea Res., 18: 51-64.

Robinson, A. and H. Stommel (1959) The oceanic thermocline and the associated thermohaline circulation. Tellus, 11: 295-308.

Rossby, C.-G. (1936) Dynamics of steady ocean currents in the light of experimental fluid mechanics. Pap. Phys. Oceanog. & Met., 5, 43 pp.

REFERENCES (continued)

Rossby, C.-G. and collaborators (1937) Isentropic analysis. Bull. Am. Met. Soc., 18: 201-209.

Scripps Institution of Oceanography/Woods Hole Oceanographic Institution (1969) Physical and chemical data from the Scorpio Expedition. SIO Ref. 69-15, WHOI Ref. 69-56, 89 pp.

Seabrooke, J. D., G. L. Hufford, and R. B. Elder (1971) Formation of antarctic bottom water in the Weddell Sea. Jour. Geophys. Res., 76: 2164-2178.

Stommel, H. and A. B. Arons (1960) On the abyssal circulation of the world ocean-II. Deep-Sea Res., 6: 217-233.

Sverdrup, H. U. (1931) The origin of the deep water of the Pacific Ocean as indicated by the oceanographic work of the *Carnegie*. Gerlands Beit. Geophysik, 29: 95-105.

Sverdrup, H. U. (1939) Lateral mixing in the deep water of the South Atlantic Ocean. Jour. Mar. Res., 2: 195-207.

Sverdrup, H. U. (1940) British, Australian, New Zealand Antarctic Research Expedition: Hydrology-discussion. BANZARE Rep., Ser. A, Vol. III, Pt. 2, Sect. II, p. 89-126.

Sverdrup, H. U., M. W. Johnson, and R. H. Fleming (1942) The Oceans. Englewood Cliffs: Prentice-Hall, 1087 pp.

Taft, B. A. (1963) Distributions of salinity and dissolved oxygen on surfaces of uniform potential specific volume in the South Atlantic, South Pacific, and Indian oceans. Jour. Mar. Res., 21: 129-146.

Tokyo Univ. Ocean Res. Inst. (1970) Oceanographic data of KH-68-4 (Southern Cross Cruise) of the *Hakuho Maru*, 67 pp.

Tolstikov, E. I. (ed) (1966) Atlas Antarktiki, Vol I. Moscow: Acad. Sci. U.S.S.R., XXIII pp. text, 225 pp. figures.

Tsuchiya, M. (1968) Upper waters of the intertropical Pacific Ocean. The Johns Hopkins Oceanog. Studies, No. 4. Baltimore: The Johns Hopkins Univ. Press, 50 pp.

von Arx, W. (1957) An experimental approach to problems in physical oceanography *in* Physics and Chemistry of the Earth, Vol. 2 (L. H. Ahrens, F. Press, K. Rankama, and S. K. Runcorn, eds). New York: Pergamon Press, pp. 1-29.

REFERENCES (continued)

Welander, P. (1959) An advective model of the ocean thermocline. Tellus, 11: 309-318.

Wooster, W. S. and B. A. Taft (1958) On the reliability of field measurements of temperature and salinity in the ocean. Jour. Mar. Res., 17: 552-566.

Wooster, W. S. and G. H. Volkmann(1960) Indications of deep Pacific circulation from the distribution of properties at five kilometers. Jour. Geophys. Res., 65: 1239-1249.

Wright, R. (1969) Deep water movement in the western Atlantic as determined by use of a box model. Deep-Sea Res., Fuglister Volume: 433-446.

Wüst, G. (1933) Das Bodenwasser und die Gliederung der atlantischen Tiefsee. Wiss. Ergebn. dt. atlant. Exped. *Meteor*, 6: 1-107. (Eng. trans., U.S. Naval Oceanog. Office TRANS-340, 1967.)

Wüst, G. (1936) Atlas zur Schichtung und Zirkulation des atlantischen ozeans. Wiss. Ergebn. dt. atlant. Exped. *Meteor*, 6, Atlas, Teil A & B, 92 Beil.

Wüst, G. (1938) Bodentemperatur und Bodenstrom in der atlantischen, indischen, und pazifischen Tiefsee. Gerlands Beit. Geophysik, 54: 1-8.

Wyrtki, K. (1961) Physical oceanography of the Southeast Asian waters (NAGA Report, Vol. 2). Scripps Institution of Oceanography, 195 pp.

VITA

Jeffrey Edwin Callahan was born in Cambridge, Massachusetts on 24 September 1943. He graduated from the United States Naval Academy in June 1965, receiving a Bachelor of Science degree and a commission in the United States Navy. After two years' duty aboard the USS *Willis A. Lee* (DL-4) in the Atlantic Fleet, he entered the graduate program in oceanography at The Johns Hopkins University. He received a Master of Arts degree from the University in 1969. The author is married to the former Evelyn Green of Bethesda, Maryland.

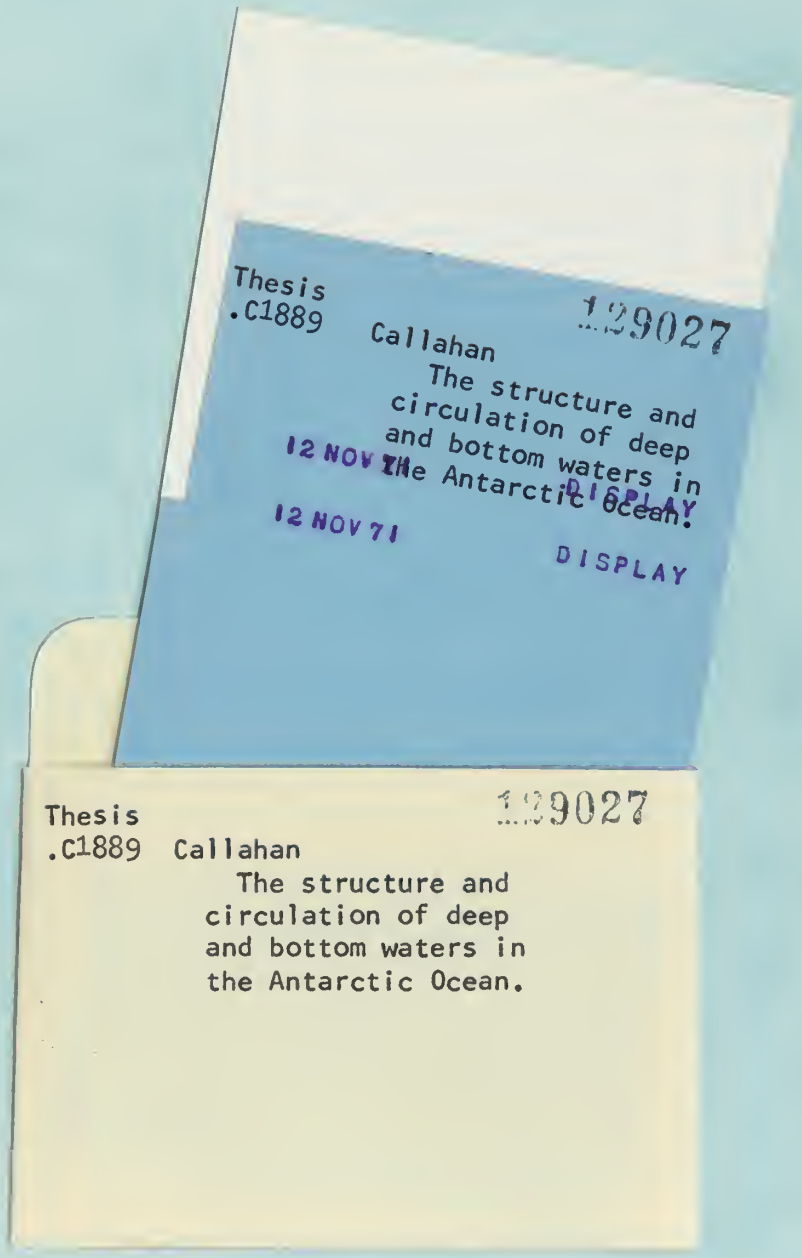

Thesis
.C1889 Callahan
129027
The structure and
circulation of deep
and bottom waters in
the Antarctic Ocean.